How Healthy Are Those Tiny Millimeter-Wave Cables? p34

SIW Filter Turns Balun for mmWave Applications p44

Accelerate Planar Filter Design Through Port Tuning p81


# Microwaves & RF®

YOUR TRUSTED ENGINEERING RESOURCE FOR OVER 50 YEARS

APRIL 2018 mwrf.com

Solving the bandwidth dilemma for the next-gen wireless network p38

# 5G & MILLIMETER WAVES


SEARCH PARTS FAST

sourceesb

Parts | Enter part... | Enter List

Your Trusted Source www.SourceESB.com


$10.00

NI AWR DESIGN ENVIRONMENT

# SIMPLY SMARTER

5G WIRELESS

NI AWR Design Environment is one platform integrating system, circuit, and electromagnetic analysis for the design of 5G communications systems. Supporting wireless standards like 5G and proprietary waveforms, the software enables designers to quickly build virtual communications systems and evaluate benefits and drawbacks, as well as share IP from design through to test.

Simply smarter 5G design.

**Learn more at awrcorp.com/5g**

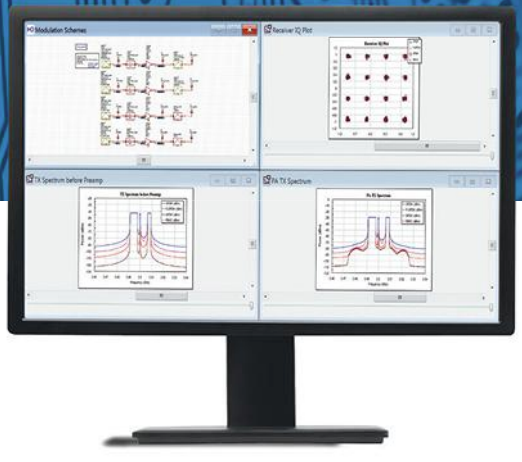

Visual System Simulator | 5G/Wireless Communications Systems Design

NATIONAL INSTRUMENTS™

©2018 National Instruments. All rights reserved.

# Planar Monolithics Industries, Inc.

## RF / Microwave Limiters - Passive & Active

PMI offers a variety of RF / microwve limiters covering the DC to 40 GHz frequency range in passive or active designs for military and industrial applications. PMI's limiters offer low loss, high speed along with low leakage levels and high peak power handling. More available at:
http://www.pmi-rf.com/Products/limiters/limiters_features.htm

LM-1G2G-4CW-1KWP-SMF-OPT10M6G

LM-100M20G-18-10W-SFF

LM-1G18G-15-25W-SMF

LM-18G40G-18-1W-292FF

### PASSIVE LIMITERS

| PMI Model No. | FREQ Range (GHz) | Insertion Loss (dB) | VSWR | Maximum Input Power | Leakage Power (dBm) | Recovery Time | Size (Inches) / Connectors |
|---|---|---|---|---|---|---|---|
| **LM-1G2G-4CW-1KWP-SMF-OPT10M6G** http://www.pmi-rf.com/Products/limiters/LM-1G2G-4CW-1KWP-SMF-OPT10M6G-Updated.htm | 0.01 - 6 | 2 | 2.0:1 | 4 W, CW 1 KW peak (1% Duty Cycle, 1 µs Max Pulse Width) | 16 | 1 µs | 1.00 x 0.75 x 0.38 SMA (F) |
| **LM-100M20G-18-10W-SFF** http://www.pmi-rf.com/Products/limiters/LM-100M20G-18-10W-SFF.htm | 0.1 - 20 | 2 | 2.0:1 | 1 W CW 10 W Pulsed (10% Duty Cycle,100 µs Pulse Width) | 18.5 | 115 ns | 0.50 x 0.50 x 0.22 SMA (F) |
| **LM-1G18G-15-25W-SMF** http://www.pmi-rf.com/Products/limiters/LM-1G18G-15-25W-SMF.htm | 1.0 - 18 | 2.5 | 2.0:1 | 10 W CW 100 W Peak (10% Duty Cycle & 40 µs Pulse Width) | 15 | 100 ns | 1.00 x 1.00 x 0.40 SMA (F) |
| **LM-18G40G-18-1W-292FF** http://www.pmi-rf.com/Products/limiters/LM-18G40G-18-1W-292FF.htm | 18 - 40 | 4 | 2.1:1 | 1 W CW | 18 | 10 ns | 0.5 x 0.5 x 0.22 2.92mm (F) |

LM-500M8G-2-33DBM-12V

LM-2G18G-2D8-33DBM-12V

LM-8G18G-7-33DBM-12V

LM-1G2G-N15-33DBM-12V

### ACTIVE LIMITERS

| PMI Model No. | FREQ Range (GHz) | Insertion Loss (dB) | VSWR | Maximum Input Power | Leakage Power (dBm) | DC Supply Voltage | Size (Inches) / Connectors |
|---|---|---|---|---|---|---|---|
| **LM-500M8G-2-33DBM-12V** http://www.pmi-rf.com/Products/limiters/LM-500M8G-2-33DBM-12V.htm | 0.5 - 6 | 2 | 2.0:1 | +33 dBm CW | 2.3 | +12 VDC @ 180 mA | 1.08 x 0.71 x 0.29 SMA (F) |
| **LM-2G18G-2D8-33DBM-12V** http://www.pmi-rf.com/Products/limiters/LM-2G18G-2D8-33DBM-12V.htm | 2.0 - 18 | 2 | 2.0:1 | +33 dBm CW | 2.8 | +12 VDC @ 180 mA | 1.08 x 0.71 x 0.29 SMA (F) |
| **LM-8G18G-7-33DBM-12V** http://www.pmi-rf.com/Products/limiters/LM-8G18G-7-33DBM-12V.htm | 8.0 - 18 | 2 | 2.0:1 | +33 dBm CW | 7.1 | +12 VDC @ 100 mA | 1.08 x 0.71 x 0.29 SMA (F) |
| **LM-1G2G-N15-33DBM-12V** http://www.pmi-rf.com/Products/limiters/LM-1G2G-N15-33DBM-12V.htm | 1.0 - 2 | 2 | 2.0:1 | +33 dBm CW | -15 | +12 VDC @ 250 mA | 1.92 x 0.78 x 0.36 SMA (F) |

**West Coast Operation:**
4921 Robert J. Mathews Pkwy, Suite 1
El Dorado Hills, CA 95762 USA
Tel: 916-542-1401, Fax: 916-265-2597

**East Coast Operation:**
7311-F Grove Road
Frederick, MD 21704 USA
Tel: 301-662-5019, Fax: 301-662-1731

sales@pmi-rf.com • www.pmi-rf.com

ISO9001 REGISTERED

- Amplifiers – Solid State
- Attenuators – Variable/ Programmable
- Couplers (Quadrature, 180° & Directional)
- Detectors – RF/Microwave
- DLVAs, ERDLVAs & SDLVAs
- DTOs, VCOs, PLO, DROs, & Frequency Synthesizers
- Filters & Switched Filter Banks
- Form, Fit, Functional Products & Services
- Frequency Discriminators & IFMs
- Integrated MIC/MMIC Assemblies (IMAs)
- IQ Vector Modulators
- Limiters – RF/Microwave
- Log Amplifiers
- Millimeter Wave Components (Up to 50 GHz)
- Miscellaneous Products
- Monopulse Comparators
- Multifunction Integrated Assemblies (MIAs)
- Phase Shifters & Bi-Phase Modulators
- Power Dividers/Combiners (Passive & Active)
- Pulse Modulators (SPST)
- Rack & Chassis Mount Products
- Receiver Front Ends & Transceivers
- SDLVAs, ERDLVAs & DLVAs
- Single Side Band Modulators
- SMT & QFN Products
- Switch Matrices
- Switched Filter Banks
- Switches – Solid State
- Systems - Radar Sense & Avoid
- Systems – Fly Eye Radars
- Threshold Detectors
- USB Products

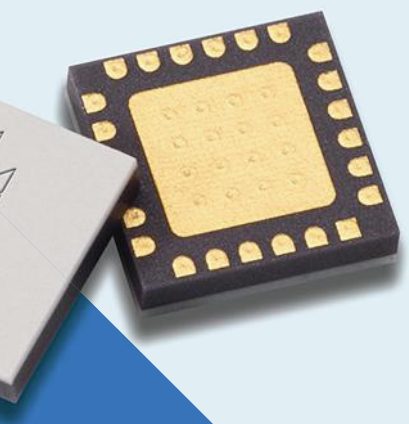

# C- AND X-BAND MIXERS WITH HIGH IP3

| CMD257C4 | CMD258C4 |
|---|---|
| 6-10 GHz<br>FREQUENCY RANGE | 7.5-13 GHz<br>FREQUENCY RANGE |
| 24 dBm<br>INPUT IP3 | 25 dBm<br>INPUT IP3 |
| 31 dB<br>IMAGE REJECTION | 29 dB<br>IMAGE REJECTION |

## Excellent as image-reject *or* single-sideband mixers

Also offering wide IF bandwidth and low conversion loss, these new GaAs MMIC mixers are the best choice for your high linearity requirements. Download complete data at **CustomMMIC.com/mixers**.

*Where can we take you next?*

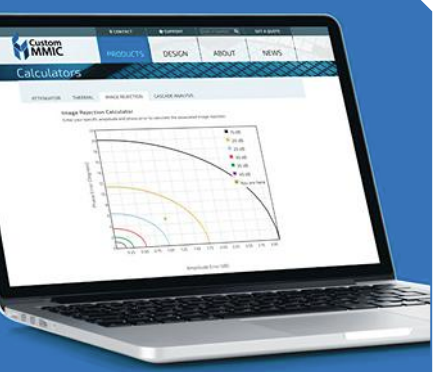


**Check out our Image Rejection Calculator**

Just plug in your phase and amplitude errors and get an instant contoured display of your image rejection. It's part of our free suite of design calculators at:

**custommmic.com/ calculators**

Custom MMIC

# Exceptional
## Phase Noise Performance
## Dielectric Resonator Oscillator

RoHS Patented Technology

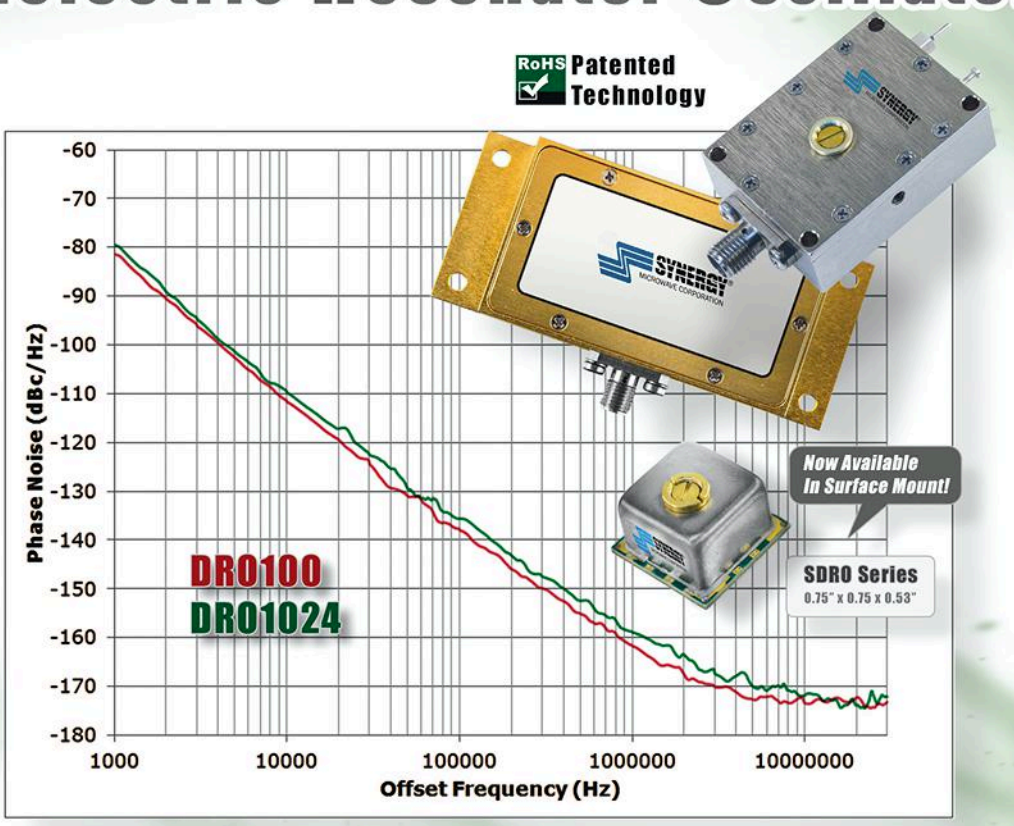


| Model | Frequency (GHz) | Tuning Voltage (VDC) | DC Bias (VDC) | Typical Phase Noise @ 10 kHz ( dBc/Hz ) |
|---|---|---|---|---|
| **Surface Mount Models** | | | | |
| SDRO1000-8 | 10 | 1 - 15 | +8 @ 25 mA | -107 |
| SDRO1024-8 | 10.24 | 1 - 15 | +8 @ 25 mA | -111 |
| SDRO1250-8 | 12.50 | 1 - 15 | +8 @ 25 mA | -105 |
| **Connectorized Models** | | | | |
| DRO100 | 10 | 1 - 15 | +7 - 10 @ 70 mA | -111 |
| DRO1024 | 10.24 | 1 - 15 | +7 - 10 @ 70 mA | -109 |

## Talk To Us About Your Custom Requirements.


SYNERGY® MICROWAVE CORPORATION

Phone: (973) 881-8800 | Fax: (973) 881-8361
E-mail: sales@synergymwave.com
Web: WWW.SYNERGYMWAVE.COM
Mail: 201 McLean Boulevard, Paterson, NJ 07504

# RF SWITCHES

## DC - 40 GHz

| Type | Failsafe | Latching | Normally Open Terminations | SMA | 2.92mm | Type-N | 7/16, 4.3-10 | SC | High Power (CW) | Low PIM (dBc) | Cycle Life |
|---|---|---|---|---|---|---|---|---|---|---|---|
| SPDT | ✔ | ✔ | ✔ | 50Ω, 2W | ✔ | ✔ | ✔ | ✔ | ✔ | 2kW | -170 | 5M |
| Transfer | ✔ | ✔ | | | ✔ | ✔ | ✔ | ✔ | ✔ | 2kW | -170 | 5M |
| SPMT* | ✔ | ✔ | ✔ | 50Ω, 2W | ✔ | ✔ | ✔ | ✔ | ✔ | 2kW | -170 | 5M |

*SP3T to SP12T designs

**Visit [www.e360microwave.com](http://www.e360microwave.com) for data sheets and more information.**

e360microwave offers relays and switches for ultra reliable test applications. Based on a 30-year heritage of innovative RF and microwave products and designs, our broad selection of relays and switches features excellent RF performance, reliability and repeatability. We can deliver 10,000s switches per month, quickly and at very competitive prices. All options are available and high-power and low PIM designs are a specialty.

RoHS Compliant REACH COMPLIANCE ISO 9001

e360 microwave

Santa Clara, CA 95054 408-650-8360 (o), 408-650-8365 (f)
techsupport@e360microwave.com
sales@e360microwave.com

# IN THIS ISSUE

## FEATURES


**27** **Why Plastic-Packaged MMIC PAs May be Essential for 5G MIMO Base Stations**
This article breaks down two new highly integrated Doherty PA designs that could have a major impact on 5G applications.

**34** **Millimeter-Wave Cables: Time for a Checkup?**
As millimeter-wave frequencies become more prevalent, it's essential that the smaller cables used at these high frequencies be properly handled due to their fragility.

**38** **What Role Will Millimeter Waves Play in 5G Wireless Systems?**
5G will mobility to mmWave communications as the next-gen wireless network attempts to serve more people and even things with a major expansion of mobile services.

**44** **SIW Filter Doubles as Balun to mmWave Frequencies**
The balun/bandpass filter, based on substrate integrated waveguide and circular complementary split-ring resonators, delivers outstanding performance in millimeter-wave-frequency applications.

**52** **Refine Biasing Networks for High PA Low-Frequency Stability**
Biasing networks can have a great deal to do with the low-frequency stability of RF/microwave power amplifiers based on many different types of high-frequency transistors.

**58** **What's the Difference Between Long- and Short-Haul Links?**
Wireless communications can be performed over near and far distances depending on factors such as transmit power, receiver sensitivity, and operating frequency.


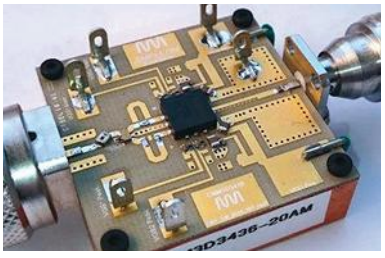

27

34

38

58

70

## PRODUCTS & TECHNOLOGY


**62** Actively-Scanned Antenna Array Simulation (Part 2)

**70** Antenna Matching with Portable VNA

**73** LDMOS Power Transistors

**76** Switchable Directional Coupler

**81** Port Tuning in Filter Design


JOIN US ONLINE

follow us @MicrowavesRF

become a fan at facebook.com/microwavesRF

## NEWS & COLUMNS


**10** ON MWRF.COM

**13** EDITORIAL
Making the Most of Millimeter Waves

**18** NEWS

**24** R&D ROUNDUP

**60** APPLICATION NOTES

**86** NEW PRODUCTS

**88** ADVERTISERS INDEX

## Fast Pulse Test Systems from Avtech

Avtech offers over 500 standard models of high-speed pulsers, drivers, and amplifiers ideal for both R&D and automated factory-floor testing. Some of our standard models include:

**AVR-E3-B:** 500 ps rise time, 100 Volt pulser

**AVRQ-5-B**: Optocoupler CMTI tests, >120 kV/us

**AVO-8D3-B**: 500 Amp, 50 Volt pulser

**AV-1010-B:** General purpose 100V, 1 MHz pulser

**AVO-9A-B**: 200 ps $t_r$, 200 mA laser diode driver

**AV-156F-B**: 10 Amp current pulser for airbag initiator tests

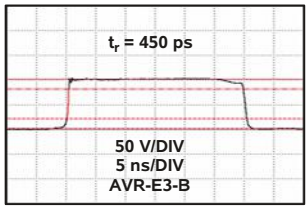


AVTECH

Nanosecond Electronics
Since 1975

**Pricing, manuals, datasheets and test results at:**
www.avtechpulse.com

AVTECH ELECTROSYSTEMS LTD.
Tel: +1-613-686-6675 Fax: +1-613-686-6679
info@avtechpulse.com

## High Output - Low Risetime Pulsers from Avtech

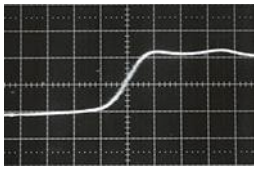

Sub-nanosecond rise time pulsers for every amplitude range!

Model AVP-3SA-C provides up to 10V with < 50 ps rise times.
← Typical waveform, 50 ps/div, 5V/div.

At the other extreme, Model AVI-V-HV2A-B provides up to 100V with < 300 ps rise times.

| Ampl | $t_{RISE}$ | Max. PRF | Model |
|---|---|---|---|
| 100 V | 500 ps | 0.1 MHz | AVR-E3-B |
| 100 V | 300 ps | 0.02 MHz | AVI-V-HV2A-B |
| 50 V | 500 ps | 1 MHz | AVR-E5-B |
| 20 V | 200 ps | 10 MHz | AVMR-2D-B |
| 15 V | 100 ps | 25 MHz | AVM-2-C |
| 15 V | 150 ps | 200 MHz | AVN-3-C |
| 10 V | 100 ps | 1 MHz | AVP-AV-1-B |
| 10 V | 50 ps | 1 MHz | AVP-3SA-C |
| 5 V | 40 ps | 1 MHz | AVP-2SA-C |

AVTECH

Nanosecond Electronics
Since 1975

**Pricing, manuals, datasheets and test results at:**
www.avtechpulse.com/

AVTECH ELECTROSYSTEMS LTD.
Tel: +1-613-686-6675 Fax: +1-613-686-6679
info@avtechpulse.com

## Pulsed Laser Diode Drivers from Avtech

Each of the 19 models in the Avtech **AVO-9 Series** of pulsed laser diode drivers includes a replaceable output module with an ultra-high-speed socket, suitable for use with sub-nanosecond pulses.

Models with maximum pulse currents of 0.1A to 10A are available, with pulse widths from 400 ps to 1 us.

GPIB, RS-232, and Ethernet control available.

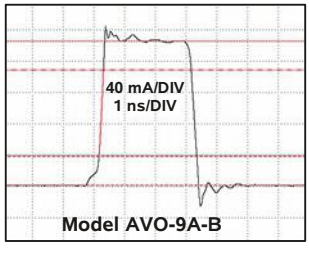


AVTECH

Nanosecond Electronics
Since 1975

**Pricing, manuals, datasheets and test results at:**
www.avtechpulse.com/laser

AVTECH ELECTROSYSTEMS LTD.
Tel: +1-613-686-6675 Fax: +1-613-686-6679
info@avtechpulse.com

## 100 to 1000 Volt Lab Pulsers

Avtech offers a full line of 100, 200, 500, 700 and 1000 Volt user-friendly pulsers capable of driving impedances of 50 Ω and higher. The **AVR Series** is suitable for semiconductor and laser diode characterization, time-of-flight applications, attenuator testing, and other applications requiring 10, 20, or 50 ns rise times, pulse widths from 100 ns to 100 us, and PRFs up to 100 kHz. GPIB & RS-232 ports are standard, VXI Ethernet is optional.

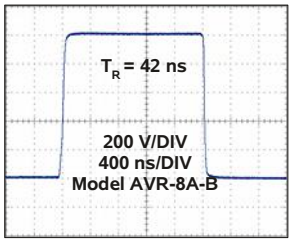


**See additional test results at:**
**http://www.avtechpulse.com/medium**

AVTECH

Nanosecond Electronics
Since 1975

**Pricing, manuals, datasheets and test results at:**
www.avtechpulse.com/medium

AVTECH ELECTROSYSTEMS LTD.
Tel: +1-613-686-6675 Fax: +1-613-686-6679
info@avtechpulse.com

# *Ultra high bandwidth Payload & RF Multipath Link Emulator*

Just released ...

Sophisticated high bandwidth (up to 600MHz) emulation of physical layer RF link effects channel modeling (delay, Doppler, AWGN, Multipath) and hardware in the loop impairments modeling (programmable Group delay, Phase noise, gain/compression distortion and non-linearity AM/AM, AM/PM simulation etc.

Comprehensive range of instruments from 72 MHz to 600 MHz bandwidth with a wide RF frequency tuning range.

Contact dBm for specifications, pricing information and demonstration/evaluation units.

- **RF physical layer Link emulation**
- **Point to Point UHF/VHF radio testing**
- **Real time control for Arial Vehicle (UAV) testing**
- **Payload and ground station emulation**
- **Multipath, 12 paths @ 600MHz BW**

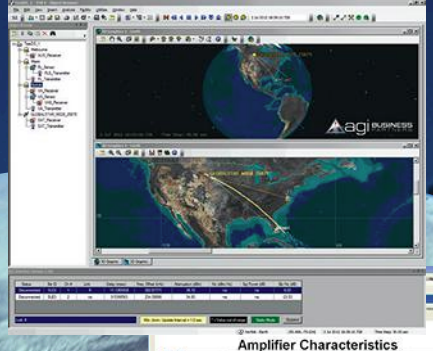


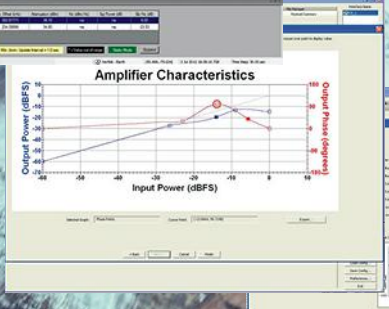


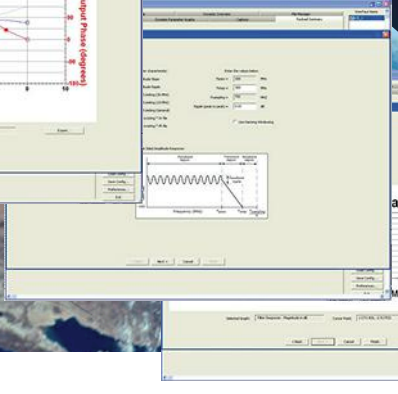

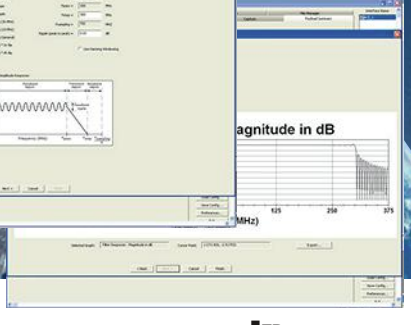

dBm

*RF Test Equipment for Wireless Communications*

**email: info@dbmcorp.com**

dBmCorp, Inc
32A Spruce Street ◆ Oakland, NJ 07436
Tel (201) 677-0008 ◆ Fax (201) 677-9444
**www.dbmcorp.com**

# RF Matters Here

## Products Being Obsoleted?
## MACOM has you covered.

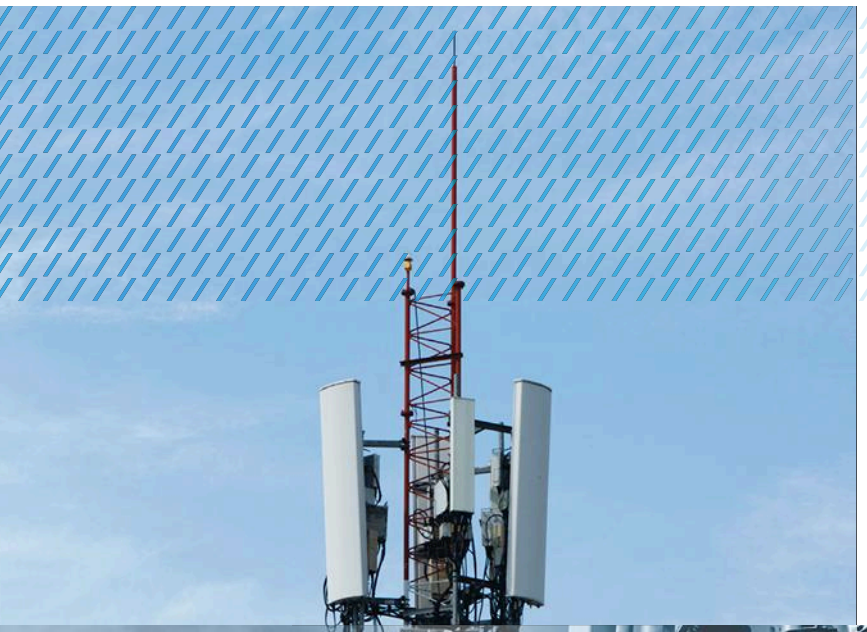

*While other suppliers are abandoning their RF customers, we remain committed to producing the best diodes, MMICs, transistors and more. Check out the MACOM Cross Reference Tool.*

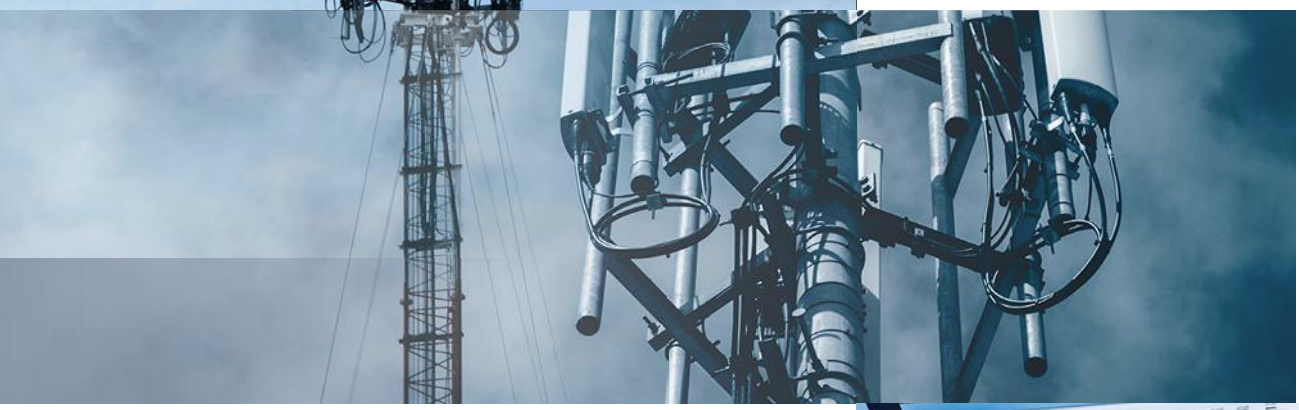

**Ka-Band 3 W Power Amplifier**
P1dB, P3dB vs. Frequency

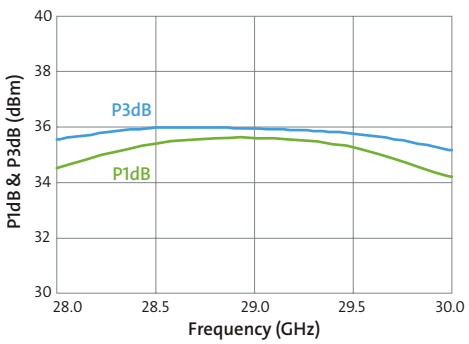


MACOM offers a family of advanced power amplifiers to meet your Ka-Band needs.

## Join the Next Generation

MACOM's 65-year legacy of innovation is driving the industry's broadest portfolio of MMICs, diodes and transistors that cover the entire RF signal chain. We deliver the engineering expertise, surety of supply and manufacturing scale to enable your most critical applications.

With our state-of-the-art technology and high-performance products, we're helping customers achieve industry-leading bandwidth, power, packaging and reliability.

Are you experiencing RF supplier obsolescence?
**Download MACOM's Cross Reference Tool at:**
**www.macom.com/home**

MACOM™

# ON MICROWAVES&RF.COM

## Are There Too Many Short-Range Wireless Standards?

Regardless of whether you agree or disagree, you're certainly not lacking for short-range wireless choices, many of which are the result of the Internet of Things. And these standards may keep on coming, according to Lou Frenzel.

*http://www.mwrf.com/community/are-there-too-many-short-range-wireless-standards*

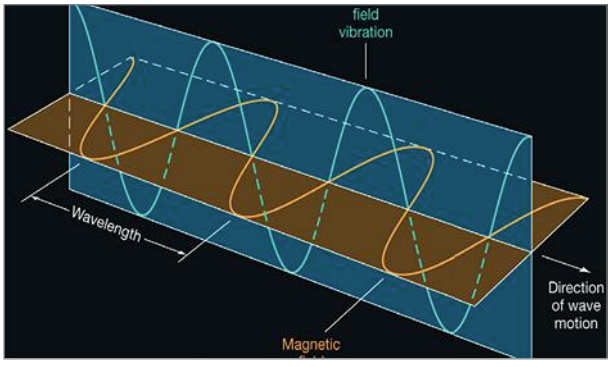


## Pursuing the Paths of EM Propagation

Propagation of electromagnetic (EM) energy, which involves a number of different paths from start to finish, makes possible many of the applications for RF/microwave signals.

*http://www.mwrf.com/systems/pursuing-paths-em-propagation*

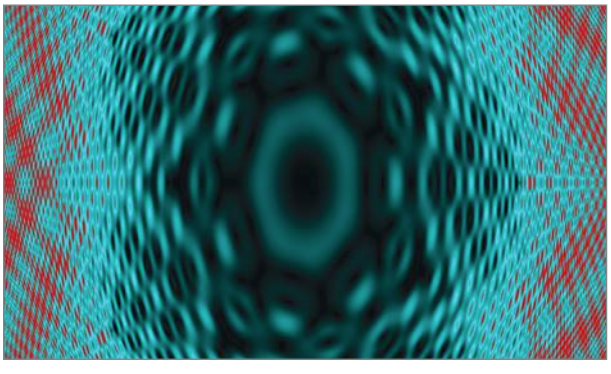

## Understanding Subarray Tradeoffs in Large Antenna Arrays

In this installment of "Algorithms to Antenna," MathWorks' Rick Gentile investigates subarrays, which allow multiple antenna elements to be mapped to specific RF channels, and the impact of model fidelity.

*http://www.mwrf.com/systems/algorithms-antenna-understanding-subarray-tradeoffs-large-antenna-arrays*

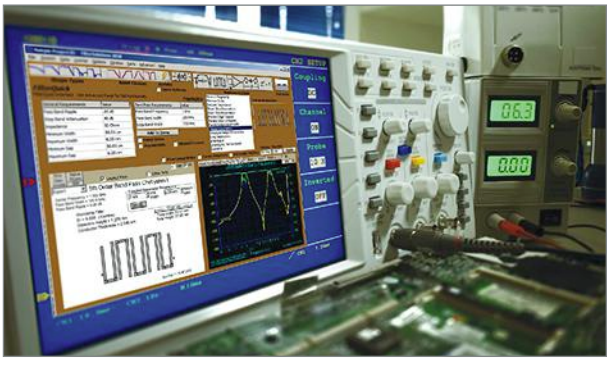

## Filters that Use Resonators with DMS Can Produce Optimal Results

Designing distributed filters that incorporate resonators with defected microstrip structures (DMSs) can help combat spurious passbands. This article explains how to efficiently design such filters with software tools.

*http://www.mwrf.com/test-measurement/get-your-hands-dirty-these-vna-tools*

twitter.com/MicrowavesRF facebook.com/microwavesrf

ANALOG DEVICES

AHEAD OF WHAT'S POSSIBLE™

# MEASURE RMS POWER TO 40GHz

## LTC5596

### IMPROVE MEASUREMENT ACCURACY & DETECTION SENSITIVITY

- RF Input 50Ω-Matched from 100MHz to 40GHz
- 35dB Log-Linear Dynamic Range to ±1dB Accuracy
- –32.6dBm Minimum Detectable Signal Sensitivity

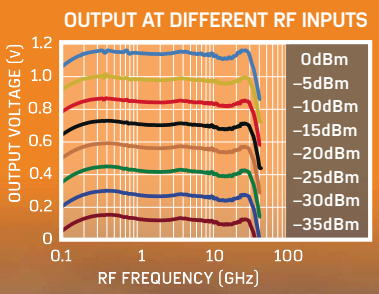


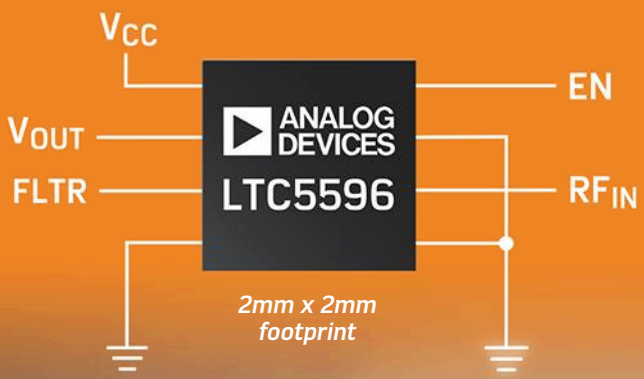


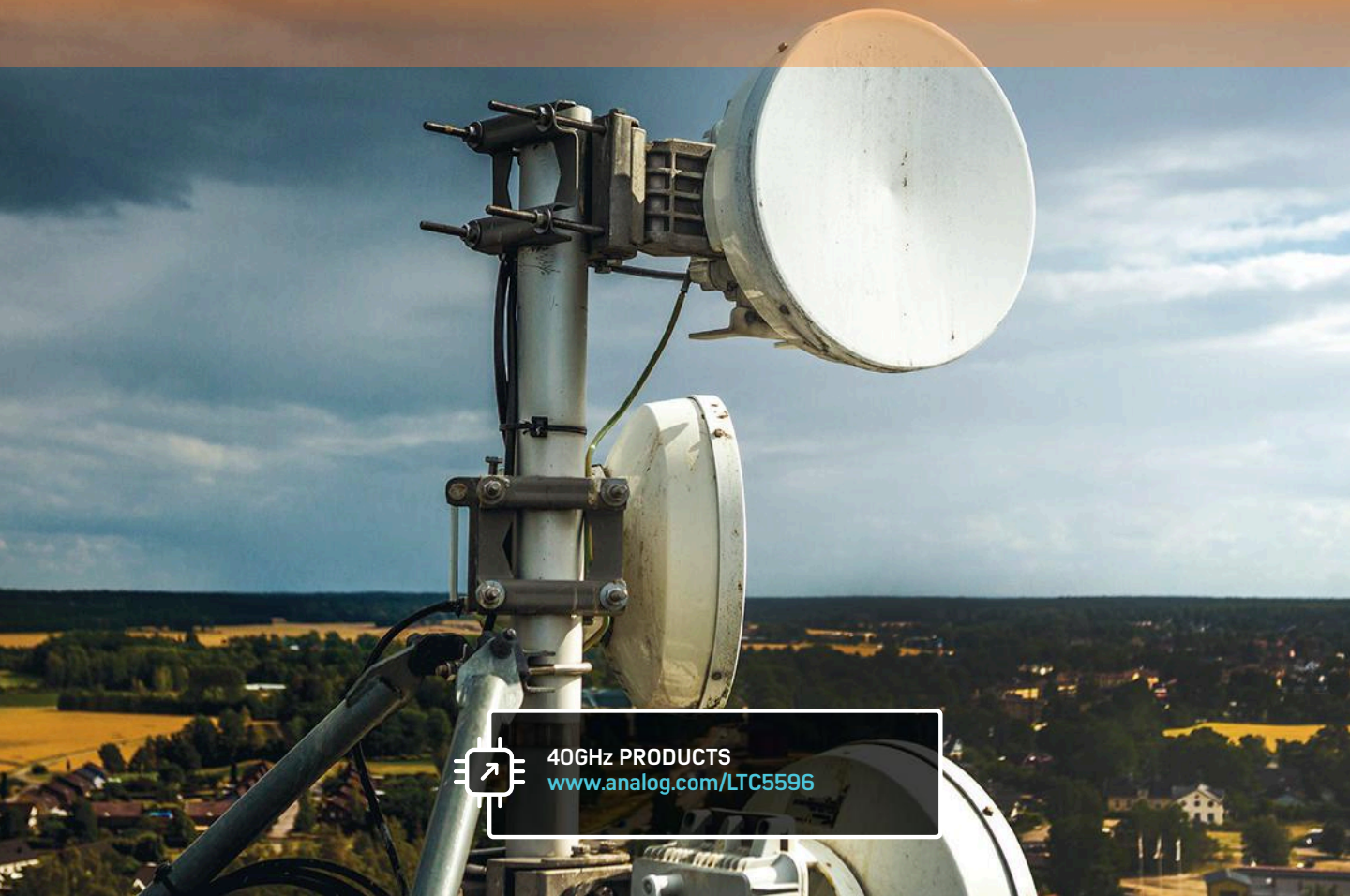

40GHz PRODUCTS
www.analog.com/LTC5596

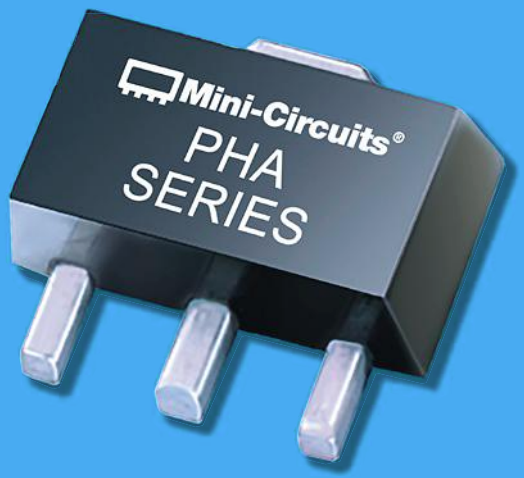


# 0.8 dB NF +45 dBm IP3

# AMPLIFIERS

## 1 MHz-2 GHz

## Stretching the Boundaries of Dynamic Range for VHF/UHF Systems

Learn more at:
**https://goo.gl/vEyVV1**

Mini-Circuits®

www.minicircuits.com (718) 934-4500 sales@minicircuits.com

574 Rev Orig_P

## Editorial

JACK BROWNE | Technical Contributor
jack.browne@informa.com

# Making the Most of Millimeter Waves

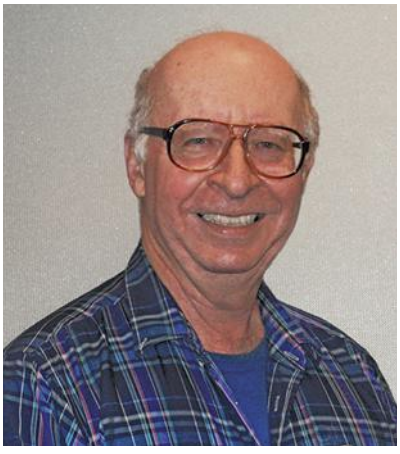

At one time, millimeter-wave (mmWave) frequencies were mainly relegated to the laboratory. They went beyond the frequency range of most test instruments and were available only in a handful of active and passive components from a small number of manufacturers. But, almost without warning, mmWave frequencies and components have become mainstream topics of conversation, largely because of highly anticipated application areas: automotive safety systems and 5G wireless technology.

Wireless networks have evolved from their humble first-generation (1G) analog beginnings based on the Advanced Mobile Phone Service (AMPS) standard to the current, quite sophisticated 4G Long Term Evolution (LTE) digital wireless standard. Already, though, LTE is being made to appear obsolete when compared to all of the services and functions that 5G will bring. Perhaps the biggest challenge facing wireless communications of any kind is that they have simply run out of bandwidth.

When commercial wireless communications went public with the AMPS system, the number of cell phones and wireless users was relatively small but growing. As the number of users grew with each new generation of wireless system, the number of functional requirements for those users also grew, from simply voice communications to adding functions such as transferring data files, high-speed Internet access, and video streaming.

Just when it appeared that 4G LTE would be the wireless network to serve all needs, it has become saturated with users. Network designers have considered the possibilities for 5G for several years, and the need for more bandwidth has turned the attention to where it's available: at mmWave frequencies.

Millimeter-wave frequencies have their share of challenges, including the small wavelengths with their short propagation distances, the significant foliage and rainfall signal attenuation, and the signal blockage cause by concrete buildings. In addition, the components for the mmWave frequency spectrum (starting at about 24 GHz) are expensive.

But for 5G to do everything that its supporters are promising, such as futuristic smartphones, connected autonomous vehicles, and Internet of Things devices everywhere that can be accessed instantly with a smartphone, bandwidth is needed. And mmWave frequencies offer that bandwidth.

The opportunities for mmWave components, test, even software developers in 5G networks are too obvious to ignore. 5G will use beamforming, MIMO, and thousands of closely spaced small cells to make mmWave technology an everyday reality. Semiconductor companies have already had a taste of the possibilities for large-volume sales of mmWave devices in the automotive radar markets. But when 5G networks are built, the demand for mmWave components and ICs will make those earlier automotive markets simply look like a wrong turn. MW

SURFACE MOUNT/DROP IN
Comb Generators from
HEROTEK

Herotek, Your Source for the Most Comprehensive Line of Comb Generators

Outline "L"

Outline "N3"

Specifications @ +25° C

| MODEL | INPUT FREQ. (MHz) | INPUT POWER (dBm) | OUTPUT FREQ (GHz) | OUTLINE |
|---|---|---|---|---|
| GC100 RL | 100 | +27 | 18 | L |
| GC200 RL | 200 | +27 | 18 | L |
| GC250 RL | 250 | +27 | 18 | L |
| GC500 RL | 500 | +27 | 18 | L |
| GC1000 RL | 1000 | +27 | 18 | L |
| GC0526 RL | 500 | +27 | 26 | L |
| GC1026 RL | 1000 | +27 | 26 | L |
| GC1526 RL | 1500 | +27 | 26 | L |
| GC2026 RL | 2000 | +27 | 26 | L |
| GCA250A N3 | 250 | 0 | 18 | N3 |
| GCA250B N3 | | +10 | | |
| GCA500A N3 | 500 | 0 | 18 | N3 |
| GCA500B N3 | | +10 | | |
| GCA1000A N3 | 1000 | 0 | 18 | N3 |
| GCA1000B N3 | | +10 | | |
| GCA0526A N3 | 500 | 0 | 26 | N3 |
| GCA0526B N3 | | +10 | | |
| GCA1026A N3 | 1000 | 0 | 26 | N3 |
| GCA1026B N3 | | +10 | | |
| GCA1526A N3 | 1500 | 0 | 26 | N3 |
| GCA1526B N3 | | +10 | | |
| GCA2026A N3 | 2000 | 0 | 26 | N3 |
| GCA2026B N3 | | +10 | | |

Note: Other input frequencies from 10 MHz to 10 GHz are available.

Herotek

The Microwave Products Source

Herotek, Inc.
155 Baytech Drive
San Jose, CA 95134
Tel: (408) 941-8399
Fax: (408) 941-8388

Made in U.S.A.

ISO 9001-2008 Certified

Website: www.herotek.com email: info@herotek.com

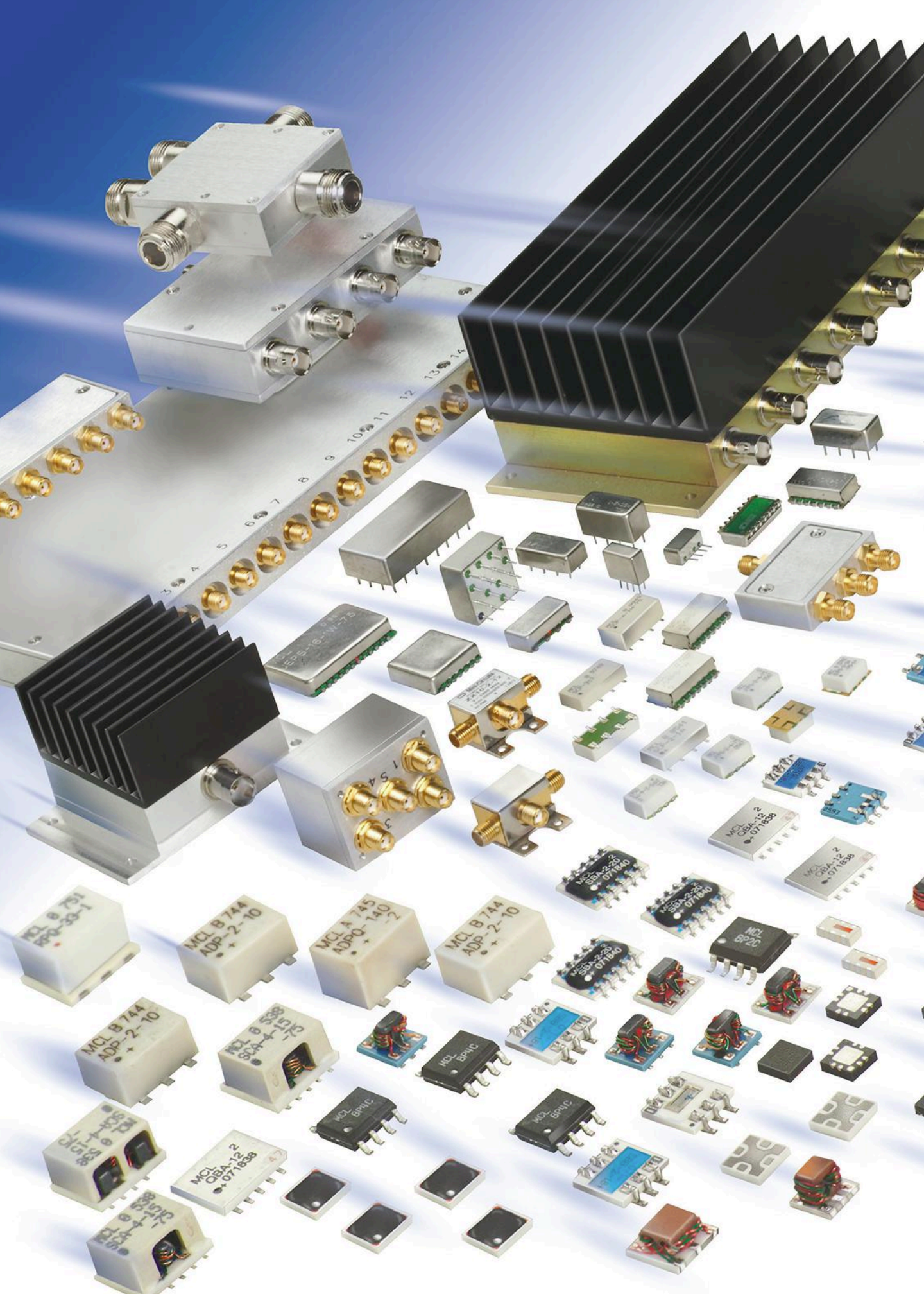

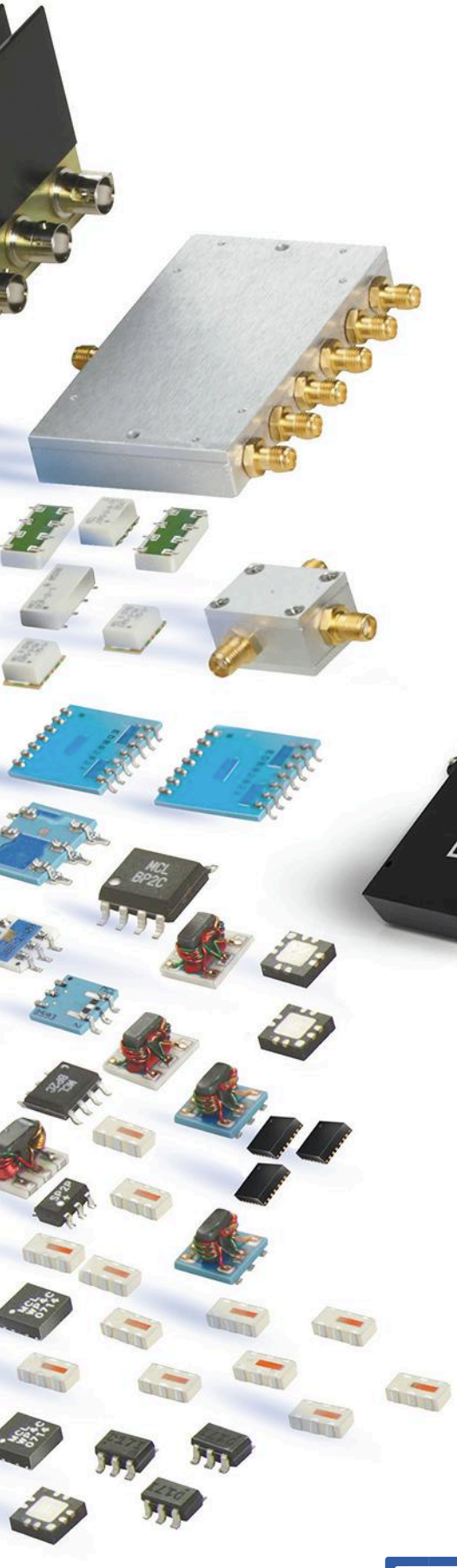

# POWER SPLITTERS/ COMBINERS

*from* **2 kHz to 40 GHz** *as low as* **89¢** *ea. (qty. 1000)*

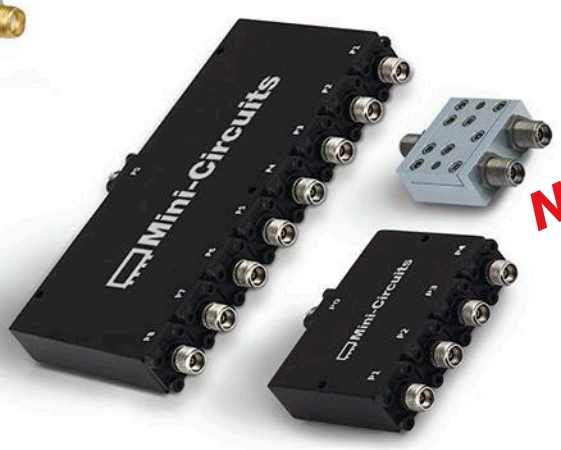


**NEW!**

***COVERING 10 to 40 GHz IN A SINGLE MODEL***

*2-WAY ZN2PD-K44+*
*4-WAY ZN4PD-K44+*
*8-WAY ZN8PD-K44+*

***The industry's largest selection includes THOUSANDS*** of models from 2 kHz to 40 GHz, with up to 300 W power handling, in coaxial, flat-pack, surface mount and rack mount housings for 50 and 75Ω systems.

***From 2-way through 48-way designs, with 0°, 90°, or 180°*** phase configurations, Mini-Circuits' power splitter/combiners offer a vast selection of features and capabilities to meet your needs from high power and low insertion loss to ultra-tiny LTCC units and much more.

***Need to find the right models fast? Visit minicircuits.com and use Yoni2®!*** It's our patented search engine that searches actual test data for the models that meet your specific requirements! You'll find test data, S-parameters, PCB layouts, pricing, real-time availability, and everything you need to make a smart decision fast!

All Mini-Circuits' catalog models are available off the shelf for immediate shipment, so check out our website today for delivery as soon as tomorrow!

***RoHS Compliant***
Product availability is listed on our website.

Mini-Circuits®

**www.minicircuits.com** P.O. Box 350166, Brooklyn, NY 11235-0003 (718) 934-4500 sales@minicircuits.com

# PIN DIODE CONTROL DEVICES

## PIN DIODE ATTENUATORS

- 0.1–20GHz
- Broad & narrow band models
- Wide dynamic range
- Custom designs

Attenuator types offered are: Current Controlled, Voltage Controlled, Linearized Voltage Controlled, Digitally Controlled and Digital Diode Attenuators.

## PIN DIODE SWITCHES

- Broad & narrow band models
- 0.1–20GHz
- Small size
- Custom designs

SPST thru SP8T and Transfer type models are offered and all switches are low loss with isolation up to 100dB. Reflective and non-reflective models are available along with TTL compatible logic inputs. Switching speeds are 1$\mu$sec.—30nsec. and SMA connectors are standard. Custom designs including special logic inputs, voltages, connectors and package styles are available. All switches meet MIL-E-5400

## PIN DIODE PHASE SHIFTERS

- 0.5-20GHz
- Switched Line
- Varactor Controlled
- Vector Modulators
- Bi-Phase Modulators
- QPSK Modulators
- Custom Designs

## SUBASSEMBLIES

Passive Components and Control Devices can be integrated into subassemblies to fit your special requirements. Call for more information and technical assistance.

**Custom Designs**

CALL OR WRITE

**waveline®** SOLID STATE INC

P.O. Box 718, West Caldwell, NJ 07006
(973) 226-9100 Fax: 973-226-1565
E-mail: wavelineinc.com



Microwaves&RF APRIL 2018

EDITORIAL

EXECUTIVE DIRECTOR, CONTENT: **KAREN FIELD** karen.field@informa.com
TECHNICAL CONTRIBUTOR: **JACK BROWNE** jack.browne@informa.com
TECHNICAL ENGINEERING EDITOR: **CHRIS DeMARTINO** chris.demartino@informa.com
ASSOCIATE EDITOR/COMMUNITY MANAGER: **ROGER ENGELKE** roger.engelke@informa.com
ASSOCIATE EDITOR/COMMUNITY MANAGER: **JEREMY COHEN** jeremy.cohen@informa.com
ASSOCIATE CONTENT PRODUCER: **JAMES MORRA** james.morra@informa.com

ART DEPARTMENT

GROUP DESIGN DIRECTOR: **ANTHONY VITOLO** tony.vitolo@informa.com
CONTENT DESIGN SPECIALIST: **JOCELYN HARTZOG** jocelyn.hartzog@informa.com
CONTENT & DESIGN PRODUCTION MANAGER: **JULIE JANTZER-WARD** julie.jantzer-ward@informa.com

PRODUCTION

GROUP PRODUCTION MANAGER: **GREG ARAUJO** greg.araujo@informa.com
PRODUCTION MANAGER: **VICKI McCARTY** vicki.mccarty@informa.com

AUDIENCE MARKETING

USER MARKETING MANAGER: **DEBBIE BRADY** debbie.brady@informa.com

**FREE SUBSCRIPTION / STATUS OF SUBSCRIPTION / ADDRESS CHANGE/ MISSING BACK ISSUES:**
OMEDA **T** | 847.513.6022 **TOLL FREE** | 866.505.7173

SALES & MARKETING

MANAGING DIRECTOR: **TRACY SMITH** **T** | 913.967.1324 **F** | 913.514.6881 tracy.smith@informa.com

REGIONAL SALES REPRESENTATIVES:

AZ, NM, TX: **GREGORY MONTGOMERY** **T** | 480.254.5540 gregory.montgomery@informa.com

AK, NORTHERN CA, OR, WA, WESTERN CANADA: **STUART BOWEN** **T** | 425.681.4395 stuart.bowen@informa.com

AL, AR, SOUTHERN CA, CO, FL, GA, HI, IA, ID, IL, IN, KS, KY, LA, MI, MN, MO, MS, MT, NC, ND, NE, NV, OH, OK, SC, SD, TN, UT, VA, WI, WV, WY, CENTRAL CANADA: **JAMIE ALLEN** **T** | 415.608.1959 **F** | 913.514.3667 jamie.allen@informa.com

CT, DE, MA, MD, ME, NH, NJ, NY, PA, RI, VT, EASTERN CANADA:
**SHANNON ALO-MENDOSA** **T** | 978.501.9116 shannon.alo-mendosa@informa.com

INTERNATIONAL SALES:

GERMANY, AUSTRIA, SWITZERLAND: **CHRISTIAN HOELSCHER** **T** | 011.49.89.95002778
christian.hoelscher@husonmedia.com

BELGIUM, NETHERLANDS, LUXEMBURG, UNITED KINGDOM, SCANDINAVIA, FRANCE, SPAIN, PORTUGAL:
**JAMES RHOADES-BROWN** **T** | +011 44 1932 564999 **M** | +011 44 1932 564998 james.rhoadesbrown@husonmedia.com

ITALY: **DIEGO CASIRAGHI** diego@casiraghi-adv.com

PAN-ASIA: **HELEN LAI** **T** | 886 2-2727 7799 helen@twoway-com.com

PAN-ASIA: **CHARLES LIU** **T** | 886 2-2727 7799 liu@twoway-com.com

PLEASE SEND INSERTION ORDERS TO: orders@informa.com

INFORMA REPRINTS: **WRIGHT'S MEDIA** **T** | 877.652.5295

LIST RENTALS/ SMARTREACH CLIENT SERVICES MANAGER: **MARY RALICKI** **T** | 212.204.4284
mary.ralicki@informa.com

DIGITAL

GROUP DIGITAL DIRECTOR: **RYAN MALEC** ryan.malec@informa.com
CLIENT SUPPORT MANAGER: **KIM BLASKI** kim.blaski@informa.com

DESIGN ENGINEERING & SOURCING GROUP

EXECUTIVE DIRECTOR, CONTENT: **KAREN FIELD** karen.field@informa.com
VP OF MARKETING: **JACQUIE NIEMIEC** jacquie.niemiec@informa.com

INFORMA MEDIA INC.

1166 AVENUE OF THE AMERICAS, 10TH FLOOR
NEW YORK, NY 10036 **T** | 212.204.4200

informa

Electronic Design | Machine Design | Microwaves & RF | Source ESB | Hydraulics & Pneumatics | Global Purchasing | Distribution Resource | Power Electronics | Defense Electronics

# RF Amplifiers and Sub-Assemblies for Every Application

## Delivery from Stock to 2 Weeks ARO from the catalog or built to your specifications!

- Competitive Pricing & Fast Delivery
- Military Reliability & Qualification
- Various Options: Temperature Compensation, Input Limiter Protection, Detectors/TTL & More
- Unconditionally Stable (100% tested)

ISO 9001:2000 and AS9100B CERTIFIED

### OCTAVE BAND LOW NOISE AMPLIFIERS

| Model No. | Freq (GHz) | Gain (dB) MIN | Noise Figure (dB) | Power-out @ P1-dB | 3rd Order ICP | VSWR |
|---|---|---|---|---|---|---|
| CA01-2110 | 0.5-1.0 | 28 | 1.0 MAX, 0.7 TYP | +10 MIN | +20 dBm | 2.0:1 |
| CA12-2110 | 1.0-2.0 | 30 | 1.0 MAX, 0.7 TYP | +10 MIN | +20 dBm | 2.0:1 |
| CA24-2111 | 2.0-4.0 | 29 | 1.1 MAX, 0.95 TYP | +10 MIN | +20 dBm | 2.0:1 |
| CA48-2111 | 4.0-8.0 | 29 | 1.3 MAX, 1.0 TYP | +10 MIN | +20 dBm | 2.0:1 |
| CA812-3111 | 8.0-12.0 | 27 | 1.6 MAX, 1.4 TYP | +10 MIN | +20 dBm | 2.0:1 |
| CA1218-4111 | 12.0-18.0 | 25 | 1.9 MAX, 1.7 TYP | +10 MIN | +20 dBm | 2.0:1 |
| CA1826-2110 | 18.0-26.5 | 32 | 3.0 MAX, 2.5 TYP | +10 MIN | +20 dBm | 2.0:1 |

### NARROW BAND LOW NOISE AND MEDIUM POWER AMPLIFIERS

| Model No. | Freq (GHz) | Gain (dB) MIN | Noise Figure (dB) | Power-out @ P1-dB | 3rd Order ICP | VSWR |
|---|---|---|---|---|---|---|
| CA01-2111 | 0.4 - 0.5 | 28 | 0.6 MAX, 0.4 TYP | +10 MIN | +20 dBm | 2.0:1 |
| CA01-2113 | 0.8 - 1.0 | 28 | 0.6 MAX, 0.4 TYP | +10 MIN | +20 dBm | 2.0:1 |
| CA12-3117 | 1.2 - 1.6 | 25 | 0.6 MAX, 0.4 TYP | +10 MIN | +20 dBm | 2.0:1 |
| CA23-3111 | 2.2 - 2.4 | 30 | 0.6 MAX, 0.45 TYP | +10 MIN | +20 dBm | 2.0:1 |
| CA23-3116 | 2.7 - 2.9 | 29 | 0.7 MAX, 0.5 TYP | +10 MIN | +20 dBm | 2.0:1 |
| CA34-2110 | 3.7 - 4.2 | 28 | 1.0 MAX, 0.5 TYP | +10 MIN | +20 dBm | 2.0:1 |
| CA56-3110 | 5.4 - 5.9 | 40 | 1.0 MAX, 0.5 TYP | +10 MIN | +20 dBm | 2.0:1 |
| CA78-4110 | 7.25 - 7.75 | 32 | 1.2 MAX, 1.0 TYP | +10 MIN | +20 dBm | 2.0:1 |
| CA910-3110 | 9.0 - 10.6 | 25 | 1.4 MAX, 1.2 TYP | +10 MIN | +20 dBm | 2.0:1 |
| CA1315-3110 | 13.75 - 15.4 | 25 | 1.6 MAX, 1.4 TYP | +10 MIN | +20 dBm | 2.0:1 |
| CA12-3114 | 1.35 - 1.85 | 30 | 4.0 MAX, 3.0 TYP | +33 MIN | +41 dBm | 2.0:1 |
| CA34-6116 | 3.1 - 3.5 | 40 | 4.5 MAX, 3.5 TYP | +35 MIN | +43 dBm | 2.0:1 |
| CA56-5114 | 5.9 - 6.4 | 30 | 5.0 MAX, 4.0 TYP | +30 MIN | +40 dBm | 2.0:1 |
| CA812-6115 | 8.0 - 12.0 | 30 | 4.5 MAX, 3.5 TYP | +30 MIN | +40 dBm | 2.0:1 |
| CA812-6116 | 8.0 - 12.0 | 30 | 5.0 MAX, 4.0 TYP | +33 MIN | +41 dBm | 2.0:1 |
| CA1213-7110 | 12.2 - 13.25 | 28 | 6.0 MAX, 5.5 TYP | +33 MIN | +42 dBm | 2.0:1 |
| CA1415-7110 | 14.0 - 15.0 | 30 | 5.0 MAX, 4.0 TYP | +30 MIN | +40 dBm | 2.0:1 |
| CA1722-4110 | 17.0 - 22.0 | 25 | 3.5 MAX, 2.8 TYP | +21 MIN | +31 dBm | 2.0:1 |

### ULTRA-BROADBAND & MULTI-OCTAVE BAND AMPLIFIERS

| Model No. | Freq (GHz) | Gain (dB) MIN | Noise Figure (dB) | Power-out @ P1-dB | 3rd Order ICP | VSWR |
|---|---|---|---|---|---|---|
| CA0102-3111 | 0.1-2.0 | 28 | 1.6 Max, 1.2 TYP | +10 MIN | +20 dBm | 2.0:1 |
| CA0106-3111 | 0.1-6.0 | 28 | 1.9 Max, 1.5 TYP | +10 MIN | +20 dBm | 2.0:1 |
| CA0108-3110 | 0.1-8.0 | 26 | 2.2 Max, 1.8 TYP | +10 MIN | +20 dBm | 2.0:1 |
| CA0108-4112 | 0.1-8.0 | 32 | 3.0 MAX, 1.8 TYP | +22 MIN | +32 dBm | 2.0:1 |
| CA02-3112 | 0.5-2.0 | 36 | 4.5 MAX, 2.5 TYP | +30 MIN | +40 dBm | 2.0:1 |
| CA26-3110 | 2.0-6.0 | 26 | 2.0 MAX, 1.5 TYP | +10 MIN | +20 dBm | 2.0:1 |
| CA26-4114 | 2.0-6.0 | 22 | 5.0 MAX, 3.5 TYP | +30 MIN | +40 dBm | 2.0:1 |
| CA618-4112 | 6.0-18.0 | 25 | 5.0 MAX, 3.5 TYP | +23 MIN | +33 dBm | 2.0:1 |
| CA618-6114 | 6.0-18.0 | 35 | 5.0 MAX, 3.5 TYP | +30 MIN | +40 dBm | 2.0:1 |
| CA218-4116 | 2.0-18.0 | 30 | 3.5 MAX, 2.8 TYP | +10 MIN | +20 dBm | 2.0:1 |
| CA218-4110 | 2.0-18.0 | 30 | 5.0 MAX, 3.5 TYP | +20 MIN | +30 dBm | 2.0:1 |
| CA218-4112 | 2.0-18.0 | 29 | 5.0 MAX, 3.5 TYP | +24 MIN | +34 dBm | 2.0:1 |

### LIMITING AMPLIFIERS

| Model No. | Freq (GHz) | Input Dynamic Range | Output Power Range Psat | Power Flatness dB | VSWR |
|---|---|---|---|---|---|
| CLA24-4001 | 2.0 - 4.0 | -28 to +10 dBm | +7 to +11 dBm | +/- 1.5 MAX | 2.0:1 |
| CLA26-8001 | 2.0 - 6.0 | -50 to +20 dBm | +14 to +18 dBm | +/- 1.5 MAX | 2.0:1 |
| CLA712-5001 | 7.0 - 12.4 | -21 to +10 dBm | +14 to +19 dBm | +/- 1.5 MAX | 2.0:1 |
| CLA618-1201 | 6.0 - 18.0 | -50 to +20 dBm | +14 to +19 dBm | +/- 1.5 MAX | 2.0:1 |

### AMPLIFIERS WITH INTEGRATED GAIN ATTENUATION

| Model No. | Freq (GHz) | Gain (dB) MIN | Noise Figure (dB) | Power-out @ P1-dB | Gain Attenuation Range | VSWR |
|---|---|---|---|---|---|---|
| CA001-2511A | 0.025-0.150 | 21 | 5.0 MAX, 3.5 TYP | +12 MIN | 30 dB MIN | 2.0:1 |
| CA05-3110A | 0.5-5.5 | 23 | 2.5 MAX, 1.5 TYP | +18 MIN | 20 dB MIN | 2.0:1 |
| CA56-3110A | 5.85-6.425 | 28 | 2.5 MAX, 1.5 TYP | +16 MIN | 22 dB MIN | 1.8:1 |
| CA612-4110A | 6.0-12.0 | 24 | 2.5 MAX, 1.5 TYP | +12 MIN | 15 dB MIN | 1.9:1 |
| CA1315-4110A | 13.75-15.4 | 25 | 2.2 MAX, 1.6 TYP | +16 MIN | 20 dB MIN | 1.8:1 |
| CA1518-4110A | 15.0-18.0 | 30 | 3.0 MAX, 2.0 TYP | +18 MIN | 20 dB MIN | 1.85:1 |

### LOW FREQUENCY AMPLIFIERS

| Model No. | Freq (GHz) | Gain (dB) MIN | Noise Figure dB | Power-out @ P1-dB | 3rd Order ICP | VSWR |
|---|---|---|---|---|---|---|
| CA001-2110 | 0.01-0.10 | 18 | 4.0 MAX, 2.2 TYP | +10 MIN | +20 dBm | 2.0:1 |
| CA001-2211 | 0.04-0.15 | 24 | 3.5 MAX, 2.2 TYP | +13 MIN | +23 dBm | 2.0:1 |
| CA001-2215 | 0.04-0.15 | 23 | 4.0 MAX, 2.2 TYP | +23 MIN | +33 dBm | 2.0:1 |
| CA001-3113 | 0.01-1.0 | 28 | 4.0 MAX, 2.8 TYP | +17 MIN | +27 dBm | 2.0:1 |
| CA002-3114 | 0.01-2.0 | 27 | 4.0 MAX, 2.8 TYP | +20 MIN | +30 dBm | 2.0:1 |
| CA003-3116 | 0.01-3.0 | 18 | 4.0 MAX, 2.8 TYP | +25 MIN | +35 dBm | 2.0:1 |
| CA004-3112 | 0.01-4.0 | 32 | 4.0 MAX, 2.8 TYP | +15 MIN | +25 dBm | 2.0:1 |

CIAO Wireless can easily modify any of its standard models to meet your "exact" requirements at the Catalog Pricing.

**Visit our web site at www.ciaowireless.com for our complete product offering.**

**Ciao Wireless, Inc.** 4000 Via Pescador, Camarillo, CA 93012

**Tel (805) 389-3224 Fax (805) 389-3629 sales@ciaowireless.com**

# News

# The Wireless World Converges at Mobile World Congress 2018

Barcelona, Spain became the focus of the mobile world once again as players from every part of the mobile/wireless ecosystem converged for the world's largest mobile communications conference. The annual Mobile World Congress (MWC) provides companies large and small the opportunity to compete for the attention of potential customers, prospective partners, and media from around the world.

With almost every player in the wireless world—with the notable exception of Apple—promoting their vision of the mobile future, it presents a valuable opportunity to assess the status of the industry and analyze the promise and problems on the path forward.

Why is the MWC so important? First, the products, components, and services presented at the event represent a major share of the world electronics, services, and media markets. Wireless communications capability is reshaping almost every category of electronics product today. If only the most obvious products with wireless capability such as smartphones, tablets, smart watches, etc. are counted, the wireless market accounted for 23% of all electronic equipment revenues in 2017.

An even larger impact is seen in the electronics components world, as semiconductors sold into wireless products drove roughly 31% of all semiconductor revenue in 2017. On the services and content side of the equation, as wireless offerings are reshaping consumer purchasing patterns, service provider and content/media generator strategies are driven by their vision of the wireless future.

The Mobile World Congress organizers had defined eight core event themes that illustrate the comprehensive reach and impact of wireless technology and products:

- The Fourth Industrial Revolution
- Future Services Provider
- The Network
- The Digital Consumer
- Tech in Society
- Content & Media
- Applied AI
- Innovation

The 2018 MWC presented some critical, high-profile issues for participants in the electronics components industry to follow as they develop future strategies for product development and supply chain management.

## SMARTPHONE INTRODUCTIONS—CAN THEY DRIVE FUTURE GROWTH?

The headlines leading up to MWC 2018 were dominated, as always, by the latest smartphone introductions. The world's smartphone market share leader, Samsung, illustrated most of the key technology trends at the conference this year with the introduction of its Galaxy S9 and S9 Plus smartphones. The S9 has a very similar look to the S8, with the most notable improvements coming in its new dual aperture camera that allows improved images in low-light settings and slo-mo video recording at 960 frames per second.

In addition, the S9 unveils Samsung's form of augmented reality (AR), AR Emoji, to compete with that of Apple's iPhone X. The new smartphone will receive a boost from Qualcomm's Snapdragon 845 chipset in the U.S. and the Samsung Exynos 9810 in other markets. Other changes are found in the positioning of the fingerprint sensor and the bezel size. Interestingly, a great deal of attention was devoted to the fact that it still includes an audio jack when many other phones are eliminating the audio jack to achieve size reductions in the phone. Finally, the phone will boost the latest Android OS, Oreo.

Stepping back from the details in Samsung's latest smartphone announcement, an overall assessment yields the impression that this phone is an incremental step forward rather than a significant innovation in the company's platform. Most smartphone players seem to be in a similar mode, with modest enhancements mainly focused around cameras, artificial intelligence, augmented reality, and additional processing power.

Some companies have chosen to not compete with Samsung in the same venue and will hold off on major new product announcements until later in the year. A list of some of the most notable smartphone introductions are below. However, the primary question that presents itself after reviewing the latest smartphone products is, "Are these smartphones able to drive future growth in the market?"

- Samsung Galaxy S9 and S9 Plus
- Nokia 8 Sirocco
- Nokia 8110
- LG V30S ThinQ
- Sony Xperia X72 and X72 Compact
- ZTE Tempo Go
- Vivo Apex

The concern over market growth emerged when Gartner Group announced that smartphone sales declined year-over-year in Q4 2017 by 5.6% for the first time. THose sales fell from 432 million units in Q4 2016 to 408 million units in Q4 2017. Gartner Group attributed the decline in sales to the fact that upgrades from feature phones to smartphones have slowed dramatically while the upgrade cycle for smartphone owners has been extended.

Prior to the era of the smartphone, the mobile industry experienced its first-ever decline in mobile handset sales in 2001. After years of high double-digit growth, sales of mobile phones declined by 1.6% between 2000 and 2001. While many reasons were given for this decline, the hard truth is that mobile phone products in 2001 did not offer compelling features to consumers that would motivate them to upgrade to a new phone. This same issue now confronts smartphone suppliers.

Will product enhancements that appear to be incremental in nature motivate consumers to purchase new phones, or will they choose to extend the use of their current phone until more innovative, "must-have" features are introduced? All participants in the supply chain for smartphones will need to carefully monitor the balance between market sell-through and production run-rates and inventories of phones and components.

## 5G TECHNOLOGIES, STANDARDS AND PRODUCTS—THE BRIGHT HOPE FOR THE FUTURE

Events leading up to MWC 2018 and the conference itself provided evidence of encouraging momentum in the creation of a 5G future. 5G technology forms one of the three key pillars in the technology triumvirate, including the Cloud and the Internet of Things, that will drive a revolutionary wave of products that will reshape the world of electronics. The timelines for the development of these technologies continues to show these technologies reaching mutual maturation for enabling new products/markets between 2020 and 2022.

The recently-concluded Winter Olympics in Pyeongchang, South Korea presented an opportunity for many carriers and equipment vendors to showcase their 5G technologies. Some of the notable participants in this showcase were KT Corp and Intel. These "pre-commercial" 5G products provided an exciting proof of concept for 5G technology and were also exhibited at MWC 2018. In addition, other important players introduced the latest incarnations of their 5G products.

Events leading up to MWC 2018 and the conference itself provided evidence of encouraging momentum in the creation of a 5G future. 5G technology forms one of the three key pillars in the technology triumvirate, including the Cloud and the Internet of Things, that will drive a revolutionary wave of products that will reshape the world of electronics.

| Freq. Range (GHz) | Insertion Loss (dB) max. | VSWR (dB) max. | Least Significant Bit | Operating Power (max) | Model Number |
|---|---|---|---|---|---|
| **Digitally Controlled Analog Attenuators, 64 dB, 8 Bits** | | | | | |
| 4.00-8.00 | 6.0 | 2.00:1 | 0.25 | <= 0 dBm | DAT-19 |
| 8.0-12.40 | 6.0 | 2.00:1 | 0.25 | <= 0 dBm | DAT-21 |
| 6.0-16.00 | 6.0 | 2.00:1 | 0.25 | <= 0 dBm | DAT-23 |
| 6.0-18.00 | 6.5 | 2.00:1 | 0.25 | <= 0 dBm | DAT-25 |
| **Linear Voltage Controlled Analog Attenuators, 64 dB** | | | | | |
| 4.0-8.0 | 5.0 | 1.9 | -- | <= 0 dBm | AAT-25 |
| 8.0-12.4 | 5.0 | 2.0 | -- | <= 0 dBm | AAT-27 |
| 6.0-16.0 | 5.0 | 2.0 | -- | <= 0 dBm | AAT-29 |
| **Switched Bit Digital Attenuators, 64 dB, 8 Bits** | | | | | |
| 0.50-1.00 | 3.7 | 2.00:1 | 0.25 | + 20 dBm | DAT-16 |
| 1.00-2.00 | 4.0 | 2.00:1 | 0.25 | + 20 dBm | DAT-17 |
| 2.00-4.00 | 6.5 | 2.00:1 | 0.25 | + 20 dBm | DAT-18 |
| **Switched Bit Digital Phase Shifters, 360°, 8 bits** | | | | | |
| 0.50-1.00 | 4.5 | 1.80:1 | 1.40 | + 20 dBm | DST-11 |
| 1.00-2.00 | 4.5 | 1.80:1 | 1.40 | + 20 dBm | DST-12 |
| 2.00-4.00 | 6.0 | 1.80:1 | 1.40 | + 20 dBm | DST-13 |

See website for complete list of 32 dB and 64 dB attenuators and phase shifters.

PULSAR
MICROWAVE CORPORATION

www.pulsarmicrowave.com

48 Industrial West, Clifton, NJ 07012 | Tel: 973-779-6262 · Fax: 973-779-2727 | sales@pulsarmicrowave.com


While Intel is preparing to capitalize on the market transition to 5G to try to capture opportunities missed in the wireless chipset market to date, Qualcomm and Huawei are also pushing their chipset solutions forward. In November, Intel announced its 5G modem, the XMM 8060. Also, prior to MWC, Qualcomm introduced the Snapdragon X24 chip designed to work with its X50 modem.

Huawei introduced its first 5G chip at MWC, the Balong 5G01. The size of the Huawei chip would seem to indicate it will be used in mobile hotspots instead of phones. Huawei states that it has invested $600 million in the network technology, which will likely be used by everything from self-driving cars to mobile devices to smart homes. All three players are creating partnerships and developing ecosystems designed to give them a competitive advantage in 5G.

Qualcomm test modeled real-world conditions in San Francisco and Frankfurt to set expectations for the speeds that could be achieved with 5G NR (New Radio) networks. The basic network test in the Frankfurt trial compared speeds between a gigabit-LTE network and 5G. In this case, browsing jumped from 56 Mbps for the median 4G user to more than 490 Mbps for the median 5G user, with roughly seven times faster response rates for browsing. Download speeds also improved dramatically, with more than 90% of users seeing at least 100 Mbps download speeds on 5G, vs. 8 Mbps on LTE. The results from the San Francisco trial were even more impressive.

# Ultra-Wideband MMIC SPLITTER/COMBINERS

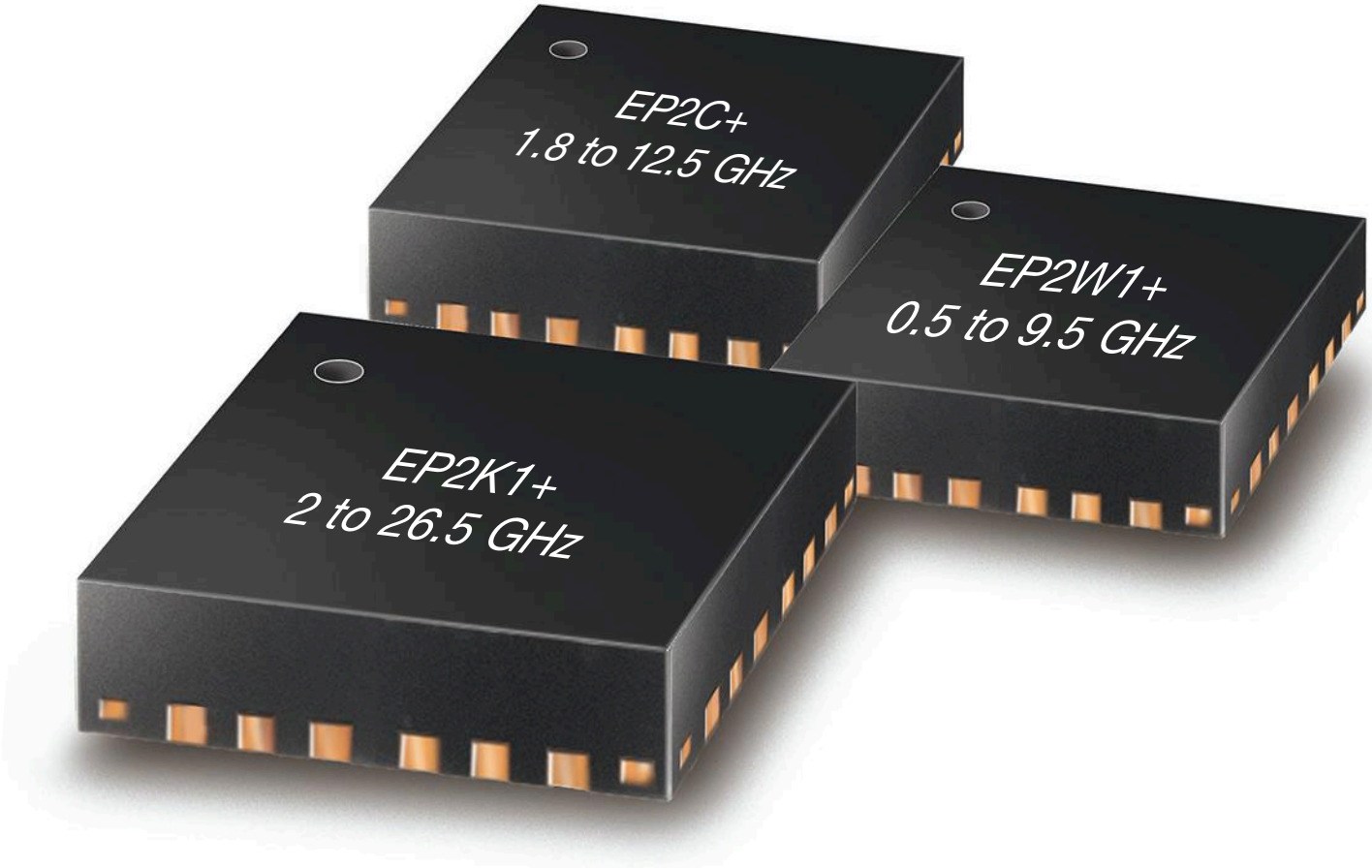


*Single Unit Coverage as Wide as* **2 to 26.5 GHz**

*Models from* $5.56 *ea. (qty. 1000)*

## THE WIDEST BANDWIDTH IN THE INDUSTRY IN A SINGLE MODEL!

Our new EP-series ultra-wideband MMIC splitter/combiners are perfect for wide-band systems like defense, instrumentation, and all cellular bands through LTE and WiFi. These models deliver consistent performance across the whole range, so you can reduce component counts on your bill of materials by using one part instead of many! They utilize GaAs IPD technology to achieve industry-leading performance, high power handling capability and efficient heat dissipation in a tiny device size, giving you a new level of capability and the flexibility to use them almost anywhere on your PCB! They're available off the shelf, so place your order on minicircuits.com today, and have them in hand as soon as tomorrow!

- Series coverage from 0.5 to 26.5 GHz
- Power handling up to 2.5W
- Insertion loss, 1.1 dB typ.
- Isolation, 20 dB typ.
- Low phase and amplitude unbalance
- DC passing up to 1.2A

EP2K-Series, 4x4x1mm
EP2W-Series, 5x5x1mm

Mini-Circuits®

www.minicircuits.com P.O. Box 350166, Brooklyn, NY 11235-0003 (718) 934-4500 sales@minicircuits.com 549 Rev B

Broadest Selection of In-Stock RF Switches

PIN Diode

Waveguide

USB Controlled

Electromechanical

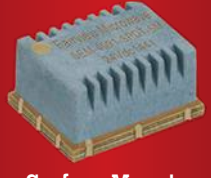

Surface Mount

- Coaxial, Waveguide and Surface Mount options available
- SPST thru SP12T and Transfer configurations
- Frequencies from 10 MHz to 110 GHz
- All in-stock and ship same-day

Fairview Microwave
RF COMPONENTS ON DEMAND. Done!



All players are working to push 5G forward as fast as they can. Networking companies like Huawei, Cisco, Ericsson, and Nokia are aggressively developing their product portfolios and partnerships. Meanwhile, major telecom operators are accelerating their timelines for introducing 5G networks. However, all players will see their race to a true commercial market paced by the development of the required standards.

The 3GPP organization is driving the 5G standard. Release 15 of the standard provides specifications for the radios for 5G and was recently approved. However, it is not due for completion until September 2018. Release 16 is the final standard for 5G and is scheduled for finalization in December 2019. Prior to the finalization of these standards, any products introduced to the market would be considered "pre-commercial."

Other critical issues being addressed at MWC related to enabling 5G include the creation of a friendly investment environment; regulatory issues; licensing terms and spectrum costs; possible public shared networks; net neutrality; potential societal benefits contrasted with possible social pushback due to technophobia; and the "digital dominance" of tech giants Facebook, Amazon, Apple, Netflix, and Google. ■

GSMA MOBILE WORLD CONGRESS

## ANALOG DEVICES Acquires Symeo to Make Positioning Radar More Precise

**ANALOG DEVICES ANNOUNCED** that it would acquire Siemens' spinout Symeo as it attempts to push higher performance and higher precision radar systems into the fast growing industrial and automotive sectors. The terms of the transaction were not disclosed.

Symeo, which has developed signal processing algorithms and radar systems that can be used to monitor forklifts driving around factory floors or buses entering a transportation depot, will join the Autonomous Transportation and Safety business unit of Analog Devices. The division is responsible for the company's 24 GHz and 77 GHz radar.

Chris Jacobs, vice president of the Autonomous Transportation and Safety business unit, said in a statement that the combination of the company's existing products and "Symeo's system and algorithm expertise will pave the way for higher performance radar solutions, enabling more accurate sensing in autonomous systems."

Symeo's local positioning radar was developed by Siemens for both indoor and outdoor applications over a decade ago. The 5.8 GHz radar technology provides between two and seven inches of accuracy and is unaffected by precipitation, dirt and grime, dust, vibrations or sunlight, according to the Munich, Germany-based company.

Symeo has also designed proprietary sensor fusion algorithms to crosscheck the radar technology with global positioning system data from GNSS and GPS satellites. The company has also developed embedded software to work with its sensors as well as a software platform for monitoring automated industrial cranes.

Analog Devices has been trying to ride revenue growth in its industrial business. Last month, the company said that it had generated about $743 million from sales of industrial products in the first quarter, representing 49 percent of its $1.52 billion revenue total. The business was 87% higher than the same quarter last year, partly because of its acquisition of Linear Technology.

Other companies are targeting so-called three-dimensional radar at the industrial market. Vayyar Imaging, based outside of Tel Aviv, Israel, recently closed a $45 million funding round to develop the high-resolution radar technology for taking stock of a car's immediate surroundings and mapping the interior of factories. ■

# The Right RF Parts. Right Away.

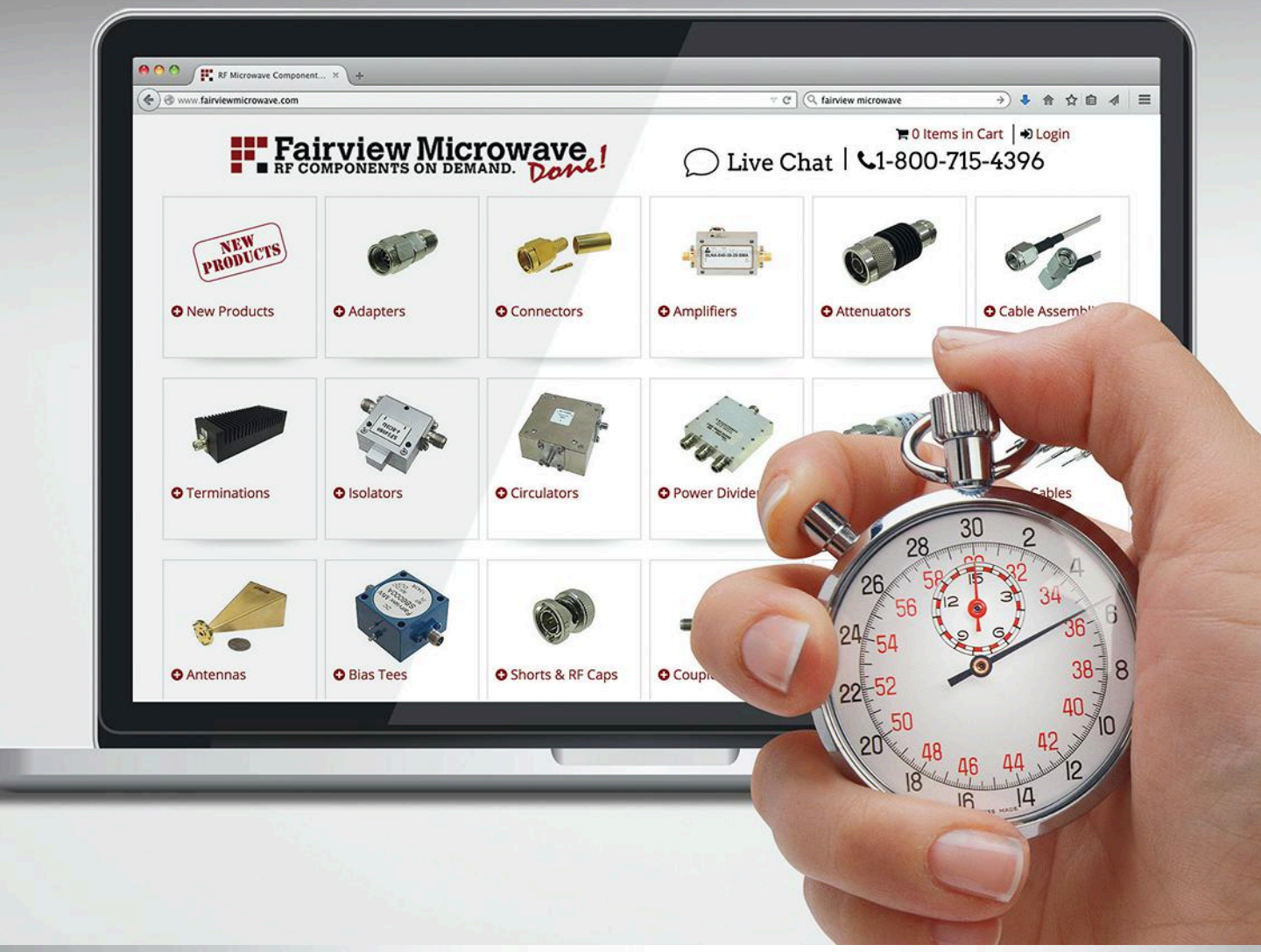


We're RF On Demand, with over one million RF and microwave components in stock and ready to ship. You can count on us to stock the RF parts you need and reliably ship them when you need them. Add Fairview Microwave to your team and consider it done.

fairviewmicrowave.com
1.800.715.4396

Fairview Microwave
RF COMPONENTS ON DEMAND. Done!

# INDENTED ARRAYS BOOST Full-Duplex Systems

The growing use of simultaneous transmission and reception (STAR) in full-duplex communications is literally putting the heat on some of the antennas in these systems, since signal leakage from the transmit antennas can double as interference for the receive antennas. Suppression or rejection of such transmit-antenna leakage can be challenging, leading some designers to explore the use of indented antenna arrays in full-duplex communications systems. The basic idea is to break the symmetry between the transmit and receive signal paths by indenting the antenna elements, thus creating an antenna aperture that is curved and less likely to cause self-interference.

The use of STAR signals within the same frequency band has often been the operating approach of continuous-wave (CW) radar systems and it is increasingly being used in full-duplex communications systems. The approach eliminates the need to separate the frequency spectrum into two different functional portions (while also eliminating the need for a diplexer to do the spectral separating) and clears the way for programmable use of different portions of the active frequency spectrum, such as by means of a software-defined-radio (SDR) communications systems approach.

To explore the effectiveness of indented antenna arrays in STAR full-duplex communications systems, researchers from the University of California at Los Angeles examined the design of a four-element standalone indented antenna array and compared its performance to a conventional antenna array operating in the approximate frequency range of 3.2 to 3.4 GHz. When making measurements at about 3.35 GHz, they found more than 15-dB improvement in return loss for the indented antenna array compared to the conventional antenna array, with much improved isolation between the transmit and receive functions for the antenna array operating within the same frequency band.

The researchers explored a number of different designs to improve transmit and receive isolation, including a standalone indented antenna array, a monostatic indented antenna array with distributed circulators, and a stacked bistatic indented antenna array. The radiation pattern of the standalone indented configuration was measured and confirmed as unchanged compared to a conventional antenna array, with dramatic improvement in transmit-to-receive isolation. In the monostatic indented array with distributed circulators, the circulators are placed after each antenna element to separate the transmit and receive paths, with that isolation limited by the leakage of the circulator. In the stacked bistatic indented antenna array, where transceivers use transmit and receive antennas, the isolation is limited only by mutual coupling between transmit and receive antennas.

The researchers performed experiments with a four-element quasi-Yagi antenna array operating from 3.2 to 3.4 GHz. Results include a 13-dB improvement in return loss of a single array; 15-dB transmit/receive isolation improvement in a monostatic array (including circulators); and a 20-dB transmit/receive isolation improvement for a bistatic array without circulators. Through the use of a standalone indented antenna array, the symmetry between transmitting and receiving paths can be disrupted by indenting the antenna elements. This achieves respectable isolation between transmission and reception without additional antenna elements or passive components, such as circulators

See "Indented Antenna Arrays for High Isolation," *IEEE Antennas & Propagation Magazine*, Vol. 60, No. 1, February 2018, p. 72.

# TERAHERTZ SPECTROSCOPY CAPTURES Metal Conductivities

**THIN METAL FILMS** such as copper are essential to the design and fabrication of high-frequency circuits, such as microstrip and coplanar waveguide (CPW) on almost-as-thin dielectric substrates in the formation of RF/microwave and even millimeter-wave printed-circuit boards (PCBs). While many studies have been performed on the analysis of the properties of dielectric materials in those PCBs, such as dielectric constant and dissipation factor, much remains to be known about the metal conductors.

In quest of that knowledge, researchers from a number of locations—including the School of Mechanical Engineering of China's Tianjin University and the School of Electrical and Computer Engineering of Oklahoma State University—pooled their resources into the investigation of different types of thin metal films. The researchers used terahertz spectroscopy to study two key material parameters (conductivity and thickness) simultaneously. They investigated three different metal films (aluminum, copper, and silver) and discovered that their measured values of conductivities for the metals were significantly different than the already-known bulk material conductivity values. Their measurements of material thicknesses were consistent with values obtained from other measurement methods.

The studies were performed with the measurement power of the terahertz time-domain spectroscopy (THz-TDS) system at Tianjin University with the aid of grants from China's National Natural Science Foundation and the Natural Science Foundation of Tianjin Province. The analysis system operates mainly in the spectrum from 0.4 to 2.5 THz. Samples were prepared by depositing metal films on 22-μm-thick Mylar substrates by means of thermal evaporation.

The researchers concluded that the differences in the measured values of conductivities and the known bulk materials could stem from a number of factors, such as defects in film metal (e.g., grain boundaries), leading to a reduction in the measured conductivities for those thin metal films compared to bulk metal values. The measurement system and test approach provide convenient means for capturing the two simultaneous conductive metal parameters. The material conductivity and thickness data gathered by the THz-TDS system, while not without some variations, does provide invaluable additional insights to computer-aided-engineering (CAE) design programs, including electromagnetic (EM) simulation software used for circuit designs.

See "Characterization of Thin Metal Films Using Terahertz Spectroscopy," *IEEE Transactions on Terahertz Science and Technology*, Vol. 8, No. 2, March 2018, p. 161.

HAND FLEX™

# CABLES

Hand Flex Cables conform to any shape required.

## NOW! DC-40 GHz!

from $12.95 ea. (qty.1-9)

***Get the performance of semi-rigid cable, and the versatility of a flexible assembly.*** Mini-Circuits Hand Flex cables offer the mechanical and electrical stability of semi-rigid cables, but they're easily shaped by hand to quickly form any configuration needed for your assembly, system, or test rack. Wherever they're used, the savings in time and materials really adds up!

***Excellent return loss, low insertion loss, DC-40 GHz.*** Hand Flex cables deliver excellent return loss (33 dB typ. at 9 GHz for a 3-inch cable) and low insertion loss (0.2 dB typ. at 9 GHz for a 3-inch cable). Why waste time measuring and bending semi-rigid cables when you can easily install a Hand Flex interconnect?

***Two popular diameters to fit your needs.*** Hand Flex cables are now available in 0.047", 0.086" and 0.141" diameters, with a tight bend radius of 3.2, 6 or 8 mm, respectively. Choose from SMA, SMA Right-Angle, SMA Bulkhead, SMP Right-Angle Snap-On and N-Type connectors to support a wide variety of system configurations.

***Standard lengths in stock, custom models available.*** Standard lengths from 3" to 50" are in stock for same-day shipping. You can even get a Designer's Kit, so you always have a few on hand. Custom lengths and right-angle models are also available by preorder. Check out our website for details, and simplify your high-frequency connections with Hand Flex! *RoHS compliant*

SMA | SMA Right Angle | SMA Bulkhead | SMP | SMP Right Angle | N-Type | N-Type Bulkhead | BNC | 2.92mm

Mini-Circuits®

www.minicircuits.com P.O. Box 350166, Brooklyn, NY 11235-0003 (718) 934-4500 sales@minicircuits.com 482 Rev Q

# RF Solutions From RF Engineers

**Largest Selection ✓**

**Expert Technical Support ✓**

**Same Day Shipping ✓**

**Actives, Passives and Interconnects**

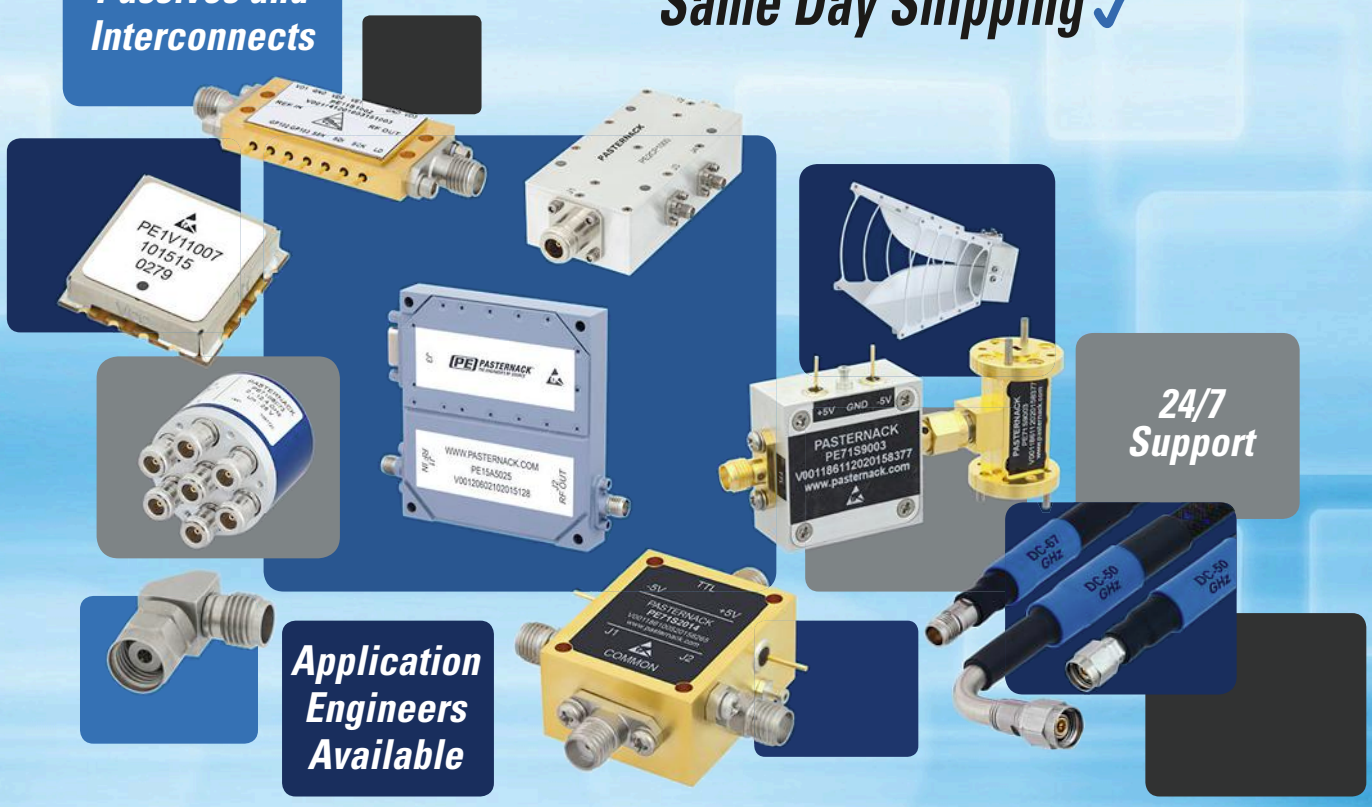


**24/7 Support**

**Application Engineers Available**

*Armed with the world's largest selection of in-stock, ready to ship RF components, and the brains to back them up, Pasternack Applications Engineers stand ready to troubleshoot your technical issues and think creatively to deliver solutions for all your RF project needs. Whether you've hit a design snag, you're looking for a hard to find part or simply need it by tomorrow, our Applications Engineers are at your service. Call or visit us at pasternack.com to learn more.*

**866.727.8376**
**www.pasternack.com**

PASTERNACK®
THE ENGINEER'S RF SOURCE

Special Report

STEPHAN MAROLDT | Ampleon
MARIANO ERCOLI | Ampleon

# Why Plastic-Packaged MMIC PAs May be Essential for 5G MIMO Base Stations

**This article breaks down two new highly integrated Doherty PA designs that could have a major impact on 5G applications.**

The introduction of 5G networks will bring higher mobile data rates to more users at once than has previously been possible. Finding the bandwidth to make this a reality will require the industry to meet a number of technical challenges.

Operators will need to move to carrier frequencies above 2.7 GHz to access more spectrum. Multiple-input, multiple-output (MIMO) antenna arrays will be utilized in 5G networks to deliver high data rates to multiple users in dense urban areas. The data rates promised by 5G will also require large instantaneous-signal bandwidths (more than 200 MHz) and the use of more complex modulation schemes.

These challenges will drive demand for small, low-power, efficient, and cost-effective power amplifiers (PAs) that can be used in 64- or even 128-way MIMO antennas. The increased complexity of the modulation schemes used in 5G will also demand that PAs remain highly efficient—even under deep output power back-off (OBO) conditions of more than 8 dB.

These requirements challenge the capabilities of today's laterally diffused metal-oxide semiconductor (LDMOS) PA technology. In response, the industry has been exploring gallium-nitride (GaN) technology to fill the performance gap. Its uptake has been limited by the cost of the semiconductor material and the use of expensive ceramic packages.

The authors have been working to address these issues, demonstrated by the construction of an ultra-compact 3.5-GHz GaN Doherty PA that can be integrated into a cost-effective QFN plastic package. We used a two-stage GaN core PA monolithic microwave integrated circuit (MMIC). Area-consuming passive networks on integrated passive devices (IPDs) were implemented in the same package.

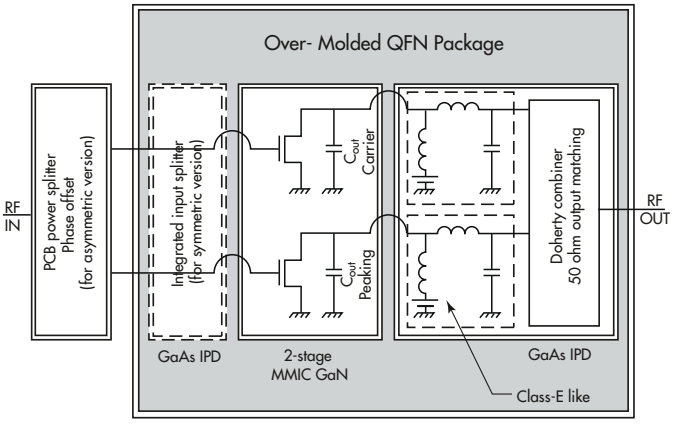


**1. The package-integrated Doherty PAs are based on two-stage GaN MMICs. The asymmetric version has an input power splitter and phase offset on the printed-circuit-board, while these features are integrated in the QFN package in the symmetric design.**

## THE TECHNOLOGY PLATFORM

The PAs are 28-V GaN MMICs that are built using a 0.25-µm gate-length GaN-on-silicon-carbide (GaN-on-SiC) technology. We chose a 28-V gallium-arsenide (GaAs) process to build the IPDs, mainly because its thick low-loss metal layer stack enables us to build high-performance inductors with quality factors (Qs) of 40 at 3.5 GHz.

The two types of die are assembled in a 7-×-7-mm QFN plastic over-molded package. To improve thermal resistance, a thick copper lead-frame is used. Standard gold bond wires are used for interconnections.

We use two different high-gain, two-stage GaN PA MMICs that each represent the heart of two different Doherty PA architectures (*Fig. 1*). The first approach uses a 20-W peak-power asymmetric MMIC, which has a carrier-to-peak size ratio of 1:2 in its final-stage transistors (*Fig. 2*). The second MMIC is designed for a symmetric PA with 26 W of peak output power. Both use a second-harmonic input short in the final stage to maximize efficiency. Output harmonics are terminated by a parallel-circuit class-E-like matching topology, which is used as the basis of an integrated Doherty combiner.

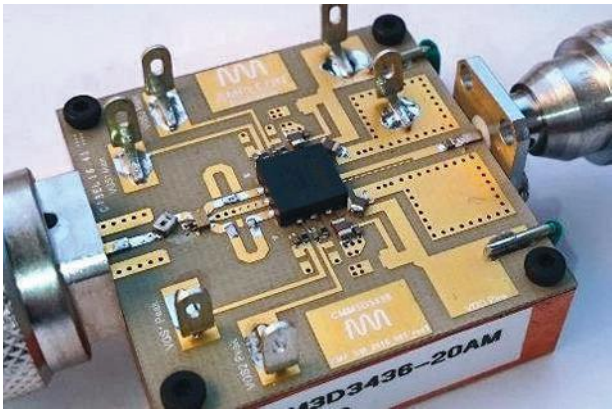

**2. Shown here is a printed-circuit-board that contains the asymmetric GaN Doherty PA in a 7-×-7-mm QFN package, with input splitter at center left and output matching at center right.**

The result is the creation of an inverted Doherty circuit, which minimizes losses in the carrier PA path by using a less-complex matching network than a classical Doherty network design. The approach integrates an input power splitter with phase offset, output matching to 50 Ω, and all the necessary phase offsets on the printed-circuit-board (PCB).

### MEASURING THE ASYMMETRIC GAN MMIC DOHERTY PA

The following measurements—save for the power sweeps—were made at an output power level of +35 dBm that corresponds to the average power with an associated OBO of about 8 dB. The large-signal S-parameters show a flat gain of 26 dB and an input return loss of better than 10 dB over the bandwidth of the PA from 3.4 to 3.6 GHz (*Fig. 3*; *red curves*).

Large-signal measurements show that the PA delivers an output power of 18 to 21 W at 3-dB gain compression (P3dB) from 3.4 to 3.6 GHz (*Fig. 4*). The maximum line-up power-added efficiency (PAE) is higher than 49%, ranging from 40 to 44% at the high OBO figure of 8.5 to 9 dB. Gain is flat for increasing output power, with about one-dB compression in the main amplifier path before the peaking amplifier sets in.

The full PA was characterized using a single-carrier 20-MHz LTE signal with 7.2-dB peak to average ratio at an average output power of +35 dBm from 3.4 to 3.6 GHz. The amplifier shows a flat frequency response with a gain that varies from 26.2 to 26.6 dB. The PAE ranges from 41.5 to 43.1%.

The asymmetric Doherty PA achieves a raw adjacent channel power ratio (ACPR) of –24 dBc. Our first results using a digital pre-distortion (DPD) scheme relevant to massive MIMO applications suggest an ACPR of better than –50 dBc with an LTE signal bandwidth of up to 40 MHz.

### MEASURING THE FULLY INTEGRATED SYMMETRIC DOHERTY PA

We built a fully integrated Doherty PA using the symmetric GaN PA MMIC. The GaN MMIC was integrated with GaAs IPDs that contained an input power splitter, input phase offset, and output Doherty combiner matched to 50 Ω. Everything was integrated into one QFN package, enabling a simplified PA demonstration board that only required the addition of decoupling capacitors along with an output dc blocking capacitor (*Fig. 5*).

This circuit achieved a higher RF bandwidth than the asymmetric version, with a small signal gain of around 30 dB (*refer*

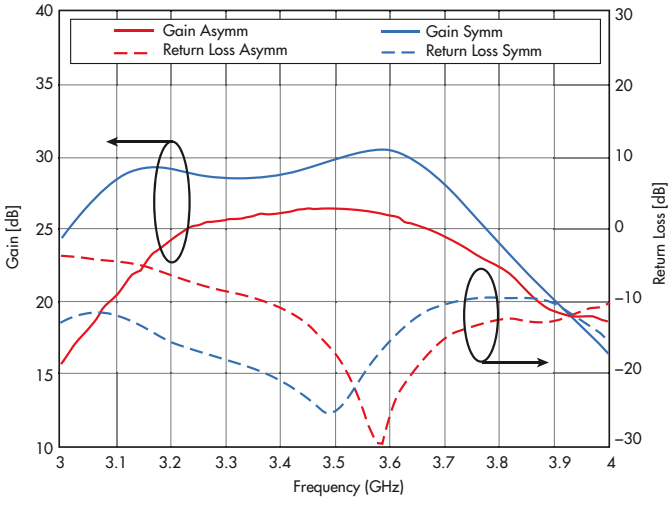


**3. These plots reveal gain and input return loss of the asymmetric (red) and symmetric (blue) Doherty PA board measured at +35 dBm and +30 dBm output power, respectively.**

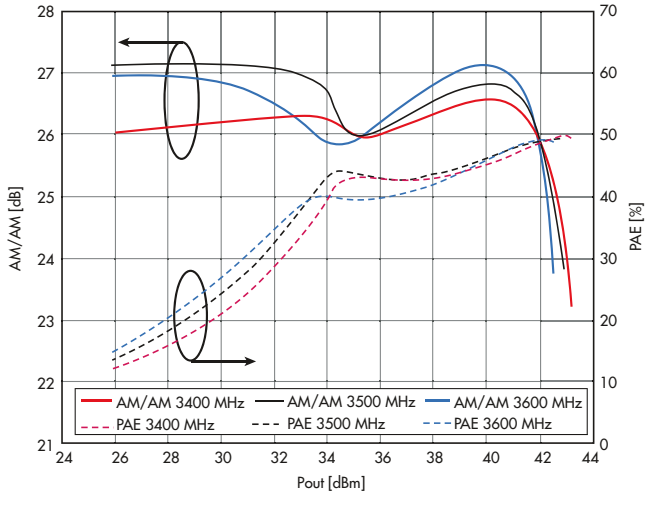


**4. CW power-sweep measurements of the asymmetric Doherty PA board were performed. Shown are AM/AM and PAE at 3.4, 3.5, and 3.6 GHz.**

# 5G

# Synthesizers Designed Specifically for Your Next 5G Application

## Superior Integrated Phase Noise Performance Over 6 to 22 GHz In-Bands

Micro Lambda Wireless, Inc has developed a product line of frequency synthesizers for the next 5G generation of systems and test equipment applications. With a focus on industry leading integrated phase noise performance over the 1Hz to 100 MHz offset frequencies which yields superior EVM performance. This family of frequency synthesizers are perfect for multiplication thru 80 GHz. Give us a call or your local representative and check out what we have available today.

**For more information contact Micro Lambda Wireless.**

**www.microlambdawireless.com**

***Micro Lambda is a ISO 9001:2015 Registered Company***

MICRO LAMBDA WIRELESS, INC.

*"Look to the leader in YIG-Technology"*

46515 Landing Parkway, Fremont CA 94538 • (510) 770-9221 • sales@microlambdawireless.com

# UP TO 100 Watt AMPLIFIERS

## NOW! 100 kHz to 26.5 GHz

$995 from ea. qty. (1-9)

**High-powered performance across wide frequency ranges.** Mini-Circuits' class A/AB linear amplifiers have set a standard for wideband high-power performance throughout the RF and microwave industry. Rugged and reliable, they feature over-voltage and over-temperature protections and can withstand opens and shorts at the output! Available with or without heat sinks, they're perfect for demanding test lab environments and for integrating directly into customer assemblies. With standard models covering frequencies from 100 kHz up to 26.5 GHz, chances are we have a solution for your needs in stock. Place your order on minicircuits.com today for delivery as soon as tomorrow! Need a custom model? Give us a call and talk to our engineers about your special requirements!

| | Model | Frequency (MHz) | Gain (dB) | Pout @ Comp. 1 dB (W) | Pout @ Comp. 3 dB (W) | $ Price* (Qty. 1-9) |
|---|---|---|---|---|---|---|
| | ZVM-273HP+ | 13000-26500 | 14.5 | 0.5 | 0.5 | 2195 |
| | ZVE-3W-83+ | 2000-8000 | 35 | 2 | 3 | 1424.95 |
| | ZVE-3W-183+ | 5900-18000 | 35 | 2 | 3 | 1424.95 |
| | ZHL-5W-2G+ | 800-2000 | 45 | 5 | 5 | 995 |
| | ZHL-10W-2G+ | 800-2000 | 43 | 10 | 12 | 1395 |
| | ZHL-15W-422+ | 700-4200 | 46 | 8 | 15 | 2295 |
| • | ZHL-16W-43+ | 1800-4000 | 45 | 12 | 16 | 1595 |
| • | ZHL-20W-13+ | 20-1000 | 50 | 13 | 20 | 1470 |
| • | ZHL-20W-13SW+ | 20-1000 | 50 | 13 | 20 | 1595 |
| | LZY-22+ | 0.1-200 | 43 | 16 | 30 | 1595 |
| | ZHL-30W-262+ | 2300-2550 | 50 | 20 | 32 | 1995 |
| | ZHL-25W-63+ | 700-6000 | 53 | 25 | - | 8595 |
| | ZHL-30W-252+ | 700-2500 | 50 | 25 | 40 | 2995 |
| | LZY-2+ | 500-1000 | 47 | 32 | 38 | 2195 |
| | LZY-1+ | 20-512 | 42 | 50 | 50 | 1995 |
| • | ZHL-50W-52+ | 50-500 | 50 | 63 | 63 | 1395 |
| NEW! | ZHL-50W-63+ | 700-6000 | 59 | 16 | 50 | 16995 |
| | ZHL-100W-251+ | 50-250 | 46 | 63 | 100 | 1695 |
| • | ZHL-100W-GAN+ | 20-500 | 42 | 79 | 100 | 2845 |
| | ZHL-100W-272+ | 700-2700 | 48 | 79 | 100 | 7995 |
| | ZHL-100W-13+ | 800-1000 | 50 | 79 | 100 | 2395 |
| | ZHL-100W-382+ | 3250-3850 | 47 | 100 | 100 | 3595 |
| | ZHL-100W-43+ | 3500-4000 | 50 | 100 | 100 | 3595 |
| NEW! | ZHL-100W-63+ | 2500-6000 | 58 | 20 | 100 | 17995 |

*Listed performance data typical, see minicircuits.com for more details*

•*Protected under U.S. Patent 7,348,854*

**Price Includes Heatsink*

Mini-Circuits®

## SUPER ULTRA WIDEBAND

# AMPLIFIERS

*up to +27 dBm output...* ***0.1 to 21 GHz***

***Ultra wide coverage and super flat gain*** make our ZVA family ideal for ECM, instrumentation, and test systems. With output power up to 0.5 Watts, they're simply some of the most usable amplifiers you'll find, for a wide range of applications and architectures!

All of our ZVA models are unconditionally stable, ruggedly constructed, and able to withstand open or short circuits at full output. For more details, from data sheets to environmental ratings, pricing, and real-time availability, just go to minicircuits.com!

*All models IN STOCK!*

*RoHS compliant*

*from* $929.95 *ea.*

*Electrical Specifications (-55 to +85°C base plate temperature)*

| | Model | Frequency (GHz) | Gain (dB) | P1dB (dBm) | IP3 (dBm) | NF (dB) | Price $ * (Qty. 1-9) |
|---|---|---|---|---|---|---|---|
| | ZVA-183WX+ | 0.1-18 | 28±2 | 27 | 35 | 3.0 | 1479.95 |
| | ZVA-183GX+ | 0.5-18 | 27±2 | 27 | 36 | 3.0 | 1479.95 |
| | ZVA-183X+ | 0.7-18 | 26±1 | 24 | 33 | 3.0 | 929.95 |
| | ZVA-213X+ | 0.8-21 | 26±2 | 24 | 33 | 3.0 | 1039.95 |
| NEW! | ZVA-213UWX+ | 0.1-20 | 15±1 | 15 | 30 | 3.0 | 1795.00 |

* Heat sink must be provided to limit base plate temperature.To order with heat sink, remove "X" from model number and add $50 to price.

**Wideband Performance**

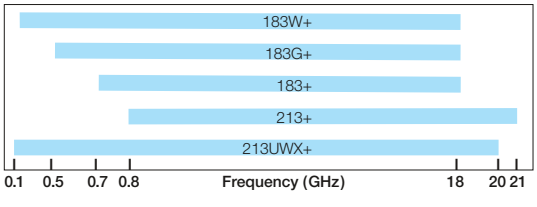


Mini-Circuits®

www.minicircuits.com P.O. Box 350166, Brooklyn, NY 11235-0003 (718) 934-4500 sales@minicircuits.com

*to Fig. 3*). Under continuous-wave (CW) conditions, the PA board yields a P3dB of +44.3 dBm with 52% maximum PAE along with a PAE of 44% at 6-dB OBO. Using a 20-MHz LTE signal at an average output power level of +36.3 dBm, the symmetric amplifier board has a gain of 28.7 dB and PAE of 40% with a raw ACPR of –25 dBc.

## PERFORMANCE COMPARISON

*Figure 6* compares the performance of the two Doherty PA boards. Output power is normalized to peak power.

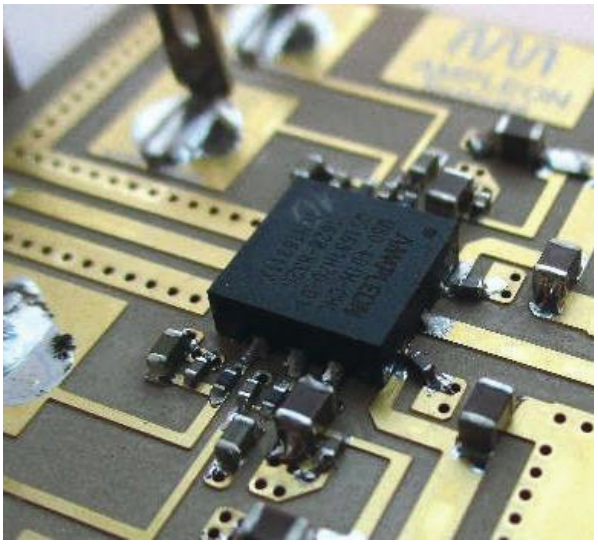

**5. Shown is the board that contains the symmetric GaN MMIC Doherty PA, which integrates the input splitter, input phase offsets, and output Doherty combiner with harmonic terminations and 50-Ω matching.**

In comparison to the asymmetric version, the symmetric Doherty achieves 2 to 3 dB more gain due to lower losses and an equal power splitting ratio in the input splitter. We also see that the symmetric PA has a PAE that is 1 to 3 percentage points higher than the asymmetric approach (down to 6-dB OBO), due to less impact from the driver transistor's power consumption.

The measurements also show that the PAE for the asymmetric PA at 8-dB OBO is 8 to 10 percentage points higher than for the symmetric approach. However, this does come at the cost of reduced linearity.

For the symmetric PA, the AM/AM compression is more smooth and the AM/PM curve increases simply monotonically to less than 10 deg. (*Fig. 7*). For the asymmetric PA, both shapes follow more complex functions. This means that the asymmetric design will need a more complex DPD algorithm for linearization.

## CONCLUSIONS

We built two versions of a Doherty PA board, using MMIC PAs assembled in a low-cost, industrial plastic QFN package. We took the parasitics of the package into account during electromagnetic (EM) simulations to minimize its contribution to overall losses. This allowed us to build a very small board to carry the PA and associated components, which is an essential step towards building massive MIMO antenna arrays for 5G networks.

## ACKNOWLEDGEMENT

The authors would like to acknowledge the great support within Ampleon that helped to accomplish this work, particularly the teams in Toulouse, Shanghai, and Nijmegen. mw

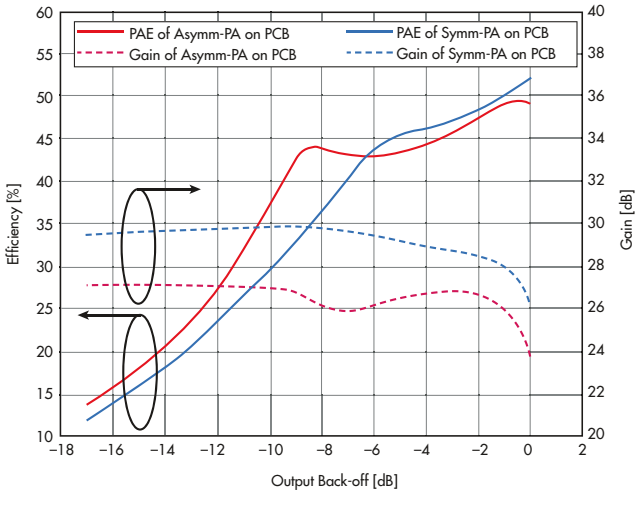


**6. These plots illustrate a comparison of gain (dashed) and PAE (continuous) of the complete asymmetric (red) and symmetric (blue) Doherty PA boards normalized to maximum output power (P3dB).**

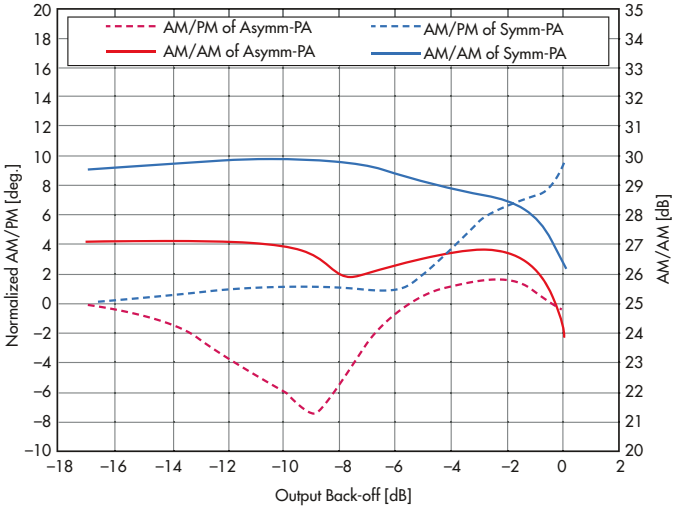


**7. This figure shows a comparison of AM/PM (dashed) and AM/AM (continuous) of the complete asymmetric (red) and symmetric (blue) Doherty PA boards normalized to a maximum output power (P3dB).**

SKYWORKS®

# Sky5™

**SKY78250**
5G NR Transmit/Receive Module with Integrated Wideband Filter

**SKY97005**
5G NR Diversity Receive (DRx) Module

**SKY85762**
Enhanced Licensed Assisted Access (eLAA) Front-end Module
*Coming Soon!*

**SKY85761**
Cellular Vehicle-to-Everything (C-V2X) Front-end Module
*Coming Soon!*

## Empowering the 5G Revolution

| | | | | |
|---|---|---|---|---|
| > 10 Gbps | < 2 Milliseconds | 75 Billion Connections | 100x 4G Speeds | 99.99 Percent |
| High Data Throughput | Extremely Low Latency | Enhanced Spectrum Efficiency | Revolutionary Speed | Network Reliability |

Enhanced Mobile Broadband

Massive IoT

Mission Critical Services

Infrastructure Upgrades

***For more information, please visit us at www.skyworksinc.com/Sky5***

sky5@skyworksinc.com | USA: 781-376-3000 | Asia: 886-2-2735 0399 | Europe: 33 (0)1 43548540 | NASDAQ: SWKS |

# Millimeter-Wave Cables: TIME FOR A CHECKUP?

**As millimeter-wave frequencies become more prevalent, it's essential that the smaller cables used at these higher frequencies be properly handled due to their fragility.**

Microwave cable assemblies are often taken for granted and subjected to various types of abuse that reduce their performance and operating lives. At lower frequencies, this can be tolerated somewhat more easily, since cables and connectors are larger. But that's not the case at millimeter-wave frequencies, which require smaller and typically more fragile cables that will not tolerate abuse.

The cellular industry, having operated below 3 GHz for its entire history, is about to exploit the spectrum between 28 and 100 GHz. In addition, the U.S. Department of Defense (DoD) has ramped up spending to counter threats from electronic warfare and radar at higher millimeter wavelengths. Consequently, there will be more millimeter-wave activity than ever before, so it's a good time for a refresher about the care and handling of these vital components.

As high-level integration combines various functions in a single package or board, it's likely that fewer microwave interconnects will be required at these frequencies. But there will still be a need for flexible, semi-flexible, semi-rigid, and other cable variants to connect subsystems even in devices like small cells. Also, every component and system operating at these high frequencies must be tested, so designers who haven't yet experienced millimeter-wave measurement challenges will soon confront them.

**1. The PE3TC1220 family of 110-GHz test cable assemblies are designed for VNAs and semiconductor probe testing.**

## TACKLING TEST EQUIPMENT

The test-and-measurement environment is one of the few that always places great importance on careful use and maintenance of cables, connectors, and assemblies (though it has not always been adhered to). Because measurement uncertainty is the bane of measurement systems, such attention to detail has been essential. Cost is another motivator due to precision vector-network-analyzer (VNA) test cables being so expensive. The same scenario applies to all types of interconnects used at millimeter wavelengths, as they are precision-machined, delicate instruments.

For example, the PE3TC1220 family of 110-GHz test cable assemblies from Pasternack are typical of those designed for use with VNAs and semiconductor probe testing (*Fig. 1*). They have male 1.0-mm connectors at each end and are armored with Nomex for protection. Insertion loss at 110 GHz is 5.6 dB or less, typical VSWR is 1.5:1, and one-time minimum bend radius is one inch. The connectors have beryllium cop-

per, gold-plated bodies and passivated stainless-steel coupling nuts. The assemblies are available in 6- and 12-in. lengths.

It's hard to overstate the importance of taking care of cables and connectors at these frequencies. Component size is related to wavelength, so cables (and connectors) at millimeter-wave frequencies are very small. This is great from a form-factor perspective, but problematic for everything else from materials to fabrication to performance. Their properties also require all who use them to be extremely careful. Even tiny bits of dust and almost imperceptible scratches and other damage can degrade measurement accuracy.

For instance, a full wavelength at 60 GHz is about 5 mm and a half-wavelength antenna at this frequency measures about 2.5 mm. Millimeter-wave connectors range from 2.92 to 1.0 mm. In addition, a 0.8-mm connector for frequencies above 110 GHz is in the wings. Larger connectors for HF through UHF frequencies are enormous compared to these connectors—a full wavelength at 100 MHz is 3 m and a full wavelength at 1 GHz measures 30 cm.

Since loss is a huge consideration at millimeter-wave frequencies, the fewest possible interconnects are used to connect a device under test (DUT) to the instruments and any other components in the transmission chain. In addition to lowering insertion loss, this reduces the number of places where discontinuities can occur, simplifies the setup, and limits points of entry for dirt and dust.

## BASIC YET CRUCIAL MATING PROCEDURES

The center conductor and dielectric of a millimeter-wave cable or connector is easily damaged if it is misaligned when mated to its counterpart. Even a slight variance from parallel between the connector and its interfacing other can have negative consequences. The proper approach is to firmly grasp the body of the connector so that it can't rotate and potentially degrade the finish and plating of contacts and transfer torque to the cable assembly. Dirty connectors or those suspected of being damaged should never be mated, nor should connectors whose pins are not aligned, have been damaged from being over-torqued, or whose coupling nut has been cross threaded.

Although few engineers would admit it, torque wrenches aren't always used to secure coupling nuts. The use of torque wrenches is sometimes even avoided in sensitive test-and-measurement environments, as novices and veterans alike develop a "feel" for when a connector is properly seated and torqued. However, once it is over-torqued, a connector will pass along its imperfections to its counterpart as well as every connector to which it is mated, with the result being "consistently inconsistent" measurement results.

A torque wrench used for millimeter-wave connectors is a precise tool. One such example is Pasternack's PE5019-16 break-over torque wrench for 1.0-mm connectors—it has a preset value of 4 in.-lbs. so that mating force will never be exceeded (*Fig. 2*). The break-over type has the advantage of stopping force at the pivot point once the preset torque value is reached. Its accuracy is ±0.15 in.-lbs. and hex size is 6 mm.

Every cable assembly has a maximum bend radius; once that's exceeded, it will initially degrade measurement results and ultimately destroy the assembly. While in some cases a tight bend might seem inescapable, it should still be avoided because just one mistake can ruin a millimeter-wave cable. Thus, the widest possible bend radius should always be used.

It's also important not to twist the cable, as this will likely damage both the cable and the integrity of the assembly and potentially damage the connector. Wrinkles or other signs of stress visible on the cable jacket are good indications that it has been severely twisted, or its bend radius specification was exceeded.

## UBER-CLEANLINESS

When tolerances are so tight, as they are in millimeter-wave components, all interfaces must be clean. Although it might seem extreme, using a microscope for examination is not a bad idea. The cleaning process is simple to perform: Simply get a lint-free cloth (polyester is a good choice), moisten it with isopropyl alcohol, and gently wipe the components clean. Filtered compressed air or nitrogen can be used. But beware of chlorinated solvents typically housed in pressurized cans. They are designed to provide deep penetration that can potentially do more harm than good.

**2. The PE5019-16 torque wrench for 1.0-mm connectors is a break-over type of wrench, which eliminates the possibility of over-torquing the connector.**

Cables used with flightline measurement systems generally experience the greatest abuse. This is because some people making these measurements understand how cables must be treated, while others who handle them may not.

Having performed this process, using a magnifying glass, inspect the surfaces, and repeat the process if necessary to ensure that any metallic particles or any other substances have been removed. While the magnifying glass is handy, it pays to inspect the interface. Potential defects include bent pins, missing pin tines, damage to the dielectric, worn or damaged threads, or any other visible appearance of damage. If any of these are spotted, replace the cable.

Cables used with flightline measurement systems generally experience the greatest abuse. This is because some people making these measurements understand how cables must be treated, while others who handle them may not. Stories abound of measurement carts being dragged along by their cables. Other adverse scenarios include cables that are used for support, as well as cables that have been pinched, crushed, stepped on, or have passed over sharp edges. This environment is also where maximum bend radius is regularly exceeded.

Although it is often difficult to eliminate these situations, whoever is responsible for maintaining the measurement system should at least do his or her best to ensure that only undamaged cable assemblies are used. A "drip loop" should always be created in outdoor measurement environments. That's because water can move down the cable and to the connector, eventually resulting in performance changes such as increased insertion loss.

Flightline conditions also place cable assemblies in hostile environments where oils and other liquids, as well as gases, may be present. In these areas, the cables may not be directly exposed, but that could be the case for those using

them. Cables designed for test-and-measurement applications are designed to meet rugged service, but not necessarily exposure to every hostile scenario.

A variety of materials are used for microwave cable jacketing. Each type has advantages and disadvantages when used in challenging environments. Polyurethane, for example, resists solvents, UV rays, radiation, and fungus, but not chemicals used for cleaning. Fluoropolymers such as fluorinated ethylene propylene (FEP), perfluoroalkoxy (PFA), and polytetrafluoroethylene (PTFE) are well-suited for cable jacketing in these environments—they can withstand high temperatures as well as exposure to chemicals, acids, and invasive solvents. They're also not flammable.

Moisture is the enemy of all types of cables, as it tends to increase cable loss over time because the outer conductor or shield becomes oxidized. When RF power is applied, water absorbed by the dielectric increases in temperature. There are several points of entry for water or water vapor, from even tiny holes in the jacketing material to spaces where the connectors meet the cable or where the connectors meet their matching interface.

In the case of cable-to-connector and connector-to-connector interfaces, a water-resistant boot can be used. However, water vapor may find its way into very small abrasions in the cable jacketing that are almost impossible to see without using a magnifying glass under bright light. Periodic attention to jacket condition is worth the time required to perform it, as over time, a damaged cable will reduce performance or ultimately fail. Not surprisingly, shipboard or coastal environments offer a major opportunity for entry of salt mist, which corrodes metal inside the cable as well as on or in the connector components if their plating has been damaged.

**SUMMARY**

Operation at millimeter wavelengths presents major challenges, which is why the mmWave region has been explored only for those few applications with suitable characteristics. Communications has rarely been one of them.

However, that will change in the next decade, as the cellular industry takes advantage of the almost unlimited available bandwidth. This development, along with defense activity, means that it will be more important than ever for designers to take extra precautions to ensure their cable assemblies not only deliver desired performance, but have long, trouble-free operating lifetimes. mw

JACK BROWNE | Technical Contributor

# What Role Will Millimeter Waves Play in 5G Wireless Systems?

**5G will bring mobility to mmWave communications as the next-gen wireless network attempts to serve more people and even things with a major expansion of mobile services.**

Wireless communications networks have evolved dramatically from their humble beginnings. The first-generation (1G) wireless network, the Advanced Mobile Phone Service (AMPS) cellular communications standard, was based on analog technology from Bell Labs. But users liked the convenience of carrying a communications device such as a telephone wherever they went, and the number of users grew quickly. Subsequently, second-generation (2G) wireless networks saw the adoption of GSM and CDMA technologies as the first digital standards.

Still, users wanted more functions from their cell phones, so third-generation networks eventually arrived as the first mobile broadband wireless systems. With 3G UMTS technology integrated as the high-speed digital standard, they could send e-mails and data as well as make voice calls. The fourth-generation (4G) wireless network, equipped with Long Term Evolution (LTE) and LTE Advanced digital technologies, was thought to be the last wireless communications network that anyone would ever need—until the need arose for the fifth generation (5G).

In spite of digital techniques and advanced modulation formats, wireless communications generations 1 through 4 have worked with essentially limited bandwidth, trying to serve a fast-growing number of users wanting more services that consume ever-increasing bandwidth.

For example, current 4G LTE wireless network infrastructure equipment in the U.S. operates at 800 MHz, 1900 MHz, 1.7 to 2.1 GHz, and 2.5 to 2.7 GHz. However, it also employs a variety of additional communications technologies, such as wired Ethernet and fiber-optic cables, to transfer data at the highest rates possible. Both fixed and mobile wireless users now expect data rates in excess of 1 Gb/s. With the coming of 5G in approximately two years, data rates are expected to reach 10 Gb/s.

## THE MMWAVE BANDWIDTH SOLUTION

Even with the advances of 4G LTE, the network is running out of bandwidth. The solution, as seen by 5G wireless network developers, is to add more bandwidth by using frequency spectrum in the millimeter-wave frequency range (*Fig. 1*). With hundreds of megahertz of wireless transmission bandwidth available at center frequencies such as 24, 28, and 38 GHz, 5G wireless networks will be capable of almost zero-latency phone calls and extremely high data speeds. Although mmWave frequencies, according to their wavelengths, range from 30 to 300 GHz, 5G innovators such as Qualcomm and other members of the Third Generation Partnership Program (3GPP) working on 5G network solutions typically refer to the mmWave frequency range as starting at about 24 GHz.

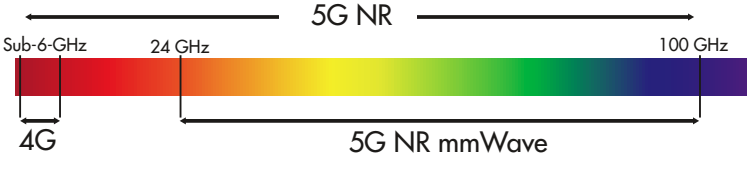


**1. The amount of bandwidth available at mmWave frequencies is enormous compared to the amount of frequency spectrum used by 4G and previous wireless network technologies.**

People are just one projected part of the many users of 5G networks. Autonomous vehicles will need that 1-ms latency of 5G networks to safely steer through traffic and maintain awareness of the traffic around them by means of vehicle-to-everything (V2X) communications. In addition, potentially billions of Internet of Things (IoT) sensors may be adding their data contributions to 5G networks within the next decade, giving people instant access to information about different things and environments around them. Due to this projected massive bandwidth consumption, developers see mmWave frequencies providing the bandwidth to make 5G possible.

However, there are many reasons why mmWave equipment has remained within astronomy, military, and research applications for so many years, beyond the high cost of the components and the relative scarcity of test equipment for aligning and evaluating the hardware. Electromagnetic (EM) energy at those higher frequencies suffers a great deal of path loss through the air (especially through air with high humidity) compared to lower-frequency signals with longer wavelengths (*see p. 58*).

Signals at 24 GHz and above can be absorbed by any objects in their propagating path, such as buildings, trees, even the hand of someone holding the smartphone that's sending the mmWave signals to a cell site to connect with a listener. But mmWave frequencies also have benefits, in addition to the generous bandwidths they offer, such as their use of much smaller antennas (to fit those smaller wavelengths) compared to lower frequencies. The small size of these antennas makes it possible to pack many of them together into small form factors to benefit from antenna arrays.

## ARCHITECTURALLY SPEAKING…

The architecture of 5G networks will be much different than earlier wireless-network generations, in part because of the use of mmWave frequencies. Smaller antennas will be used in mobile handsets to transmit and receive those higher-frequency signals but, as noted, the propagation distances for mmWave frequencies is less than for signals at the lower frequencies traditionally used in cellular networks.

As a result, 5G network infrastructure must be erected with many more, smaller cell sites or base stations than lower-frequency wireless networks (*Fig. 2*). In addition, within those smaller cells, many antennas will be used to produce three-dimensional (3D) antenna beams, as part of a process known as beamforming.

It is a technology that has long been in use by the military as part of phased-array radar systems, to create and direct high-energy pulses for reflection from a target. In 5G systems, multiple-element antennas in closely spaced, smaller base stations will use hundreds of antenna elements to form directional beams for transmission and to receive similar 3D beams from adjacent base stations. A user with a mobile handset will have an antenna array with much fewer elements, possibly around 30 within a battery-powered mobile device, to send and receive signals within microwave and mmWave frequency bands.

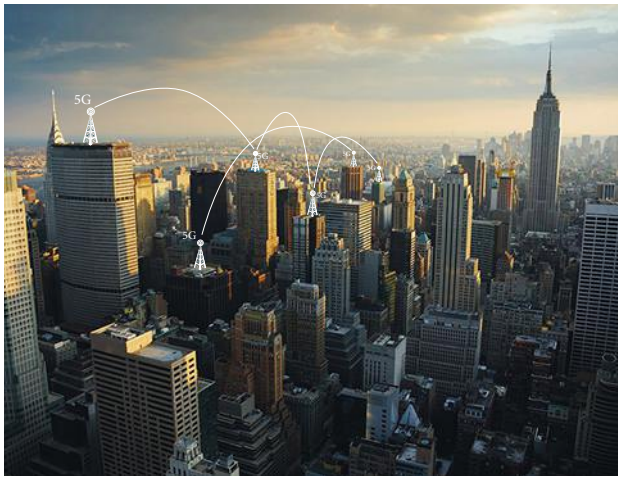


**2. The infrastructure for 5G wireless networks will employ many more closely spaced base stations than earlier wireless networks, to support the shorter propagation distances of mmWave signals.** *(Courtesy of Verizon)*

The actual application of mmWave frequency bands in 5G wireless networks has yet to be determined, although the additional bandwidth they offer is vital to the improved performance promises of 5G networks. The mmWave frequencies, for example, may only be for outdoor use, with indoor cell sites operating at under-6-GHz frequencies and providing indoor and outdoor-to-indoor coverage. The plan for the buildup of 5G New Radio (NR) infrastructure is not to abandon 4G LTE, but to add to the capacity and coverage already provided by 4G LTE networks.

## LOOKING AHEAD

Forward-looking companies such as Qualcomm, Skyworks, and Ericsson have been at work on 5G components and subsystems for some time. Qualcomm has worked closely with the 3GPP on developing its 5G NR standard as a means of cost-effectively incorporating mmWave technology into compact 5G base stations and mobile handsets. It will do so using 3D beamforming and multiple-input, multiple-output (MIMO) antenna techniques.

The company has developed smart, closed-loop algorithms for beam switching, steering, and tracking to maximize the amount of energy transmitted and received between 5G access points at mmWave frequencies. These algorithms look for reflected energy when a mmWave line-of-sight (LOS) signal path is blocked by a building or other obstruction, and combine the signal energy from alternative signal paths into the maximum received signal energy.

# ARE YOU 5G-READY?

## *LET US BE YOUR ONE-STOP SHOP FOR MMWAVE COMPONENTS & SUBASSEMBLIES.*

SAGE Millimeter, Inc.

**WWW.SAGEMILLIMETER.COM**

MADE IN USA


www.sagemillimeter.com | 3043 Kashiwa Street, Torrance, CA 90505
T: 424-757-0168 | F: 424-757-0188 | sales@sagemillimeter.com

## *VIEW PRICING, LEADTIME, AND INVENTORY*

# NEW SAGE WEBSITE

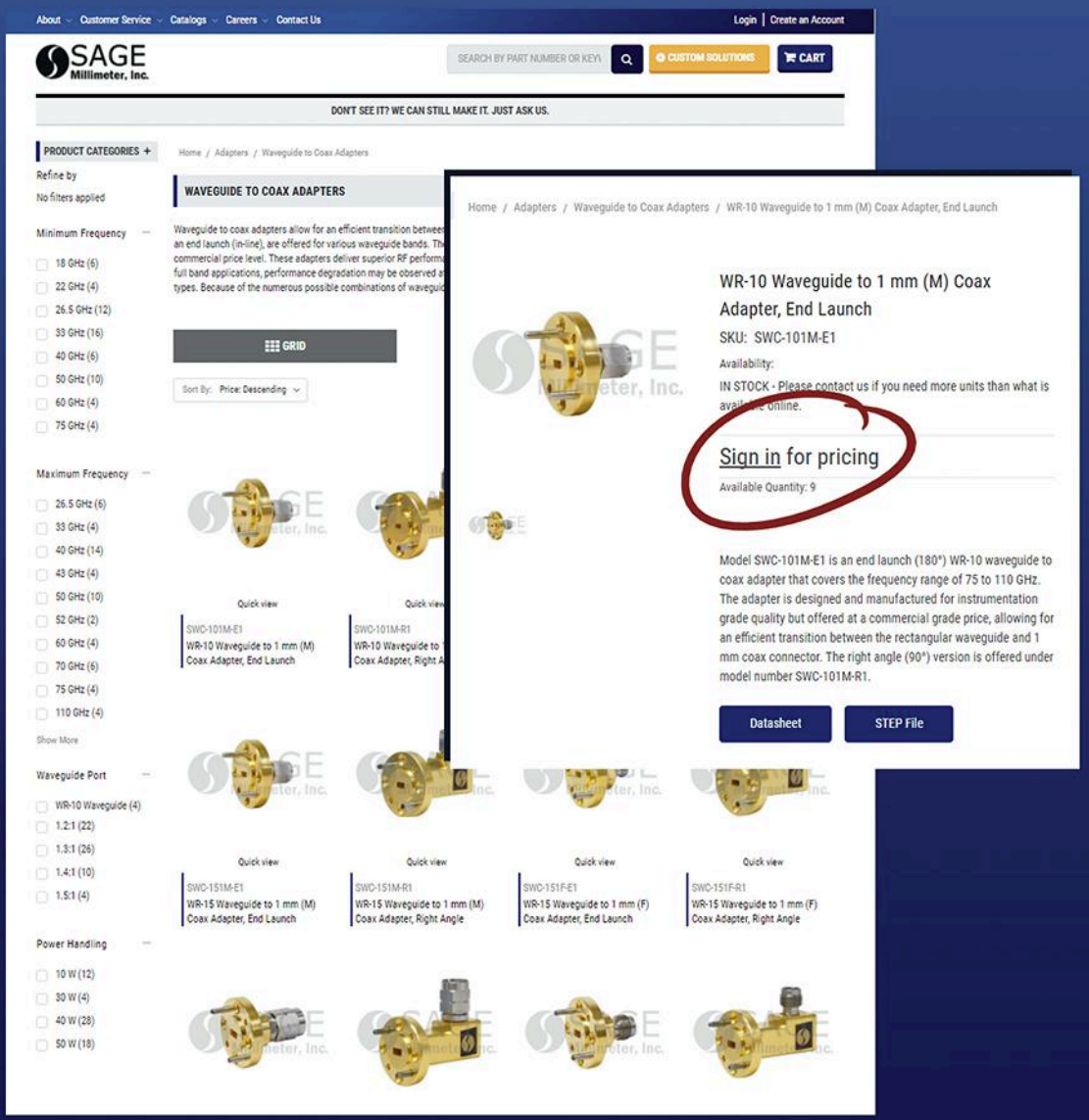


WWW.SAGEMILLIMETER.COM/STOCKROOM

***Over 2,500 millimeterwave components off-the-shelf, in stock, and ready to ship guaranteed in only 1-3 days.***

SAGE STOCKROOM

The architecture of 5G networks will be much different than earlier wireless-network generations, in part because of the use of mmWave frequencies.

In fact, Qualcomm has already successfully demonstrated (November 2015) a 5G system at mmWave frequencies. Along the way, the firm has performed a wide range of simulations and measurements from 22 through 67 GHz, comparing the propagation of the mmWave signals to 2.9 GHz as a lower-frequency reference.

Extensive over-the-air (OTA) testing of prototype 5G NR base station units and mobile devices has been conducted, even within vehicles moving at speeds to 30 mph, and reliable communications at mmWave frequencies were achieved even through the walls of buildings. Qualcomm showed what it calls its 5G NR shared spectrum (SS) approach to managing mmWave signal propagation at the most-recent Mobile World Congress (MWC), using the live demonstration of a prototype circuit board.

The company offers its Snapdragon X50 5G modem as a building block for 5G infrastructure. The modem features an integrated antenna array and RF front end. It's designed for use at 28 GHz, achieving as much as 800 MHz bandwidth through 8 × 100-MHz carrier aggregation. The modem employs the company's adaptive beamforming and beam-tracking techniques as well as MIMO antenna methods to extend the typical LOS range of mmWave frequencies to longer, non-LOS ranges that also support mobile users. Qualcomm recently announced additions to the Snapdragon X50 5G modem family with 5G NR multimode chipsets compliant with the 3GPP 5G NR standard. They also support operation at frequencies below 6 GHz for compatibility with 4G LTE networks as well as earlier 2G and 3G systems. The first commercial products with Snapdragon X50 5G modems are expected in 2019.

In providing components for the expected rapid buildup of 5G infrastructure during the next several years, Skyworks Solutions (*www.skyworksinc.com*) offers circuits at the RF front end. It has announced its Sky5 product family for 5G networks. The line includes the highly integrated SKY78250 5G NR power-amplifier (PA) module with integrated filtering and dual-path low-noise amplifier (LNA).

For its part in the 5G NR planning, Ericsson (*www.ericsson.com*) has paid a great deal of attention to concerns about the security of 5G wireless networks. The company now offers a downloadable white paper on its website, "5G Security—Enabling a Trustworthy 5G System," which explains the steps being taken as part of the initial 5G NR 3GPP standard to protect the privacy of future 5G users.

Advances in semiconductor and integrated-circuit (IC) technologies will play major roles in the development of affordable integrated and modular circuit solutions for 5G base stations and mobile devices, especially with the complexity of mmWave antennas and radio circuits. Components for mmWave frequencies, both active and passive, have traditionally been expensive—even the coaxial connectors (depending upon frequency) for hybrid circuits were precision machined and expensive. But the imminent buildup of 5G networks and its expanding contingent of mobile devices has brought a new awareness to the high-frequency industry concerning the need for more cost-effective components, circuit materials, and test instruments for frequencies above 24 GHz.

Moreover, major instrument manufacturers are addressing the coming needs for test equipment that can evaluate 5G systems and their components, at both mmWave frequencies and below 6 GHz. Anritsu Corp., for example, recently announced the expected launch of its MT8000A Radio Communication Test Station for developing chipsets and terminals for 5G wireless networks. The tester has built-in support for the broadband signal processing and beamforming technologies used in 5G in a compact desktop configuration. It will be capable of RF and protocol tests at mmWave frequencies and at 6 GHz and below.

In addition, Keysight Technologies has issued a memorandum of understanding to develop test equipment for 5G NR standards. On the computer simulation side, high-frequency model master Modelithics recently released a new mmWave and 5G library of devices for the popular Advanced Design System (ADS) suite of software circuit and system simulation programs from Keysight. 5G system simulations have also been performed on specialized modeling tools, such as MATLAB from MathWorks.

With this first 5G NR standard as embraced by the 3GPP, it's apparent that development is accelerating for 5G wireless communications networks, with plans to provide sufficient bandwidth to support mobile users as well as cars, IoT devices, and even unmanned drones. The enormous number of devices to be connected by means of 5G wireless network technology may even make that additional bandwidth seem like it's not enough before long. But this initial use of mmWave frequency bands for commercial communications will provide generous frequency spectra through 60 GHz and above, as the high-frequency industry seeks to learn how to cost-effectively produce mmWave components and possibly even test equipment and software in large volumes for the first time. mw

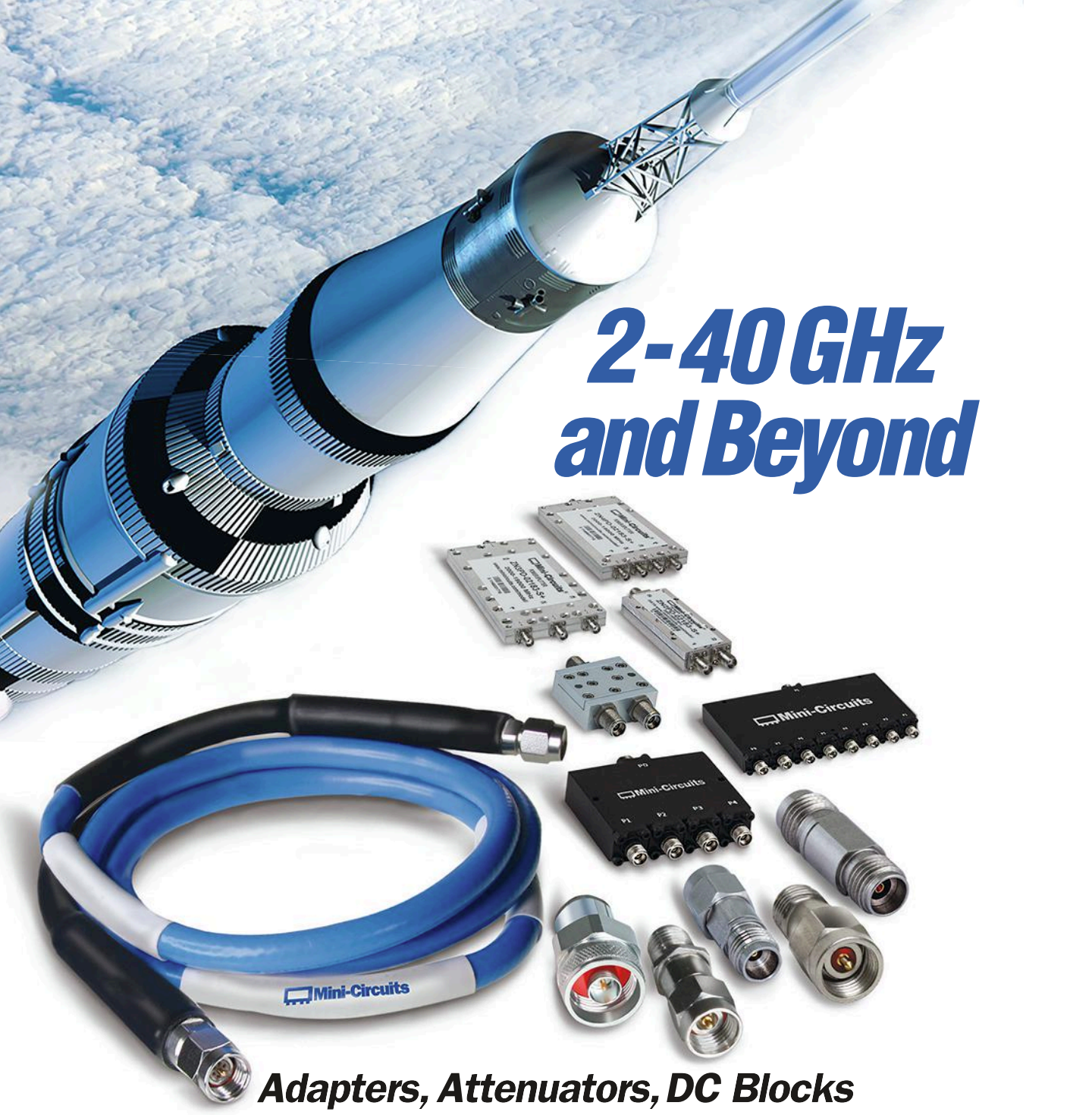


# 2-40 GHz and Beyond

## Adapters, Attenuators, DC Blocks Splitters, Terminations & Test Cables

***Breaking Through Barriers to the Next Generation of Wireless Applications***

From 5G test systems to Ka-Band SatCom and more, Mini-Circuits is your source for coaxial components from DC to 40 GHz and beyond. We're not just giving you more innovative products and greater capabilities with a growing selection of adapters, splitter/combiners, terminations and test cables to 40 GHz and attenuators to 50 GHz. We're giving you the speed, flexibility, and technical partnership you need in your development efforts to break through the barriers to higher frequencies and next generation wireless standards. Check out our latest additions on minicircuits.com today or give us a call for custom solutions with fast turnaround and industry-leading application support.

Mini-Circuits®

www.minicircuits.com P.O. Box 350166, Brooklyn, NY 11235-0003 (718) 934-4500 sales@minicircuits.com 566 RevC

DR. BOUCHRA RAHALI | Researcher, STIC Laboratory, Department of Electrical Engineering, Faculty of Technology, University of Tlemcen, Post Box 230, Pole of Chetouane, 13000 Tlemcen, Algeria; e-mail: b_rahali@hotmail.fr

# SIW Filter Doubles as Balun to mmWave Frequencies

**This balun/bandpass filter, based on substrate integrated waveguide and circular complementary split-ring resonators, delivers outstanding performance in millimeter-wave-frequency applications.**

Bandpass filters are among the most useful building-block high-frequency components in modern communications networks, for functions such as providing signal isolation and spectral cleaning. Waveguide bandpass filters provide outstanding electrical performance, but are relatively large in size. However, substrate-integrated-waveguide (SIW) transmission-line technology delivers good performance from compact planar formats such as printed circuit boards (PCBs), and can be readily integrated with other transmission-line formats, e.g. microstrip, as needed for high-frequency component and subsystem design.[1]

In fact, SIW components can be thought of as traditional rectangular waveguide in planar form. This allows a transition of most classical waveguide components into more compact SIW forms. There are inevitable tradeoffs between the two formats, with conventional waveguide lower in loss but larger in physical size. However, the very good electrical performance of SIW components combines well with the compact, planar formats that can be made to fit many system designs.

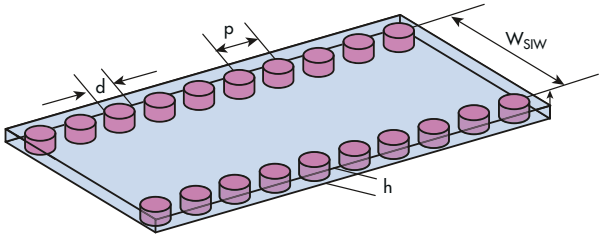


**1. This graphical depiction of a rectangular SIW circuit structure shows how it is formed with two rows of drilled, metallized viaholes along the dielectric material.**

SIW technology is the catalyst behind a wide range of passive high-frequency components, including planar SIE phase shifters,[2] power dividers,[3] circulators,[4] directional couplers,[5] six-port circuits,[6] and low-cost filters.[7] A variety of resonator-based filters have been developed with SIW approaches, too, including post, iris, and cavity-type filters.

Overall, the low insertion loss, sharp rejection cutoff, and low cost of these filters has made them invaluable for modern wireless communications systems. To explore the design of SIW bandpass filters, some examples will be shown using circular complementary split-ring resonators (CSRRs) fabricated on readily available commercial PCB material and with design guidance using the High Frequency Structure Simulator (HFSS) electromagnetic (EM) simulation software from ANSYS *(www.ansys.com)*.

CSSRs have been proposed for the synthesis of negative-permittivity and left-handed (LH) metamaterials in planar circuit configurations.[8] They can serve as useful circuit design elements: CSRRs etched in the ground plane or conductor of a planar transmission-line format, such as microstrip or coplanar waveguide (CPW), provides a negative effective permittivity with resulting stopband behavior in the vicinity of the frequency of the resonant structures. CSSRs have been applied to the design of compact bandpass filters (BPFs) to achieve low bandpass loss with high out-of-band rejection.[7]

A balun, which is a balanced/unbalanced network, enables an unbalanced input signal to be transformed to a pair of balanced output signals 180 deg. out of phase, as might be used in balanced frequency mixers.[9] It is possible to combine the highpass characteris-

tics of SIW transmission lines and the bandstop characteristics of CSSRs to form an SIW balun/BPF in compact, planar format with good electrical performance.[10,11]

The graphic representation of a rectangular SIW section *(Fig. 1)* is based on a circuit structure fabricated on commercial DiClad dielectric substrate material from Arlon, now part of Rogers Corp. *(www.rogerscorp.com)*. The substrate material has a relative permittivity or dielectric constant (εr) of 3.38, dissipation factor (tanδ) of 0.0009, and height (h) of 0.81 mm.[1-3]

The SIW circuit structure is formed by drilling and metalizing two rows of holes through the circuit-board material to establish contact between the two metal planes of the dielectric substrate material. Parameter $W_{eq}$ represents the width of the corresponding rectangular waveguide circuit or component that is replaced by the rectangular SIW (RSIW) circuit structure.[3] Parameters for the SIW circuit include the width of the RSIW ($W_{SIW}$), the diameter of the via holes (d), and the space between the viaholes (p).[2]

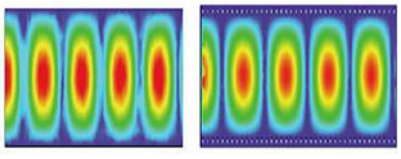

**2. These electric-field distributions represent the TE10 mode at 12 GHz for an equivalent rectangular waveguide structure (left) and an RSIW structure (right).**

Based on previous work,[2] empirical equations were derived for determining the width of the equivalent rectangular waveguide, using the same fundamental-mode propagation characteristics as the RSIW of *Figure 2*. The same height and dielectric material parameters were used for the RSIW filter, and parameter analysis was performed by using the finite-element method (FEM) included as part of the HFSS EM simulation software:[12]

$$W_{eq} = W_{SIW}\{\xi_1 + \xi_2/[(p/d) + (\xi_1 + \xi_2 - \xi_3)/(\xi_3 - \xi_1)]\} \quad (1)$$

with

$$\xi 1 = 1.0198 + 0.3465/(W_{SIW}/p - 1.0684)$$

$$\xi 2 = -0.1183 - 1.2729/(W_{SIW}/p - 1.2010)$$

$$\xi 3 = 1.0082 - 0.9163/(W_{SIW}/p + 0.2052)$$

and

$$p \le 2d$$

## DESIGNING AN SIW BPF

Complementary split-ring resonators (CSRRs) are sub-wavelength planar structures that have been produced as metamaterial resonators,[8] and can be thought of as electric dipoles. According to the theory of evanescent-mode propagation for a waveguide loaded by electric dipoles, a bandpass below the waveguide cutoff frequency can be obtained by properly loading the CSRRs.

SIW technology is suitable for loading CSRRs on a waveguide surface, so that SIW-loaded complementary resonators such as CSRRs are effective structures for achieving compact BPFs. The technique yields miniature waveguide filters, in contrast to much larger, conventional waveguide filters based on bulk resonators.

To offer some insight into the compact size and high-performance possibilities in designing an RF/microwave BPF with integral balun using SIW transmission-line technology with SSRRs, a filter was designed on a CPW circuit configuration. The filter design is relatively simple *(Fig. 3)*, consisting of two CSRRs printed on circuit material with thickness (h) of 0.81 mm and dielectric constant ($\varepsilon_r$) of 3.38.

ANSYS's HFSS EM simulation software was used to simulate the RF/microwave performance of the SIW BPF design with integrated balun from 3 to 13 GHz. *Figure 4* shows the response for the full-wave simulation, with levels about as expected at 9.48 GHz; the design features negligible return loss of 14.86 dB and quite low insertion loss of 0.31 dB. The SIW BPF consists of input and output coupling lines with CSRR-loaded SIW.[3,4] An SIW filter with bandpass response[7] was achieved by combining the highpass characteristics of the SIW and the bandstop characteristics of the CSSRs.[8]

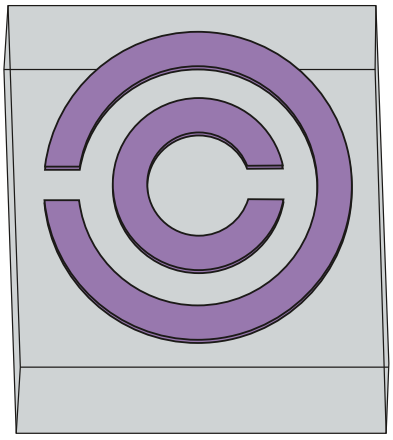

**3. A bandpass filter can be realized in a simple CSRR printed-circuit configuration such as this, using circular slotted split rings.**

*Figure 5* shows the design of the filter based on a single CSRR cell. Simulations were performed on the dielectric substrate material used for the filter and other circuit structures, since various SIW-planar structure transitions were needed to integrate the filter, balun, and other circuit functions within the same circuit material.

The design of the SIW-to-microstrip transition is straightforward,[13] making use of a tapered microstrip line to excite the waveguide mode *(Fig. 5, again)*. The transition offers excellent performance over a broad bandwidth capable of covering the full SIW operating bandwidth. As the HFSS simulations show, the filter achieves a bandpass of 7.71 to 8.58 GHz, with excellent return loss of 29.15 dB and low bandpass insertion loss of only 0.74 dB, both at 8.20 GHz *(Fig. 6)*.

After creating the design for this single cell, multiple cells were cascaded together to form a complete BPF for use with the SIW filter/balun structure. The full bandpass characteristics of the design are achieved by cascading the cells *(Fig. 7)*.

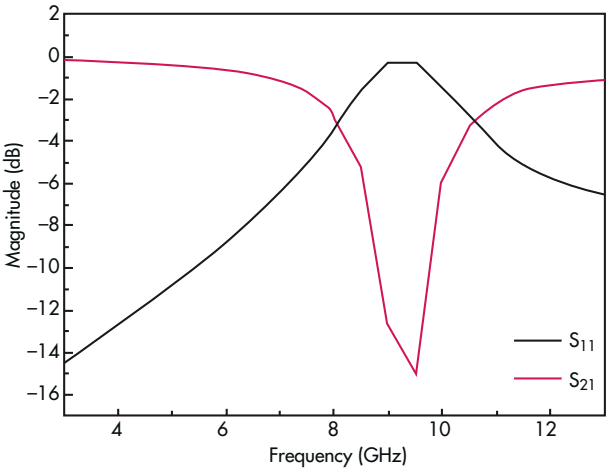


**4. This HFSS simulation shows the modeled response of the CSRR circular ring filter structure for 3 to 13 GHz.**

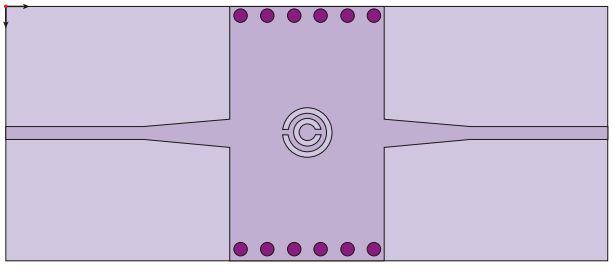

**5. This SIW planar transmission line includes a circular single-ring CSRR structure.**

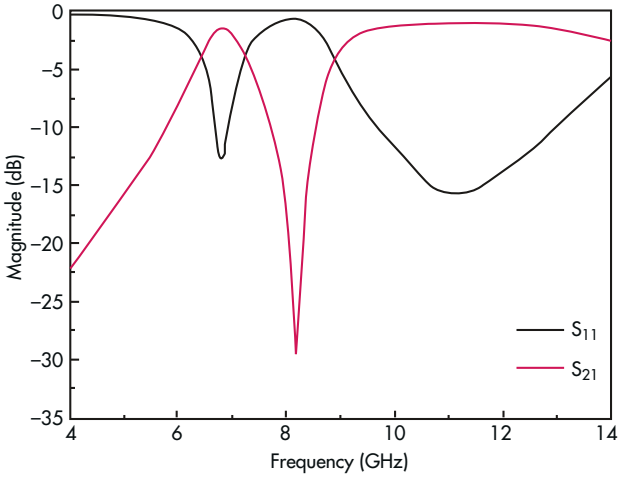


**6. These simulated plots show the forward transmission ($S_{21}$) and reflection coefficient ($S_{11}$) for the SIW with single-ring CSRR and tapered transitions (of Fig. 5).**

This larger SIW BPF structure with cascaded CSRRs shows promising simulated performance for both return loss and bandpass insertion loss, with simulated return loss of 30.41 dB at 8.66 GHz and simulated insertion loss of 1.04 dB at the same bandpass frequency. The filter portion of the integrated design offers respectable return loss and insertion loss across a fairly wide bandpass, from 7.59 to 9.89 GHz *(Fig. 8)*.

## SIW BALUN BPF

A balun is a circuit that converts signals from an unbalanced state to a balanced state, as might be needed within different systems. An unbalanced-to-balanced line transformer was first proposed by Marchand in 1944.[9] Because of its output-balanced characteristics and output phase difference of 180°, it is useful for many applications.

Many microwave circuits, for example, require balanced inputs and outputs to reduce noise, minimize higher-order harmonics, and improve dynamic range. Baluns are often used as "building-block" components to realize designed performance functions in wireless communications systems, working together with balanced frequency mixers, push-pull amplifiers, and antenna feed networks.[10,11]

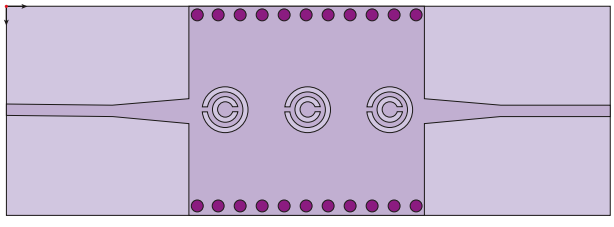

**7. An SIW bandpass filter was designed using three circular ring CSRR cells.**

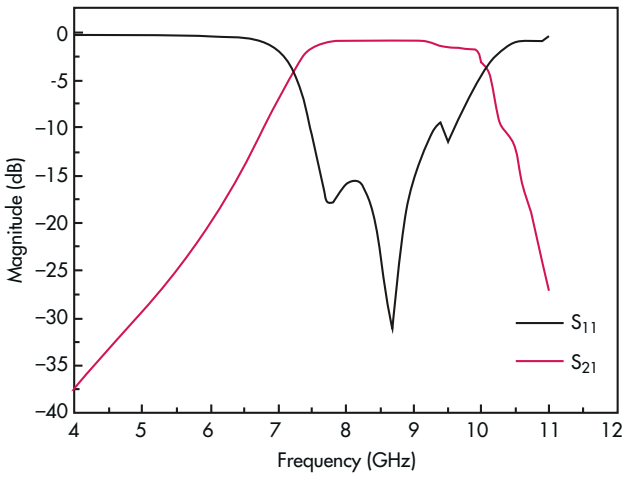


**8. These simulations plot the forward transmission ($S_{21}$) and reflection coefficient ($S_{11}$) for the SIW BPF based on the three CSRR cells.**

# Your Job just GOT a whole lot EASIER

## NEW for 2018!

Customize your workspace with personalization features that will save you time:

- Customized Parts Library – build and organize parts into an easy-to-manage library
- Product Categories - tag only the one's that matter to you
- Part/Product Alerts – keep up-to-date on product availability
- Search "Authorized Only" Distributors – your reliable source for truly vetting authorized distributors

SourceESB has built-in engineering tools and functionality, designed just for you. If streamlining your workflow and increasing productivity are important, then you will appreciate the new features added to SourceESB in 2018.

SourceESB®

SourceESB.com

*The most trusted electronics parts search engine that serves the engineer from design to purchase.*

Passive baluns can be constructed with coplanar waveguide (CPW) transmission lines, coaxial lines, or microstrip transmission lines. As an alternative approach, a broadband passive balun transformer was designed using SIW transmission-line technology *(Fig. 9)*. This SIW balun design consists of a −3-dB SIW power divider, which provides a split of a single input port to two, evenly divided output power levels, and microstrip lines that are placed on different sides of a dielectric substrate at balanced ports to obtain a 180-deg. phase shift.[3,5] Since the SIW power divider features broadband characteristics, the resulting balun structure also provides broadband frequency response that's useful for many wireless communications applications.

This use of a power divider and microstrip lines with specific electrical lengths makes it possible to realize a broadband, high-frequency balun in SIW circuit technology.[9,10] As had been shown earlier, the SIW transmission-line technology is also useful for designing and fabricating a compact BPF. By combining the circuit structures with a common SIW circuit technology, the equivalent of a multiple-function component with filtering and line-matching capabilities can be designed using a common SIW circuit architecture.

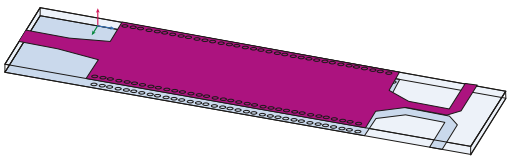

**9. The other ingredient in the SIW balun/BPF, the unbalanced/balanced transformer, is shown here in SIW transmission-line technology.**

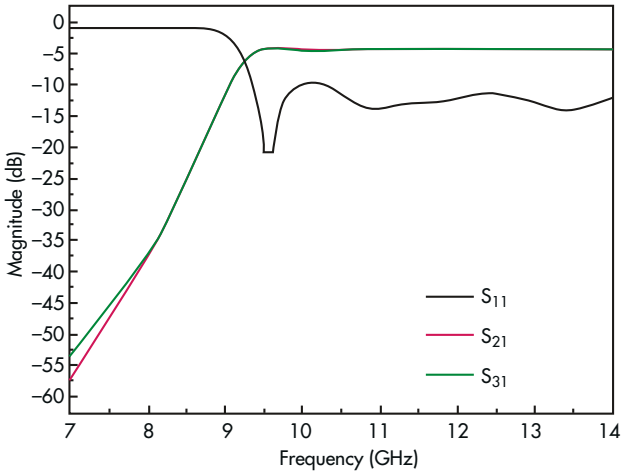


**10. The simulated performance for three scattering parameters for the SIW balun are shown here, using HFSS simulation software.**

Be ahead in 5G.
Be ready for the future.

Your 5G NR test and measurement challenges are our motivation to provide innovative solutions for your success. Bring your products to market more quickly and safely with Rohde&Schwarz test solutions. As a world market and technology leader in all areas of RF and microwave test and measurement equipment, we support the entire mobile technology lifecycle for performing measurements in the lab, in production and in the field.
Be ahead with Rohde&Schwarz in
- 5G NR testing in the sub 6 GHz and mmWave range
- Over-the-air (OTA) antenna and transceiver characterization
- Network and mobile endpoint security

Discover the Rohde&Schwarz test solutions at
**www.rohde-schwarz.com/5G**

ROHDE&SCHWARZ

Simulations of the multiple-function circuit design were performed with commercial ANSYS HFSS EM simulation software[12] to predict the amplitude response and the phase balance of the SIW planar balun, with simulated levels of scattering parameters S21 and S31 close to −3.76 dB with return loss (S11) of −20.51 dB at 9.56 GHz and with the phase responses of parameters $S_{21}$ and $S_{31}$ having a 180-deg. difference between them *(Figs. 10 and 11)*.

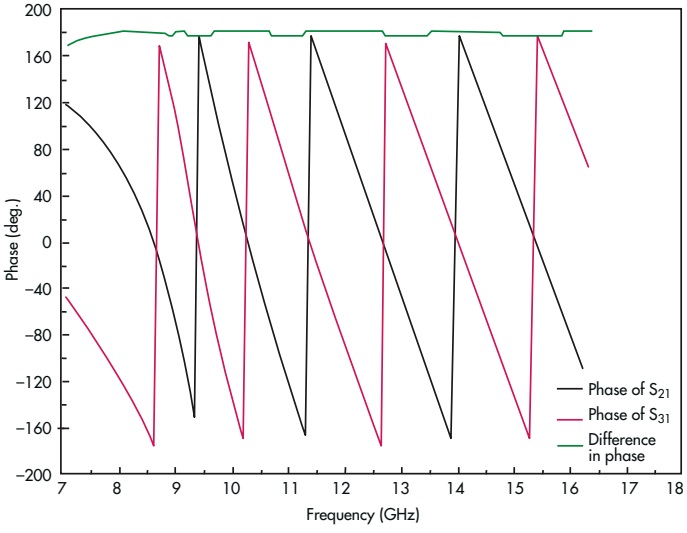


**11. The differences in phase for the outputs of the SIW balun were simulated with HFSS software.**

Using SIW CSRRs, a combination of the balun and the bandpass filter was designed for fabrication on a common circuit board.[14] Critical to the performance of the balun/filter circuit structure is the performance of the SIW power divider (presented earlier), and the cascade of 10 CSRRs that are etched on the PCB's top metal plane *(Fig. 12)*.[8] Tight control of these structures during the design and fabrication stages of this circuit help to maintain required frequency tolerances for the filtering bands with proper suppression of undesired spurious or harmonic signal content in order to achieve the widest-possible operating bandwidth for the balun/filter combination component.[9]

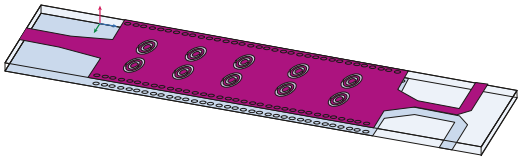

**12. The combination of the bandpass filter and the balun is modeled using SIW transmission-line technology.**


FULL LINE OF
5G Products

LV1000 Flux Coating
- Low-voiding
- Minimal flux residue
- No ECM impact

InFORMS®
- Improves bondline planarity
- Increases joint strength
- No ECM Issues

Thermal Interface Materials
- Excellent thermal conductivity
- Free from outgassing
- No pump-out or bake-out
- Reclaimable and recyclable

Implementation of 5G is happening fast and design criteria are dynamic! Let us help you with products that enable superior reliability and performance for all your packaging needs.

Contact our engineers today: shomer@indium.com
Learn more: www.indium.com/MICRV




©2018 Indium Corporation

**The balun BPF was designed in the form of a compact SIW power divider with good simulated results. It was realized with two balanced output ports on both sides of the circuit substrate to achieve a 180-deg. phase difference between the output ports.**

With the help of the HFSS software, 180-deg. reverse phase characteristics between the two output ports can be easily modeled and realized with a multilayer SIW power divider. The multilayer power divider's performance parameters are finely tuned to achieve good wideband performance. The simulation results shown in *Figure 13* indicate that the power levels of scattering parameters $S_{21}$ and $S_{31}$ are close to −3.78 dB in the frequency range from 8.26 to 13.04 GHz with return loss ($S_{11}$) of greater than −10 dB across the frequency range of 9.02 to 11.94 GHz or for 27.86% of the bandwidth. *Figure 14* shows the phase response of parameters $S_{21}$ and $S_{31}$ with a full 180-deg. difference in phase.

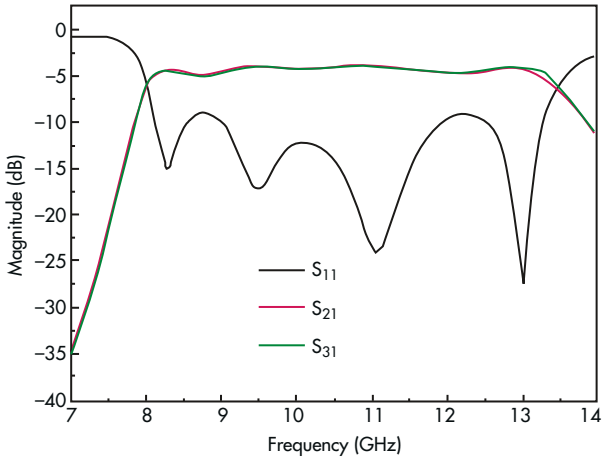


**13. The simulated performance for three scattering parameters for the SIW balun/BPF combination are shown here, using HFSS simulation software.**

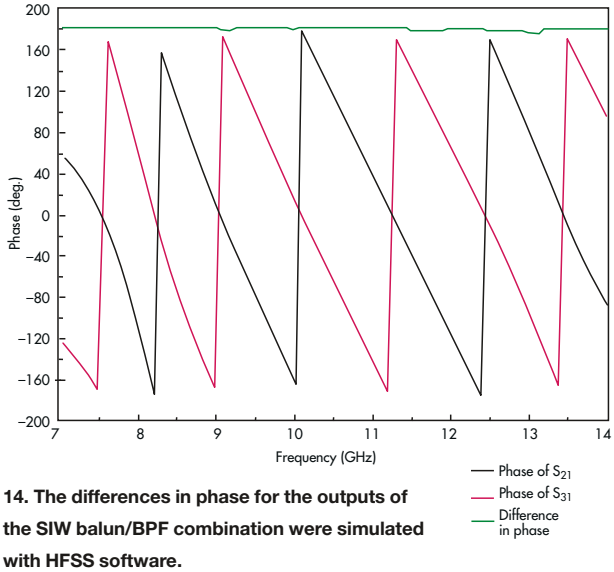


**14. The differences in phase for the outputs of the SIW balun/BPF combination were simulated with HFSS software.**

The balun BPF was designed in the form of a compact SIW power divider with good simulated results. It was realized with two balanced output ports on both sides of the circuit substrate to achieve a 180-deg. phase difference between the output ports. For good high-frequency selectivity, 10 CSRRs were etched on the top metal plane of the circuit substrate. As the EM simulations show, it is possible to achieve good balanced electrical performance and high selectivity with this SIW configuration. In fact, performance approaches that of a traditional waveguide component structure, but in a much more compact SIW component. mw


REFERENCES

1. D. Deslandes and K. Wu, "Design Consideration and Performance Analysis of Substrate Integrated Waveguide Components," European Microwave Conference, October 2002, pp. 1-4.
2. Y. Cassivi, L. Perregrini, P. Arcioni, M. Bressan, K.Wu, and G. Conciauro, "Dispersion Characteristics of Substrate Integrated Rectangular Waveguide," *IEEE Microwave Wireless Components Letters,* Vol. 12, No. 9, 2002, pp. 333-335.
3. Rahali Bouchra, "Contribution à la Modélisation Electromagnétique des structures Complexes Hyperfréquencesen Technologie SIW," Thèse dedoctorat, Département de Génie Electriqueet Electronique, Faculté de Technologie, Université AbouBekrBelkaid de Tlemcen Algérie, May 2013.
4. Nathan Alexander Smith, "Substrate Integrated Waveguide Circuits and Systems," thesis for the degree of Master of Engineering, Department of Electrical & Computer Engineering, McGill University, Montréal, Québec, Canada, May 2010.
5. Bouchra Rahali and Mohammed Feham, "Design of K-Band Substrate Integrated Waveguide Coupler, Circulator, and Power Divider," *International Journal of Information and Electronics Engineering,* Vol. 4, No. 1, January 2014, pp. 47-53.
6. Ke Wu, Dominic Deslandes, and Yves Cassivi, "The Substrate Integrated Circuits - A New Concept for High-Frequency Electronics and Optoelectronics," *Microwave Review*, December 2003.
7. Bouchra Rahali,Mohammed Feham, Achour Ouslimani, Abed-Elhak Kasberi, and Junwu Tao, "Fabricate C-Band Components with Rectangular SIW," *Microwaves & RF*, April 2016.
8. J. Bonache, F. Martin, R. M. Sillero, F. Falcone, T. Lopetegi, M. A. G. Laso, J. Garcia-Garcia, I. Gil, M. F. Portillo, and M. Sorolla, "Equivalent-Circuit Models forSplit-Ring Resonators and Complementary Split-RingResonators Coupled to Planar Transmission Lines," *IEEE Transactions on Microwave Theory & Techniques,* Vol. 53, No. 4, April 2005.
9. N. Marchand, "Transmission-Line Conversion Transformers," *Electronics*, Vol. 17, No. 12, December 1944, pp. 142–145.
10. Z. Y. Zhang, Y. X. Guo, L. C. Ong, and M. Y. W. Chia, "Improved Planar Marchand Balun with a Patterned Ground Plane," *International Journal on RF/Microwave CAE*, Vol. 15, No. 3, May 2005, pp. 307–316.
11. R. Sturdivant, "Balun Designs for Wireless Mixers, Amplifiers and Antennas," *Applied Microwaves*, 1993, pp. 34–44.
12. User's guide – High Frequency Structure Simulator (HFSS), v11.0, Ansoft Corp. *(www.ansoft.com).*
13. Dominic Deslandes, "Design Equations for Tapered Microstrip-to-Substrate Integrated Waveguide Transitions," 2010 IEEE International Microwave Theory & Techniques Symposium (MTT-S), Symposium Digest, pp. 704-707.
14. Z. C. Hao, W. Hong, J. X. Chen, X. P. Chen, and K. Wu,"Planar Diplexer for Microwave Integrated Circuits," *IEE Proceedings on Microwave Antennas & Propagation,* Vol. 152, No. 6, December 2005.

# Amazingly Low Phase Noise

# SAW VCO's

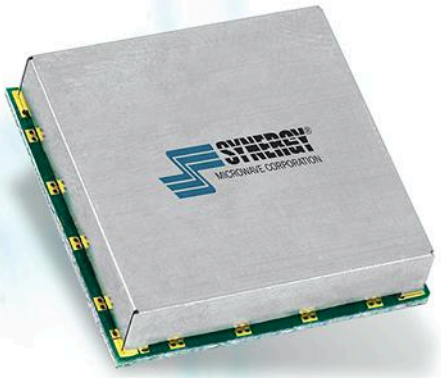


RoHS REL∞PRO® Patented Technology

## Features:

- Very Low Post Thermal Drift
- Small Size Surface Mount *

| Model | Frequency [MHz] | Tuning Voltage [VDC] | DC Bias VDC @ I [Max.] | Phase Noise @ 10 kHz (dBc/Hz) [Typ.] |
|---|---|---|---|---|
| HFSO600-5 | 600 | 0.5 - 15 | +5 VDC @ 35 mA | -146 |
| HFSO640-5 | 640 | 0.5 - 12 | +5 VDC @ 35 mA | -151 |
| HFSO745R84-5 | 745.84 | 0.5 - 12 | +5 VDC @ 35 mA | -147 |
| HFSO776R82-5 | 776.82 | 0.5 - 12 | +5 VDC @ 35 mA | -146 |
| HFSO800-5 | 800 | 0.5 - 12 | +5 VDC @ 20 mA | -146 |
| HFSO800-5H | 800 | 0.5 - 12 | +5 VDC @ 20 mA | -144 |
| HFSO800-5L | 800 | 0.5 - 12 | +5 VDC @ 20 mA | -142 |
| HFSO914R8-5 | 914.8 | 0.5 - 12 | +5 VDC @ 35 mA | -139 |
| HFSO1000-5 | 1000 | 0.5 - 12 | +5 VDC @ 35 mA | -141 |
| HFSO1000-5L | 1000 | 0.5 - 12 | +5 VDC @ 35 mA | -138 |
| HFSO1600-5 | 1600 | 0.5 - 12 | +5 VDC @ 100 mA | -137 |
| HFSO1600-5L | 1600 | 0.5 - 12 | +5 VDC @ 100 mA | -133 |
| HFSO2000-5 | 2000 | 0.5 - 12 | +5 VDC @ 100 mA | -137 |

** Package dimension varies by model ( 0.5" x 0.5" or 0.75" x 0.75").*

## Talk To Us About Your Custom Requirements.

SYNERGY® MICROWAVE CORPORATION

Phone: (973) 881-8800 | Fax: (973) 881-8361
E-mail: sales@synergymwave.com
Web: WWW.SYNERGYMWAVE.COM
Mail: 201 McLean Boulevard, Paterson, NJ 07504

Design Feature

DR. OSMAN CEYLAN | Design Engineer
DR. LAZARO MARCO-PLATON | System Engineer
DR. SERGIO PIRES | Senior Director—Innovation and Advanced Concepts
Ampleon Netherlands B.V., Halfgeleiderweg 8, 6534 AV, Nijmegen, The Netherlands

# Refine Biasing Networks for High PA Low-Frequency Stability

**Biasing networks can have a great deal to do with the low-frequency stability of RF/microwave power amplifiers based on many different types of high-frequency transistors.**

High-frequency active-device performance depends very much on the dc biasing conditions. For optimum performance, a solid-state device (SSD) requires an application-specific biasing network. Such bias networks are not only essential parts of RF/microwave circuits with SSDs, but properly designed bias networks contribute a great deal to the performance and stability of high-frequency circuits using SSDs.

SSD gain is inversely proportional to frequency, with higher gain at lower frequencies, so attention should be paid to SSD circuit design because of the strong connection between device gain and stability. For example, the response of an RF/microwave power amplifier (PA) should be carefully compensated to prevent oscillations due to the higher gain at lower frequencies.

At lower frequencies, the impact of the biasing networks is dominant compared to the impedance-matching networks. That's because the small value of the dc blocking capacitor has a high impedance at lower frequencies, and neutralizes the effects of the matching networks. Thus, a properly designed biasing network can be employed to improve SSD low-frequency stability.

Although the stability analysis of RF/microwave circuits is a major topic, partial analysis allows for inferring some ideas about the low-frequency stability issues induced by biasing networks. The influences of PA biasing networks on low-frequency stability can be shown by analyzing the simplified low-frequency equivalent of a high-power field-effect transistor (FET) and its biasing networks.

Class AB type biasing will be considered for the low-frequency stability analysis. Following the analysis, design suggestions will be presented regarding gate and drain biasing, with attention paid to RF/microwave performance parameters such as insertion loss and efficiency. Finally, a resonance investigation study of a PA and its measured results will be presented.

## POWER-AMP ABCs

A typical PA consists of an active device and at least four passive subcircuits: input impedance matching, gate biasing, output impedance matching, and drain biasing. *Figure 1* depicts such a structure. It is assumed that the values of the dc blocking capacitors are small enough to ignore the influence of matching networks on the analysis of the low-frequency response of the PA.

To better understand the challenges of achieving low-frequency amplifier stability, the intrinsic transistor components and drain biasing structure will be used to show the initial conditions of low-frequency stability regarding input impedance and transfer function. The circuit complexity will be increased step by step to demonstrate the effects of the gate-biasing components.

The analysis steps are to determine the input impedance analysis without the gate-biasing components; include

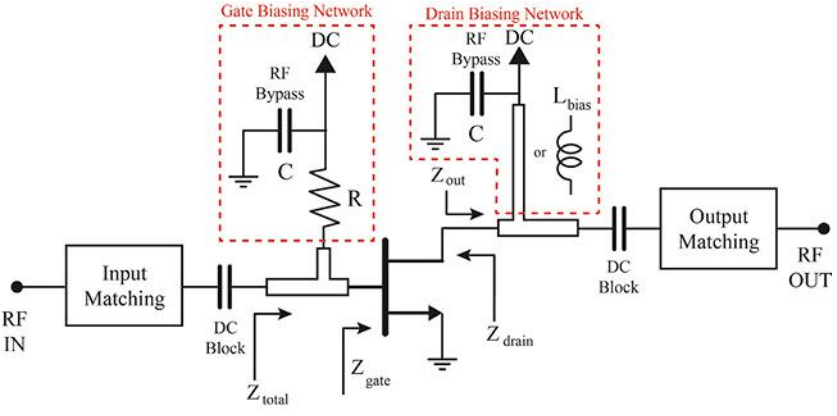


**1. This is a conventional biasing structure for an RF/microwave power amplifier (PA).**

the serial bias resistor at the gate with an ideal RF bypass; and replace the ideal RF bypass capacitors with realistic capacitor models. This analysis will be performed for a narrowband high-frequency PA, with the term "low frequency" considered as applying to frequencies to a few hundred megahertz.

A conventional biasing structure of a PA includes a resistor at the gate and an inductor at the drain *(Fig. 1, again)*. These components are RF shorted out at the dc supply point with a couple of RF bypass capacitors. Values of the dc blocking capacitors are often selected at picofarad level due to their low effective serial resistance (ESR) at the fundamental frequency and high self-resonance frequency (SRF). Therefore, the influence of matching networks can be neglected due to the high impedance of dc blocking capacitors in low frequency region.

If an ideal RF bypass is assumed at the drain, then bias inductor $L_{bias}$ has an ideal RF ground. The values of the intrinsic gate-source and drain-source capacitors, $C_{gs}$ and $C_{ds}$, respectively, are in the picofarad range so that they can be neglected as well at low frequencies. Capacitance $C_{gd}$ is the intrinsic gate-drain capacitance of the transistor. Although $C_{gd}$ is even smaller than $C_{gs}$ and $C_{ds}$, it is a feedback component of the circuit, so it has a significant role on stability.

With these assumptions, the low-frequency equivalent of a PA without gate-biasing network can be depicted *(Fig. 2)*. Impedance Zgate is the impedance observed at the transistor gate:

$$Z_{gate} = (Z_{Cgd} + Z_{Lbias})/(1 + g_m Z_{Lbias}) \quad (1)$$

$$Z_{gate}(s) = 1/sC_{gd} + sL_{bias})/(1 + g_m sL_{bias})$$

$$= (1 + s^2 L_{bias} C_{gd})/(sC_{dg} + s^2 g_m L_{bias} C_{gd}) \quad (2)$$

$$Z_{gate}(j\omega) = (1 - \omega^2 L_{bias} C_{gd})/(j\omega C_{gd} - \omega^2 g_m L_{bias} C_{gd}) \quad \text{where } s = j\omega \quad (3)$$

Since ω is in the megahertz frequency range and the gate-drain capacitance $C_{gd}$ is less than a few picofarads, $\omega^2 L_{bias} C_{gd} << 1$ and Eq. 4 holds:

$$Z_{gate}(j\omega) = 1/(j\omega C_{gd} - \omega^2 g_m L_{bias} C_{gd}) \quad (4)$$

and

$$\mathrm{Re}\{Z_{gate}\} \approx 1/(\omega^2 g_m L_{bias} C_{gd}) \quad (5)$$

Oscillation startup conditions at a particular frequency can be described as[1]:

$$\mathrm{Re}\{Z, \omega\} < 0, \mathrm{Im}\{Z, \omega\} = 0 \quad (6)$$

$$(\partial \mathrm{Im}\{Z, \omega\})/\partial\omega|_{\omega = {}_{\omega}0} > 0 \quad (7)$$

Eq. 5 shows that the real part of the impedance is negative at low frequencies. Although the negative resistance is not the only condition needed to cause oscillations (Eqs. 6 and 7), its elimination is a significant step in taking a PA into a safe zone against low-frequency oscillations. It is obvious that making the real part of impedance positive with the configuration of *Fig. 2* is not possible.

Since gate-drain capacitance $C_{gd}$ and transconductance $g_m$ are the intrinsic device parameters that depend on the transistor's dc operating points, varying them affects circuit performance using that transistor. Therefore, a designer is only able to change the drain-biasing inductance value to decrease the negative resistance.

Yet, the drain-biasing inductance cannot simply be changed without consideration of other circuit parameters. For example, if the drain-biasing transmission line is a quarter-wavelength (λ/4) line, the low-frequency inductance of the line is given by[2]:

$$L = Z_0(l/c) \quad (8)$$

where c is the speed of light; l is the length of the microstrip line; and $Z_0$ is the characteristic impedance of the microstrip line. The width of the microstrip line should be decreased to increase $Z_0$ and inductance of the microstrip line. But a microstrip transmission line with reduced width is not suitable for high-power applications because it has reduced current-handling capability and increased resistance.

In addition to the impedance analysis, the circuit transfer function can also give valuable information about stability. The pole and zero locations of the transfer function can be analyzed to understand the stability behavior of the circuit.

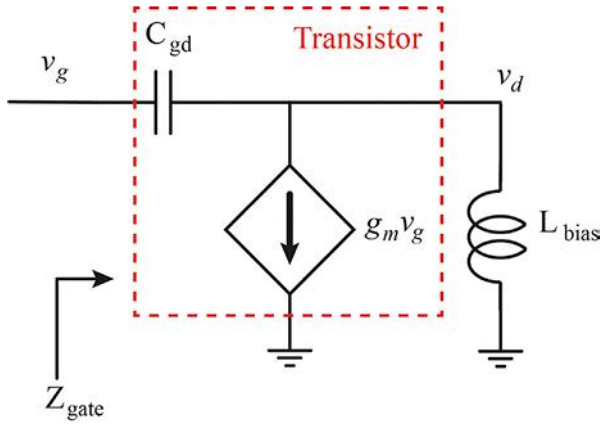


**2. Shown is a low-frequency equivalent circuit of an RF/microwave PA without biasing circuitry or biasing components.**

The voltage transfer function of the circuit depicted in *Fig. 2* is shown in Eqs. 9 and 10:

$$\upsilon_d(s)/\upsilon_g(s)$$

$$= (1 - g_m ZC_{dg})/(1 + ZC/ZL_{bias}) \quad (9)$$

$$\upsilon_d(s)/\upsilon_g(s)$$

$$= (s^2 L_{bias} C_{dg} - sg_m L_{bias})/(s^2 L_{bias} C_{dg} + 1)$$

$$= s(s - g_m/C_{dg})/(s^2 + 1/L_{bias} C_{dg})) \quad (10)$$

From Eq. 10, it can be seen that the circuit transfer function has zeros at s = 0 and s = $g_m/C_{gd}$ and poles at s = ±j/($L_{bias}C_{gd}$). The circuit is marginally stable because the poles are on the imaginary axis Y. The stability of a marginally stable system depends on the type of input signal, so that a particular signal can cause oscillation. On the other hand, since the poles on the Y-axis are inclined to shift due to the temperature changes, nonlinear behavior of components, etc., a marginally stable system is not practically realizable.

Inserting a serial resistor to the gate-biasing network is a frequently used method to improve the stability. In this section, the contribution of the gate-biasing resistor to the low frequency stability is analyzed. *Figure 3* shows the low-frequency equivalent circuit of a PA with a gate-biasing resistor.

If Eq. 4 is used to derive total impedance including the gate resistor, then $Z_{total}$ is

$$Z_{total} = R//Z_{gate} = RZ_{gate}/(R + Z_{gate}) \quad (11)$$

$$Z_{total} = [R(1 - \omega^2 L_{bias} C_{gd})]/(1 - \omega^2 L_{bias} C_{gd} + j\omega RC_{gd} - j\omega^2 g_m R L_{bias} C_{gd}) \quad (12)$$

Since the frequency under consideration is in the megahertz range, the gate-drain capacitance $C_{gd}$ is very small, and bias inductor $L_{bias}$ is at a nanofarad value, the $\omega^2 L_{bias} C_{gd}$ term in the numerator is smaller than unity. Therefore, $Z_{total}$ is almost equal to R for small values of R. For example, assuming that R = 10 Ω, a frequency of 200 MHz, $L_{bias}$ of 10 nH, $C_{gd}$ of 0.3 pF, and $g_m$ of 1000 mS, $Z_{total}$ = 9.9 + j0.44 Ω. However, this assumption is not correct for larger values of R. For example, if R = 1 kΩ, then $Z_{total}$ = 49.5 + j217 Ω.

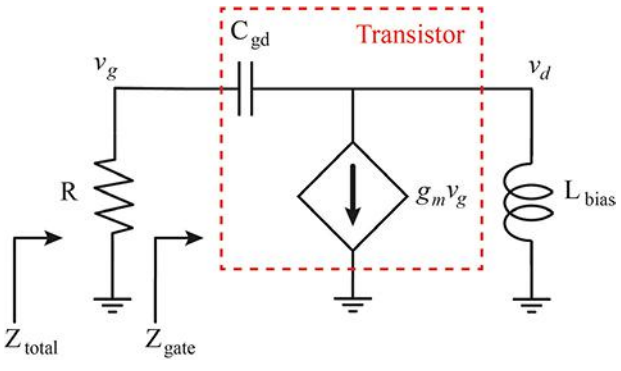


**3. Here's a low-frequency equivalent circuit of an RF/microwave PA with a biasing resistor.**

Eq. 12 shows that a suitable bias resistor at the gate provides positive input resistance in the low-frequency region. While gate resistor R may seem to be a form of "magic" component for achieving low-frequency stability, the assumption is valid with an ideal RF bypass circuit. Microfarad- and nanofarad-valued capacitors tend to have high parasitic series inductance and resistance values, causing strong resonances in the low-frequency region. Any inductance of significant value due to an RF choke or a microstrip transmission line can affect the low-frequency resonances.

*Figure 4* shows $Z_{gate}$ and $Z_{total}$ input impedances, with and without a gate-biasing resistor, and when considering real capacitor models (100 pF and 33 μF with 10-nH series inductance) instead of an ideal RF bypass capacitor. Strong resonances in the bias network can cause low-frequency oscillations in addition to reducing the video bandwidth and degrading the intermodulation-distortion (IMD) performance of an amplifier.

The structure of a PA biasing network will involve tradeoffs among stability, linearity, and complexity. Gate- and drain-biasing networks should contribute to improvements in overall performance and reliability. By understanding some of the essential rules for biasing networks, it is possible to achieve a desired compromise among the key design goals, including low-frequency stability, for an RF/microwave PA.

## SEEKING STABLE BIAS NETWORKS

As has been shown, a series resistor in the gate biasing circuitry is a vital component for achieving low-frequency stability. The value of the resistor depends on a number of factors, including class of operation, saturation level, transistor technology, and device size. A smaller resistor may not have enough resistance to provide a wide-range positive input impedance. Conversely, a larger-valued resistor may cause undesired resonances and voltage swings on gate biasing due to gate current in different devices, such as in HEMTs.

A small amount of current, such as 1 to 2 mA, can flow down a transistor gate under the compressed operation of a high-power HEMT. The peak value of the gate current will depend on the SSD technology and will be proportional to the physical size of the SSD. For example, the gate current of a 100-W, 50-V GaN HEMT device is a few milliamperes.[4] The voltage swing on the gate bias caused by a bias resistor changes the dc operating point of a PA, resulting in fluctuations in drain current and amplitude modulation of the signal.

*Figure 5* and *Table 1 (online only)* show some gate-biasing structures and component values for several power levels and frequencies commonly used for Ampleon PA demonstration boards. *Fig. 5's* resistor-based biasing network "A" is suitable for under-1-GHz applications. Bias network "C" is well-suited for higher-frequency applications. In some cases, the gate-biasing network is also part of the impedance matching network, and bias network "D" is an example of that type of configuration. A shunt resistor, such as R2 in bias networks "A" and "C" in Fig. 5, relieves stability problems, but is not suitable for depletion-mode HEMTs due to their requirement of negative bias. A dc blocking capacitor, such as C2 in bias network "B" of *Fig. 5*, may be needed in some cases.

As shown in *Fig. 4*, the wideband response of all components in a gate-biasing network should be inspected for resonances. However, such an investigation can be cumbersome and sometimes impossible due to insufficient models of biasing components. A measurement-based analysis can be useful and time-

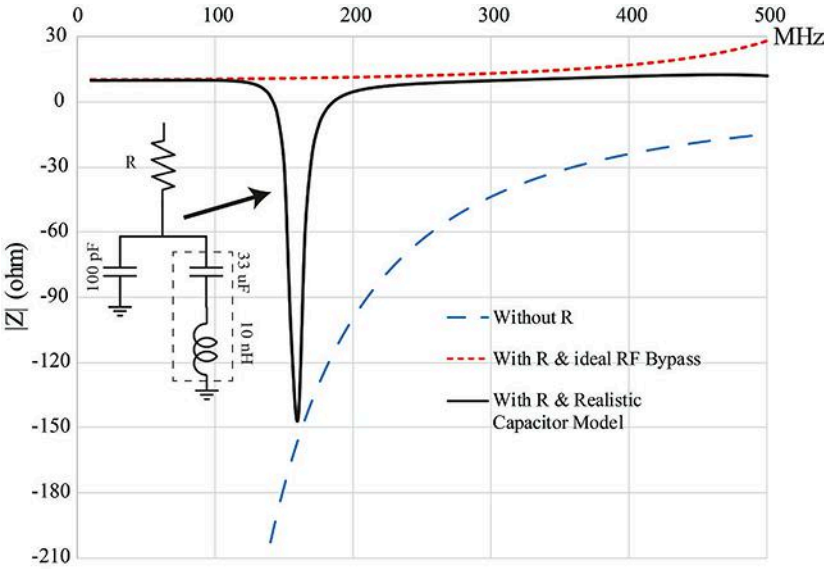


**4. Input impedance variance of a SSD at low-frequency region; without resistor, with resistor, and ideal RF-bypass, with resistor and realistic component model ($C_{dg}$=23 fF/W, $g_m$=30 mS/W [3], L=10 nH, R=10 Ω, P=30 W).**


PicoVNA™
Vector Network Analyzer

- 300 kHz to 6 GHz
- > 5000 .s2p points/s
- To 118 dB and 0.005 dB RMS
- 8/12 term cal. incl. unknown thru

The PicoVNA 106 brings you full-function bidirectional vector network analysis at an unprecedented low price. Fast, professional-grade measurement and analysis that you can afford.

For more information, visit
**www.picotech.com/A72**

pico® Technology

only $5995

Email: sales@picotech.com. Errors and omissions excepted.
Please contact Pico Technology for the latest prices before ordering.

saving, as will be shown in an example in which resonances are removed with the aid of S-parameter measurements and modeling.

The drain-biasing network influences the overall efficiency and RF performance of the PA directly. Moreover, extra attention is required during its design to increase the reliability of the PA due to the existence of the high voltage and current on the drain-biasing line. The dc, low-frequency, and high-frequency circumstances must be considered at the same time to achieve desired the PA performance, and stable and reliable operation.

The tradeoffs between these conditions shape the structure of a biasing network:

- The current-handling capability and dc resistance of its dc characteristics.
- The low-frequency stability and biasing induced memory effects of its low-frequency characteristics.
- The isolation and RF leakage of its high-frequency characteristics.

Eq. 5 shows that a larger value of the drain biasing inductance aids low frequency stability. But a narrower microstrip line is needed to increase the characteristic impedance of the biasing line for a larger inductance (Eq. 8). Decreasing the width of microstrip line increases its resistance and reduces its current-handling capability. A microstrip line with high dc resistance not only results in power loss and heating effects, but also a voltage swing at the drain, causing signal envelope distortion, PA linearity degradation, and asymmetry at adjacent channels. It complicates digital predistortion (DPD) efforts and can cause a failure in a DPD attempt. *(Continued on mwrf.com)*

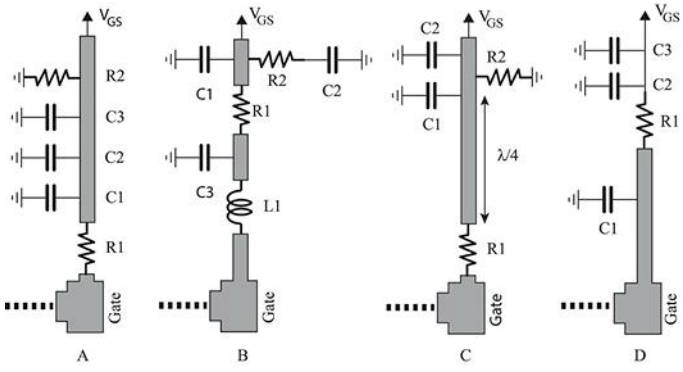


**5. Frequently used gate-biasing networks for Ampleon PA demonstration PCBs.**

TO READ this article in its entirety (including references), or download a PDF of the article, please visit *www.mwrf.com*.

# FOCUSED

## & #FIERCELY INDEPENDENT

Good work comes from determination, focus and free thinking. As engineers you know this. We hold ourselves to the same truth - a determination to bring you bold insights and information that helps you do your jobs better - with a promise to deliver unbiased, expert content. Informa Design Engineering & Sourcing is the only independent insight and information source holding the promise of your truth.

Electronic Design. Machine Design. Power Electronics. Microwaves&RF. SourceESB.

JACK BROWNE | Technical Contributor

# What's the Difference Between Long- and Short-Haul Links?

**Wireless communications can be performed over near and far distances depending on a number of factors, including transmit power, receive sensitivity, and operating frequency.**

Wireless technology has become an essential part of modern lives, almost as much as electricity. High-frequency wireless signals are applied in many different forms, typically for communications. Signals may travel as far as from the Earth to an orbiting satellite, and back again, to as nearby as inches from a wireless transceiver in an office building.

Such communications systems operate by means of long- and short-haul links, requiring such critical components as antennas, receivers, and transmitters. But, while the block diagrams for these links may appear quite similar, the performance requirements for wireless communications links can be quite different, as typified by the many different standards that capture the operating parameters specific to each type of communications system.

For a wireless communications link, the maximum possible distance while maintaining normal radio operation will be determined by a number of factors, including transmit power, receive sensitivity, signal frequency/wavelength, and interference from other radio waves and the surrounding environment. Radio links are usually considered under ideal conditions, which is the line-of-sight (LOS) distance between the transmitter and the receiver. As a condition of electromagnetic (EM) propagation, the radio waves will suffer some amount of path loss even with optimum LOS operating conditions and no obstructions. Path loss refers to the decrease in strength of radio waves over distance.

Transmit power is one of the main factors in achieving an RF/microwave link of any considerable distance. This is due to the fact that radio waves follow an inverse square law in terms of distance traveled. When the distance of a radio link is doubled, there will be one-fourth the amount of transmitted power at the receiver.

From the point of view of the transmitter, if the transmit power for an RF/microwave link is quadrupled, or raised by 6 dB from a starting point, it will double the distance that can be covered by that radio link, assuming the same sensitivity at the receiver for both transmitter power levels. Wireless communications systems designers typically use a link budget to account for the various gains and losses in a link to estimate the amount of signal power that's expected to be available at the receiver.

## THE LONG AND THE SHORT OF IT

Although there's no absolute definition as to what constitutes a short-haul wireless link versus a long-haul link, a short-haul link is considered anything covering a few kilometers or less while a long-haul link is usually 20 to 50 km or longer. The relatively long wireless links between cellular communications systems, such as 4G LTE, can usually be identified, at least at one end, by their fairly large parabolic dish antennas *(Fig. 1)*.

**1. Long-haul microwave links can be identified by their use of large, parabolic dish antennas at each end of the link.**

Frequency plays a part in any link budget, especially for longer links, since long-distance links require the longer propagation distances of larger-wavelength, lower-frequency signals rather than smaller-wavelength, higher-frequency signals. Long-distance microwave radio links are usually operating at lower frequencies licensed by an applicable government organization, such as the Federal Communications Commission (FCC). Licensed bands at 6 and 11 GHz are now used for long-haul links in 4G LTE systems, to transfer callers from their local access point to their intended listener.

With the growing number of users for 4G LTE wireless services, the avail-

able bandwidth of these licensed link frequencies is quickly being saturated. Today's wireless users seek more than voice service, using their smartphone or other mobile device for internet access, e-mail, high-speed data transfers, and video streaming.

The rapid consumption of network and link capacity in 4G LTE has spurred the design and development of the next or fifth-generation (5G) wireless network with its totally different radio link structure. Rather than linking large cells or base stations over relatively long distances *(Fig. 2)*, a 5G network will use higher-frequency backhaul links over shorter distances, relying on a much greater number of smaller, closely spaced cell sites to create a wireless network. The shorter links will be made at licensed and unlicensed millimeter-wave frequencies with their abundance of available bandwidth to serve the growing number of users.

The smaller cells and higher frequencies of 5G radio links will employ smaller antennas than 4G LTE systems. In either network approach, installing a long-haul link with optimum performance requires precise alignment of the antennas at both ends of the link.

In 4G LTE systems, with their larger antennas, antennas are aligned with the aid of both software and hardware. Simulation software can be used to perform a site survey at each end of the link, to model the effects of signal-absorbing objects like foliage as well as signal reflections from nearby metal surfaces. The LOS bearing of the antenna at each end of the link must be approximated and then the appropriate test equipment, such as a microwave signal generator and spectrum analyzer, used to generate in-band signals and measure the signal strength for both link directions. Shifting the position of either antenna will impact the received signal strength.

When greater distance is needed between antennas in a long-haul link, say, because of available sites for LOS antenna placement, a number of options

**2. Current 4G LTE cellular communications networks rely on larger antennas and base stations than those that will be used in 5G systems.**

are available for extending the operational distance of a long-haul microwave link. For example, the gain of one or both of the antennas in the link can be increased to boost the signal strength. As a complement, the loss of associated components in the link, such as interconnecting coaxial cables, couplers, and filters, can be minimized through careful specification of these components.

Further distance, as noted earlier, can also be achieved by increasing the transmit power on both sides of the link. Similarly, receivers with enhanced receive sensitivity can extend the effective link distance. Of course, all of these options result in higher equipment costs, which may be unavoidable due to available site locations.

## 5G'S SHORTER RADIO LINKS

Although 5G will employ somewhat shorter radio links than 4G LTE systems, with smaller antennas as a function of shorter wavelengths, the antenna alignment procedure may be made somewhat more complicated by the use of mmWave signals. While smaller antennas can be easier to align over shorter distances than larger antennas over longer distances, the required gain of the antennas will play a role in the alignment difficulty, with high gain making alignment more difficult. 5G's radio links will enhance antenna performance through the use of multiple smaller antennas, for focused beamforming use and in multiple-input, multiple-output (MIMO) architectures.

Many wireless users are quite familiar with short-haul wireless links from their daily use of wireless local-area networks (WLANs) and the many short-range wireless standards for connecting devices like mobile phones, computers, and even a growing number of Internet of Things (IoT) sensors. The IEEE has developed many standards for WLAN equipment and networks as variations on the initial IEEE 802.11 WLAN standard at 2.4 GHz and 2 Mb/s, including popular Wi-Fi short-haul applications.

Other versions of IEEE 802.11 include IEEE 802.11a, which uses more available bandwidth at 5 GHz to achieve data rates to 54 Mb/s; IEEE 802.11ac, which combines three data streams each at 433 Mb/s to provide data rates to 1.3 Gb/s; and even a 60-GHz standard, IEEE 802.11ad, which is capable of data rates to 7 Gb/s. While these standards detail frequencies, bandwidths, modulation types, and other operating parameters, they don't specify link distance.

Most users associate wireless standards for WLAN as being short-haul wireless applications. However, they're not limited to any specific range, and can be extended in operating distance by means of the same practices applied to long-haul links or by adding repeaters that relay signals over longer distances.

Longer-range versions of Wi-Fi equipment have been developed in recent years to create longer unlicensed radio links than possible with conventional Wi-Fi equipment. These long range Wi-Fi networks, which operate within the established, unlicensed 2.4-GHz ISM band for Wi-Fi, offer options to cellular networks and even satellite links for longer-distance point-to-point communications. Still, the link budget requirements apply, and the radio link can only go as far as its frequencies, antennas, receivers, and transmitters will allow. mw

# SMARTPHONE Manufacturers Confront 5G Challenges

The pressure is on for smartphone manufacturers to add 5G New Radio (NR) support to handset designs even while 5G standards are still being developed. Initial mobile deployments will utilize the non-standalone (NSA) 5G NR specification, which creates additional RF challenges due to the need to simultaneously enable 4G LTE and 5G connectivity. These topics and more are discussed in Qorvo's white paper "Is Your Handset RF Ready for 5G?," which delves into what the advent of 5G means to smartphone manufacturers.

Qorvo Inc.,
7628 Thorndike Rd.,
Greensboro, NC 27409;
(336) 664-1233;
www.qorvo.com

The white paper explains that uncertainties still exist regarding key details of fundamental RF specifications for 5G. Specific points mentioned include power back-off levels, regional band combinations, uplink multiple-input, multiple-output (MIMO), and supplemental uplink (SUL). Furthermore, inclusion of 5G content in time for planned network deployments places pressure on smartphone manufacturers to develop the implementation strategies needed to meet tough 5G RF requirements.

Various challenges are associated with adding 5G support to handsets that are already densely packed with 4G LTE functionality. Enabling the dual 4G LTE/5G connectivity required for the 5G NSA specification results in significantly greater levels of RF complexity. In many cases, operators are expected to combine 4G FDD-LTE bands with a 5G band. The NSA specification allows the handset to transmit on one or more of these LTE bands while also receiving on a 5G band. However, this scenario means that harmonics of the transmit frequencies can potentially de-sense the receiver.

Dual connectivity is associated with other challenges, such as accommodating two primary cellular antennas in a handset. Power management is another concern, due to the need for an additional dc converter. 4-×-4 MIMO represents a challenge, too, as does the unprecedented bandwidth and new waveforms utilized for 5G communications.

The white paper notes that many existing 3G/4G spectrum allocations will be refarmed for 5G NR bands, resulting in additional complications. The document concludes by noting that RF suppliers must raise the bar in areas like power-amplifier (PA) design, RF front-end (RFFE) module integration, antenna tuning, and antenna-plexers.

# SYSTEM SIMULATION SOFTWARE Unravels RF Links

**ACCURATELY PREDICTING RF LINK** performance early in the design cycle is important for cellular, radar, and satellite applications. Although spreadsheets and rule-of-thumb methods have traditionally been used, they provide limited insight into RF links of next-generation wireless systems. An alternative approach is to utilize RF system simulation software, which is the topic of the white paper "Predicting Critical Metrics for Wireless RF Links" from National Instruments.

Spreadsheets have traditionally been used to calculate parameters, such as cascaded noise figure (NF) and 1-dB compression (P1dB). The white paper notes that spreadsheets offer the benefit of being readily available. They also allow for simple data entry.

However, new complex 5G specifications bring to light the limitations of spreadsheets. The white paper notes that spreadsheets are based on standard equations. Therefore, they do not typically account for other factors, such as mismatches between components. And spreadsheets usually do not support data files (such as touchstone files) and spur tables. Neither yield analysis nor optimization techniques, which are becoming increasingly important, are supported as well.

AWR Corp.,
1960 E. Grand Ave.
Suite 430, El Segundo, CA
90245; (310) 726-3000;
www.awrcorp.com

The white paper explains that a more modern approach is to use a system design software tool. With the Visual System Simulator (VSS) software, designers can start from a spreadsheet interface to define components such as amplifiers and mixers. They can then define the circuit measurements and automatically generate a system diagram.

Three examples are presented to demonstrate the capabilities of system design software. The first involves an RF link that's analyzed with both a traditional spreadsheet and design software, with each producing different results. Analyzing the local-oscillator (LO) path with the system design software revealed the cause of the discrepancy. Such analysis could not be performed with a spreadsheet, demonstrating the benefits of design software. The second example shows how the software can be used to vary an inductor value of a filter in the link, and then observe the changes in link NF. The third example highlights a spur analysis tool within the software.

# PRECISION ATTENUATORS

## 2 W to 100 W

*50 W & 100 W models*

NEW
*BW-V Series*
*50 GHz models*

## DC-50 GHz *from* $29.95 ea. (1-49)

Customers trust Mini-Circuits BW-family precision fixed attenuators for accuracy, reliability, and repeatability. Now, we've expanded your choices by adding the BW-V series, covering even more applications from DC up to 50 GHz! With fixed attenuation values from 3 to 20 dB, these new, ultra-wideband models feature 2.4mm connectors and provide outstanding attenuation accuracy, excellent VSWR, and RF power handling up to 1W. Our full "BW" family of fixed precision attenuators now includes over 70 models with attenuation values ranging from 1 to 50 dB and power handling from 1 to 100W to meet your requirements with performance you can count on.

Visit minincircuits.com for free data, curves, quantity pricing, designer kits, and everything you need to find the right BW attenuator for your needs. All models are available off the shelf for delivery as soon as tomorrow!

*RoHS compliant*

Mini-Circuits®

**www.minicircuits.com** P.O. Box 350166, Brooklyn, NY 11235-0003 (718) 934-4500 sales@minicircuits.com 

JOHN DUNN | EM Technologist, AWR Group, NI
*www.awrcorp.com*

# Dive into EM/Circuit Co-Simulation of a T/R Front-End Module and Actively-Scanned Array, Part 2

**This concluding part examines multi-technology simulation of an actively-scanned antenna array, involving technologies ranging from parameterized 3D cells to 3D EM extraction.**

5G is poised to bring more integrated and sophisticated antenna and circuit modules to the modern defense and commercial electronics markets. Part one of this article examined today's multi-technology circuit and electromagnetic (EM) simulation challenges and the software tools needed to support the successful design of 5G products.

Part two presents examples that illustrate the use of multi-technology in an EM simulation and EM/circuit co-simulation of an actively-scanned antenna array. Advanced technologies such as parameterized 3D cells, shape preprocessing and simplification, 3D EM extraction, and in-situ measurements are described.

## EXAMPLE: MULTI-TECHNOLOGY RFIC/MMIC PACKAGE ON BOARD

In this case, we'll illustrate the use of multi-technology in an EM simulation. The area of interest is the launch from the board onto the package and then onto the chip within the package *(Fig. 1)*. The board uses a printed-circuit-board (PCB) library. The device package utilized is quad, flat, no-leads (QFN).

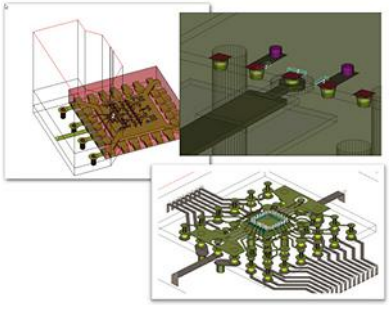

**1. Shown is an RFIC/MMIC in a QFN/flip-chip/wire-bonding package on a PCB.**

The package is connected to the chip by means of bond wires. Three libraries are used in this example, one each for the board, package, and chip layout cells. The designer is interested in answering questions about the performance of the launch, grounding issues, package resonances, layout optimization, and performing yield analysis for manufacturability issues.

Hierarchy is being used in this EM project to control the multiple technologies. Each level uses one technology, ports and boundaries are added at the top level, and the final layout is then flattened and sent to the simulator *(Fig. 2)*. Shown on the left is the list of layout cells. Notice the listing for "board partial package" at the top level, which uses a board technology. Also depicted is "full chip," which is a sub-cell that leverages gallium-arsenide (GaAs) chip technology.

The NI AWR Design Environment employs the same stackup and material menus in each of the different technology libraries, making it easier to create and maintain the various technologies. In addition, different EM simulators use the same menus, enabling the designer to easily switch between EM simulators without worrying about different stackup or materials settings. For example, it is possible to switch between two different supported 3D simulators without any changes required other than for the simulator selection setting. Different simulators may implement the various settings differently, such as how they handle boundary conditions.

*Figure 3* shows the stackup for a typical board. This same stackup can be used in AXIEM, Analyst, or third-party simulators without modification. The stackup also includes shape simplification rules, which simplify the geometry to produce a smaller mesh and reduce the problem size. The same simplification rules can be used for all simulators.

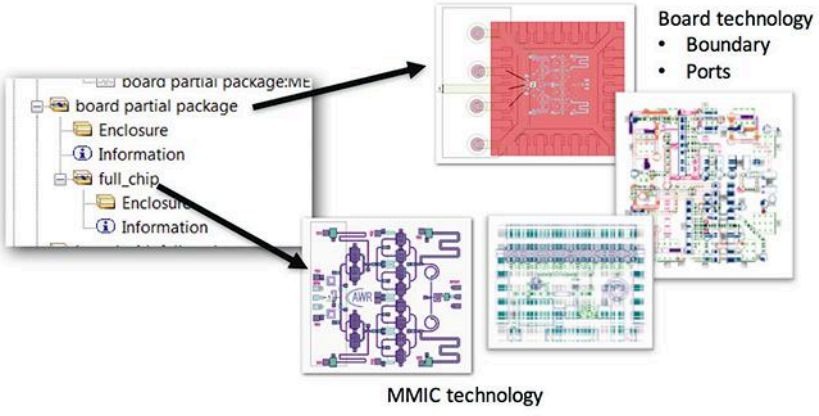


**2. With hierarchy, each level uses one technology, ports and boundaries are added, and the final layout is flattened.**

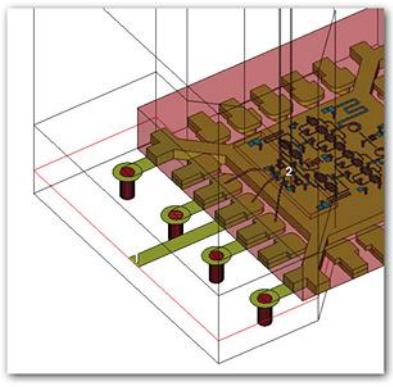

**4. Ports 1 and 2 are wave ports in Analyst and CST, but lumped ports in HFSS.**

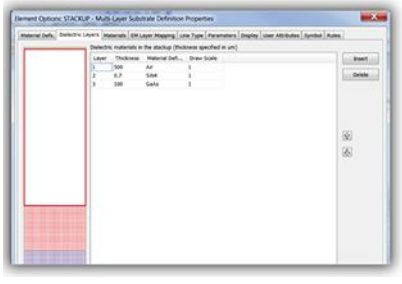

**3. Each technology gets its information from the appropriate stackup block.**

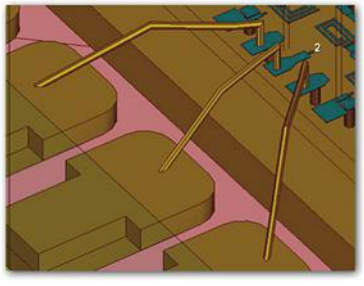

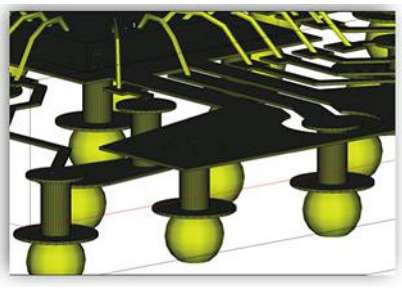

**5. PCells can represent common types of 3D objects, such as bond wires, BGAs, QFN packages, and SMA connectors.**

Ports and boundaries are placed at the top level of the layout. Note that a boundary for Analyst does not need to enclose an entire layout. Only EM effects inside the boundary will be simulated. Therefore, designers should be careful that important effects, such as coupling between the elements, are not left out when using this feature. The port type depends on the simulator. In *Figure 4*, Ports 1 and 2 are wave ports in Analyst, lumped ports in HFSS, and wave ports in CST *(www.cst.com)*, a Dassault Systèmes company.

## PARAMETERIZED 3D CELLS

Libraries can contain 3D cells of predrawn shapes, which the designer can place in the layout. The cells can be parameterized, making it possible to modify the shapes by simply changing various parameter values—for example, the diameter or height of a BGA ball can be changed with parameters. These cells are sometimes called 3D parameterized cells (3D PCells). The layout in *Figure 5* shows several 3D PCells being used, which in this case are bond wires and BGAs.

The grounding vias in *Figure 6* represent another example of using 3D cells from the library. These vias were selected from the standard via parts list that ships with the library. The layout can be used for vias, multi-metal layer lines, and spirals. *Fig. 6* shows the grounding vias from the board process design kit (PDK).

It is possible for designers to create their own cells by drawing them in the 3D layout editor integrated within Microwave Office. Parameters can be used in the drawing, which are then exposed in the software so that the layout can be easily changed. The custom cells can be added into the 3D parts library for use in other projects. In this way, companies are able to have their own proprietary parts libraries, which are shareable among all engineers.

## SHAPE PRE-PROCESSING AND SIMPLIFICATION

Many features in EM layout are needed mechanically in the drawing, but are not necessary for the simulation. These features create many meshes when the problem is solved, which uses more memory and takes longer for the simulator to solve. Furthermore, very small meshes can be created, leading to a poorly conditioned problem and possible solver error.

Many features in EM layout are needed mechanically in the drawing, but are not necessary for the simulation. These features create many meshes when the problem is solved, which uses more memory and takes longer for the simulator to solve.

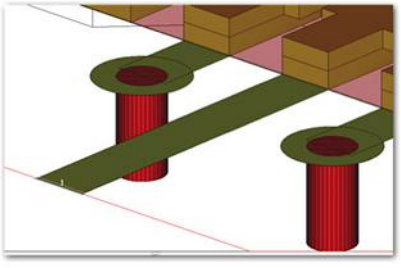

6. This figure illustrates grounding vias from the board PDK.

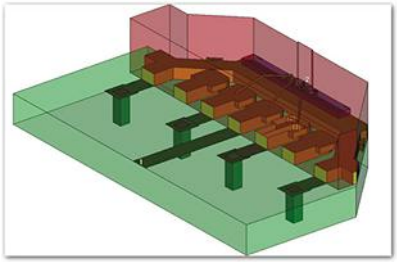

7. The board vias become squares after simplification rules have been applied.

The shape simplification technology in NI AWR Design Environment software is designed to solve this problem. PDKs have rules for shape simplification that remove small sides, unite vias, reduce the number of sides of circles/vias, and remove small indentations in multiple metal layers. *Figure 7* illustrates how the board vias become squares after simplification rules have been applied.

Simplification of the geometry, however, has its dangers. The various shapes may disconnect or nets can become shorted, although the engine tries to prevent this from happening. An annotation in the layout permits the designer to see the net connectivity after geometry simplification and meshing. *Figure 8* is an example in which the various colors show the different dc connected nets.

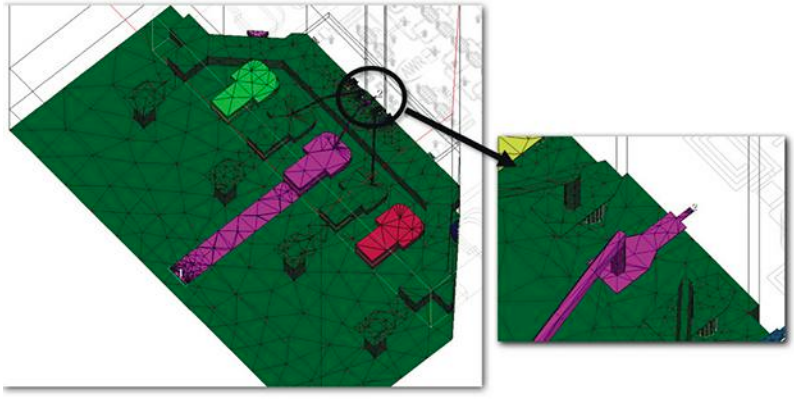

8. Here's a mesh example that shows connectivity.

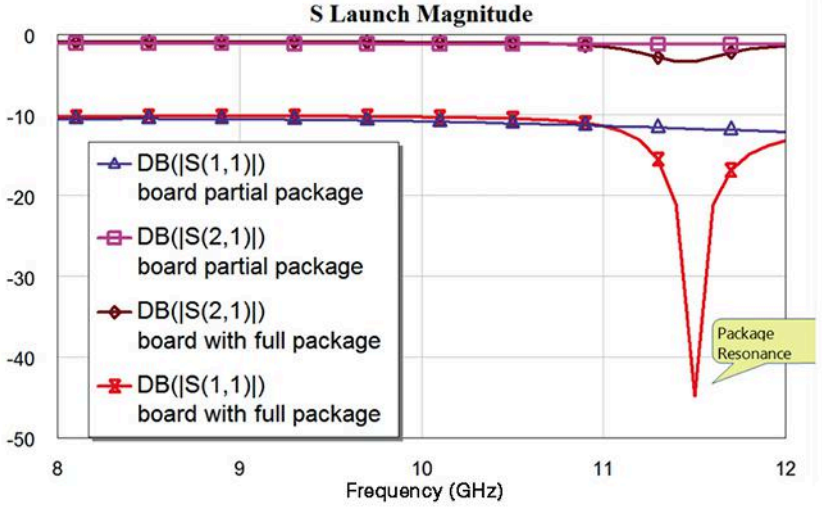


9. Shown are the simulation results of the front end of the package along with the entire package from Fig. 5.

## SIMULATION RESULTS

*Figure 9* shows the results from simulating the package in *Fig. 1*. First, the front end only was simulated using the boundaries shown in *Fig. 4*. The boundary was then extended to include the entire package and subsequently the results were compared. The difference can be seen in the large dip in the magnitude of $S_{11}$ due to a package resonance, indicating that the package needs better grounding.

## 3D EM EXTRACTION

EM extraction sends the layout of a schematic to the EM simulator automatically. This process usually involves a 2D layout that's delivered

## Tiny LTCC Bandpass Filters Offer Center Frequencies from 415 to 618 MHz

Mini-Circuits' BFTC Series low-temperature-cofired-ceramic (LTCC) bandpass filters combine high out-of-band rejection and low passband insertion loss in compact ceramic packages measuring only 0.150 × 0.150 × 0.059 in. (3.81 × 3.81 × 1.50 mm). The RoHS-compliant hermetic LTCC filters are temperature stable from -40 to +85°C and feature typical 25-dB out-of-band rejection and 4-dB passband insertion loss for passbands with center frequencies ranging from 415 to 618 MHz. As an example, model BFTC-415+ has a passband of 330 to 500 MHz with typical passband insertion loss of 4 dB and typical passband VSWR of 1.50:1. It provides at least 25 dB lower stopband rejection from 1 to 240 MHz and 25 dB upper stopband rejection from 650 to 1800 MHz, and handles input power levels to 4 W.

## Ultra-Thin Hand-Formable Cables Connect DC to 18 GHz

Mini-Circuits' 047 Series Hand-Flex™ hand-formable coaxial cables provide outstanding flexibility. These new, ultra-thin models are just 0.047 in. in diameter with a 3.2-mm minimum bend radius, making them ideal for reliable connections in the tightest layouts. Like all Mini-Circuits Hand-Flex cables, 047-Series models are hand-formable to almost any shape without special bending tools. The 50-Ω cables, which have a frequency range from DC to 18 GHz, feature gold-plated beryllium copper construction with outer shield of tin-plated and tin-soaked copper braid to minimize signal leakage while maintaining flexibility. The cables are available in standard lengths of 3, 6, and 12 in. and can be supplied with SMP female, right-angle SMP female, and 180-deg.-rotated right-angle SM female blind-mate, push-on connectors.

## Electromechanical SPDT Switch Guarantees 10 Million Cycles to 26.5 GHz

Mini-Circuits' MSP2T-26-12+ Xtra Long Life single-pole, double-throw (SPDT) reflective switch is a rugged failsafe switch in make-before-break configuration for applications from DC to 26.5 GHz. The 50-Ω switch is guaranteed for 10 million switching operations and can handle as much as 20 W cold-switched power with 20-ms typical switching speed. Designed for 12 V DC, the SPDT switch has low insertion loss of typically 0.20 dB or less from DC to 8 GHz, 0.30 dB or less from 8 to 18 GHz, and 0.64 dB from 18 to 26.5 GHz. It offers high isolation of typically 100 dB from DC to 1 GHz, 90 dB from 1 to 8 GHz, 80 dB from 8 to 12 GHz, and 66 dB from 12 to 26.5 GHz. The reliable SPDT switch maintains low VSWR, of typically 1.05:1 from DC to 1 GHz, 1.20:1 from 1 to 12 GHz, and 1.29:1 or less from 12 to 26.5 GHz. The RoHS-compliant switch is supplied with SMA connectors.

## Coaxial 2.4-mm Adapter Links DC to 50 GHz

Mini-Circuits' model 24M-24M+ is a 2.4-mm male to 2.4-mm male coaxial adapter with low loss, low VSWR, and flat response across a wide frequency range of DC to 50 GHz. The RoHS-compliant coaxial adapter offers extremely low insertion loss for interconnections of cables and coaxial equipment, with loss of typically only 0.04 dB from DC to 5 GHz, 0.08 dB from 5 to 10 GHz, 0.10 dB from 10 to 20 GHz, 0.15 dB from 20 to 40 GHz, and 0.21 dB from 40 to 50 GHz. It exhibits similar low VSWR, typically only 1.20:1 from DC to 10 GHz, 1.04:1 or less from 10 to 40 GHz, and 1.06:1 from 40 to 50 GHz. The RoHS-compliant adapters measure 0.685 in. (17.4 mm) in length and 0.362 in. (9.2 mm) in diameter with passivated stainless-steel body and handle operating temperatures from -55 to +100°C.

## GaAs MMIC Directional Coupler Extends from 5.0 to 43.5 GHz

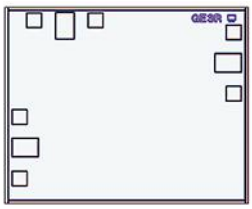

Mini-Circuits' model EDC19-KA-DG+ GaAs MMIC directional coupler features a broad frequency range of 5.0 to 43.5 GHz, well suited for many applications, including test equipment, military systems, and 5G base stations. Supplied as unpackaged die, the coupler can be integrated into hybrid circuits. It has typical nominal coupling of 26.0 dB from 5 to 10 GHz, 21.4 dB from 10 to 20 dB, 18.3 dB from 20 to 40 GHz, and 18.9 dB from 40 to 43.5 GHz. The coupling flatness is typically ±2.7 dB or better from 5 to 20 GHz and typically ±0.9 dB or better from 20 to 43.5 GHz. Directivity is typically 9.1 dB from 5 to 20 GHz, 9.3 dB from 20 to 40 GHz, and 6.1 dB from 40 to 43.5 GHz. The chip coupler handles input power to 1 W at operating temperatures from -40 to +85°C and can pass as much as 1.3 A DC current.

## Fast USB-Controlled SP16T Switch Handles 1 to 8000 MHz

Mini-Circuits' model USB-1SP16T-83H is a single-pole, 16-throw (SP16T) solid-state absorptive switch with 90-dB typical isolation from 1 to 8000 MHz. The 50-Ω switch handles power levels to 1 W (+30 dBm) with low insertion loss of 5.5 dB from 1 to 3000 MHz, 7.5 dB from 3000 to 7000 MHz, and 9.5 dB from 7000 to 8000 MHz. It provides high isolation between RF ports, of typically 90 dB from 1 to 3000 MHz, 88 dB from 3000 to 7000 MHz, and 78 dB from 7000 to 8000 MHz. With USB and TTL power and control and typical switching speed of 5.5 µs, the 50-Ω SP16T switch is a good fit for production testing. It is equipped with 17 female SMA RF connectors, internal DC blocking capacitors at all RF ports, and D-Sub 9-pin port for power and TTL control. Full software support is provided for USB control.

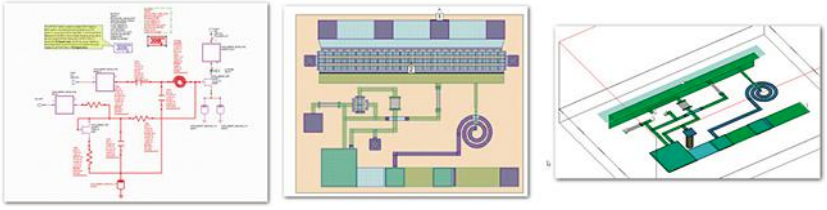

10. In this example, a MMIC spiral is going to AXIEM for simulation.

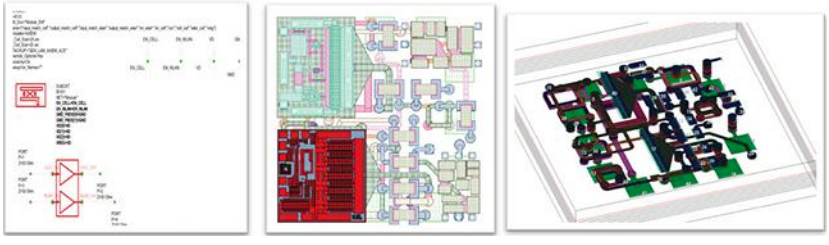

11. Shown here is a module PCB going to AXIEM for simulation.

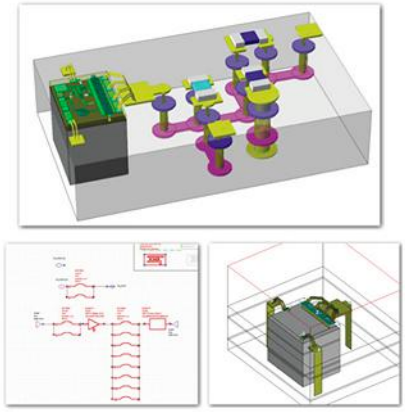

12. This figure depicts a MMIC multi-technology module in 3D (top) along with bond wires selected in the schematic (bottom left) and the extracted transition in Analyst (bottom right).

to a planar simulator. *Figure 10* shows an example of a MMIC spiral going to AXIEM. The picture on the left of *Fig. 10* is a MMIC schematic with selected elements for extraction (highlighted in red), while the picture in the middle is the schematic layout. The picture on the right is the EM extracted layout in AXIEM.

*Figure 11* shows an example of a module on a PCB going to AXIEM. Again, the picture on the left of *Fig. 11* is the module schematic with selected elements for extraction. The picture in the middle is the schematic layout, while the picture on the right is the EM extracted layout.

It is also possible to send a 3D EM extraction to a 3D simulator. Extracted shapes include thick, finite dielectric blocks, bond wires, boundaries, and ports. *Figure 12* shows a 3D view of a MMIC module in which a MMIC chip is on top of a ceramic substrate with associated interconnects. In the top picture of *Fig. 12*, two different PDKs are used in the multi-technology example; the chip is attached to the substrate by bond wires. The picture at the bottom left shows the bond wires selected in the schematic, while the picture at the bottom right is the extracted transition in Analyst.

The straps from the ports to the bottom ground plane are used to obtain the correct port ground definitions. They are not made of metal; rather, they are mathematical surfaces used in exciting the meshes touching them.

NEW!

Planar Back (Tunnel) Diodes, MBD Series

ECLIPSEmdi
MICROWAVE & RF PRODUCTS

| Model Number | $I_P$ | | $C_J$ | Y | $R_V$ | $I_P / I_V$ | $V_R$ | $V_F$ |
|---|---|---|---|---|---|---|---|---|
| | MIN µA | MAX µA | MAX pF | Typ. mV / mW | Typ. Ω | MIN | MIN mV | MAX mV |
| MBD1057-C18 | 100 | 200 | 0.30 | 1,000 | 180 | 2.5 | 420 | 135 |
| MBD2057-C18 | 200 | 300 | 0.30 | 750 | 130 | 2.5 | 410 | 130 |
| MBD3057-C18 | 300 | 400 | 0.30 | 500 | 80 | 2.5 | 400 | 125 |
| MBD4057-C18 | 400 | 500 | 0.30 | 275 | 65 | 2.5 | 400 | 120 |
| MBD5057-C18 | 500 | 600 | 0.30 | 250 | 60 | 2.5 | 400 | 110 |

The MBD series of planar back (tunnel) diodes are fabricated on germanium substrates using passivated, planar construction and gold metallization for reliable operation up to +110 °C. Unlike the standard tunnel diode, $I_P$ is minimized for detector operation and offered in five nominal values with varying degrees of sensitivity and video impedance.

www.eclipsemdi.com
408.526.1100
Let's talk shop.

● Zero bias operation ● Excellent temperature stability ● Low video impedance

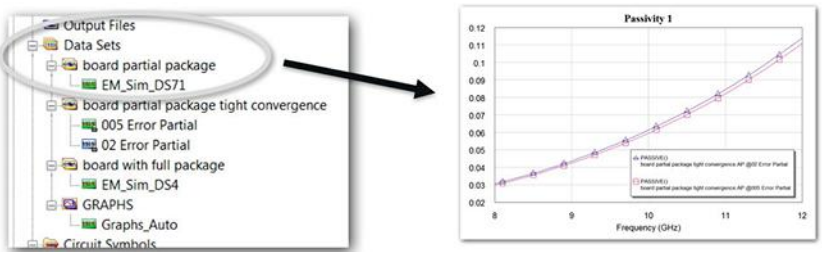


**13. Data sets in a project (left) can be easily plotted in multiples (right).**

mance or changing power in some of the elements. This is not caused by the antennas; rather, it is because the load to the PAs has changed and must be accounted for.

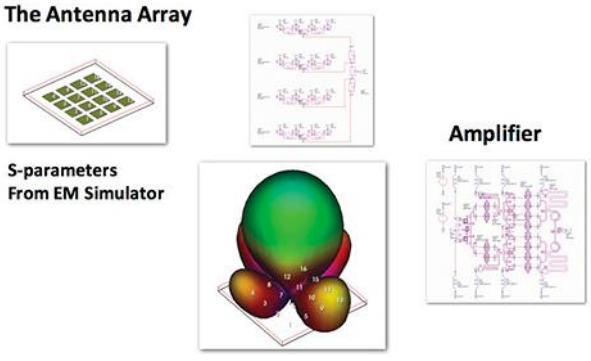


**14. This is an example of a 16-patch microstrip driven by 16 amplifiers.**

## DATA SETS

Microwave Office uses data sets to help the designer manage the data from the various EM and circuit simulations. Data sets store simulation data, enabling designers to swap between data sets quickly to compare results on graphs and change the data used by a schematic *(Fig. 13)*. Designers can take advantage of data sets to keep old simulation results and easily compare them with newer results. The data sets include the layout of the EM simulation and the log file.

## EM/CIRCUIT CO-SIMULATION OF AN ACTIVELY-SCANNED ANTENNA ARRAY

The antenna array and attached driving circuitry affect each other. To help designers overcome this issue, Microwave Office allows for co-simulation of the antenna and attached circuitry. First, the antennas must be simulated in an EM simulator, which produces an S-parameter file that describes the array's behavior. Antenna patterns are also calculated from the known currents on the antennas. The problem is that the power amplifiers (PAs) driving the array are highly nonlinear and their performance depends on the loads they are driving (in this case, the inputs to the array).

As the beam of the array scans, the impedances of the ports change, which then affects the amplifiers. The antenna's performance and the driving circuitry are therefore coupled together. *Figure 14* shows a 16-patch microstrip example driven by 16 amplifiers. As the array is scanned, the load to each element changes, potentially degrading perfor-

## IN-SITU MEASUREMENT FEATURE

Traditionally, the designer must calculate the input impedance to the array, feed the results back into the circuit simulation, and then adjust the PA's performance. The resulting output power is fed back into the array to see how the beam has changed. This cycle is repeated until the results converge—a time-consuming and painstaking process.

The in-situ (inside the circuitry) measurement feature in Microwave Office enables communication between the circuit and antenna, thus automatically accounting for the coupling between the circuit and the antenna array in an easy-to-use framework. The designer determines the measurement under consideration (such as the power radiated over scan angle) involving the circuitry that drives the various ports of the array by pointing to the S-parameter block on the circuit schematic.


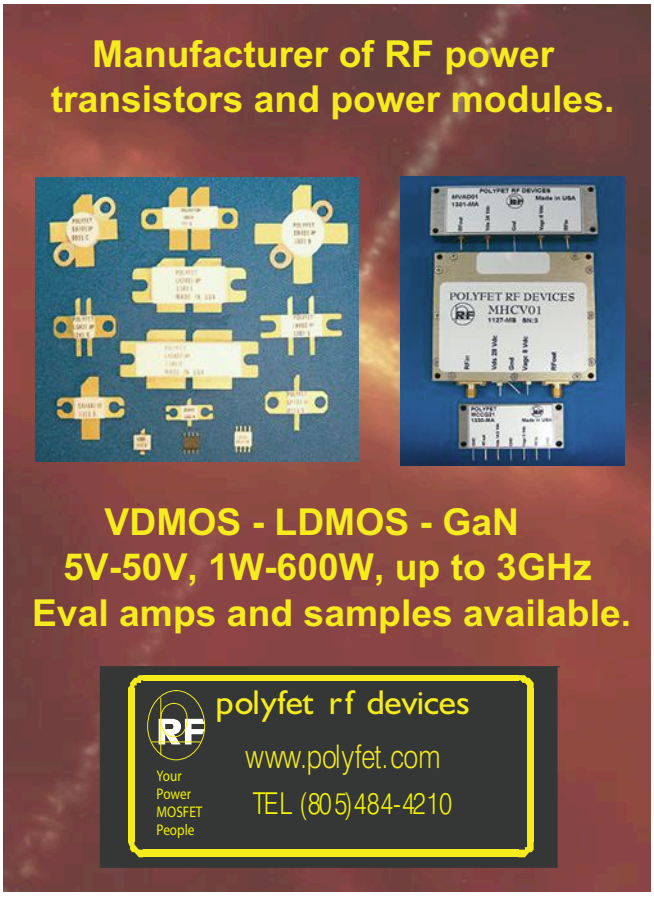

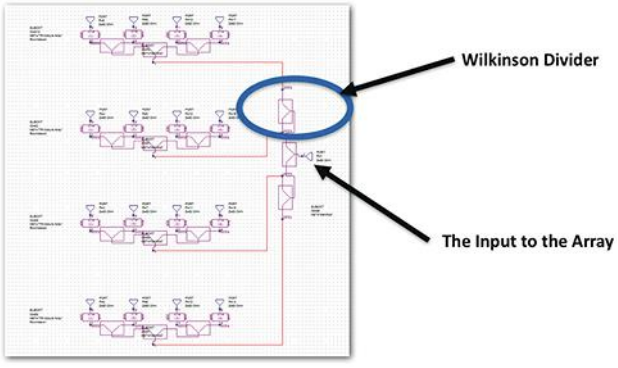


**15. The corporate feed network is attached to the array in the circuit simulator.**

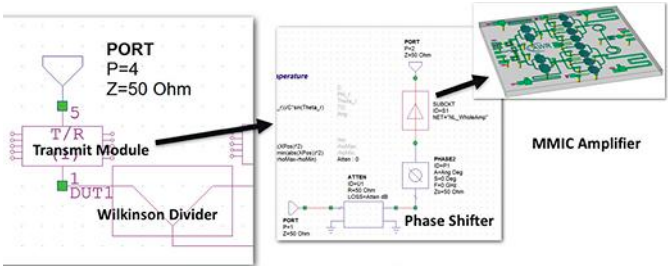


**16. The MMIC amplifier is inside this transmit module.**

The schematic in *Figure 15* shows the corporate feed network attached to a 16-element array. The input to the array appears on the right side of the schematic. Wilkinson power dividers are used to split the power among the 16 elements (the blue circle indicates one of the Wilkinson dividers).

Before the signal reaches each of the 16 elements, it is sent through a transmit module. Each transmit module contains a phase shifter, an attenuator, and a PA. *Figure 16* shows one of the transmit modules with the phase shifter, attenuator, and amplifier inside. The amplifier is driving the element and the array's beam is steered by changing the attenuation and phase shift of each signal going into the antenna elements.

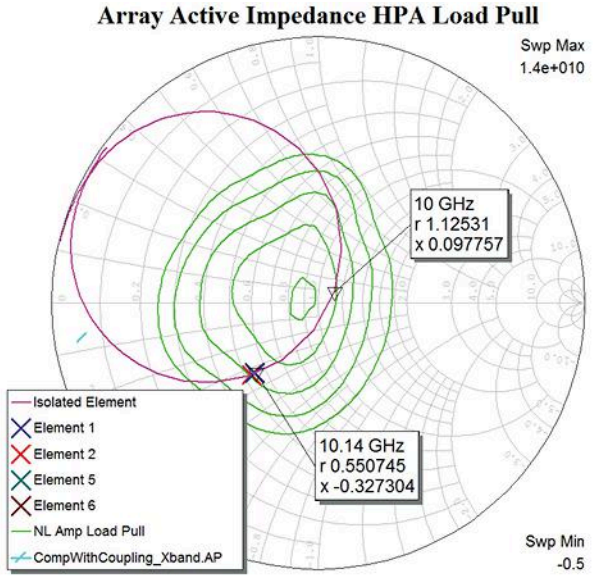


**17. Shown is the input impedance of an isolated patch element from 6 to 14 GHz (purple circle), as well as load-pull curves (green) for the amplifier and power output for various loads.**

Because the PA is nonlinear, obtaining the correct performance requires accounting for the changing load in the PA as the attenuation is changed. *Figure 17* shows the input impedance of an isolated patch element from 6 to 14 GHz (purple circle), as well as load-pull curves (green) for the amplifier and power output for various loads. As the antenna is scanned, the point on load-pull curves will change and the designer can account for those changes. In this example, the impedances of the array's elements are about the same as the isolated patch, which meets expectations.

The pattern measurement is set up the same way. Since the power going to the elements is known, harmonic balance can be used for the circuit simulation in Microwave Office. *Figure 18* shows the measurement of the total radiated power in Theta direction.

**HF Amplifiers**
We stock the complete parts list and PC boards for the Motorola amplifier designs featured in their Application Notes and Engineering Bulletins

AN779L (20W) AN758 (300W)
AN779H (20W) AR305 (300W)
AN762 (140W) AR313 (300W)
EB63A (140W) EB104 (600W)
EB27A (300W) AR347 (1000W)

**NEW ! NEW ! NEW !**
We stock the new rugged FREESCALE 1KW transistor and parts for the 2M and 88-108MHz amplifier designs.

HF Broadband RF Transformers 2 to 30MHz

COAX WIRE
TC-12 TC-18
TC-20 TC-22
TC-24

RF Transformers Type "U" 2 to 300MHz

HF Power Splitter / Combiners 2 to 30MHz

2 Port
PSC-2L 600W PEP
PSC-2H 1000W PEP
4 Port
PSC-4L 1200W PEP
PSC-4H 2000W PEP
PSC-4H5 5000W PEP

CCI Communication Concepts, Inc.
www.communication-concepts.com

508 Millstone Drive,
Beavercreek, OH 45434-5840
Email: cci.dayton@pobox.com
Phone (937) 426-8600
FAX (937) 429-3811

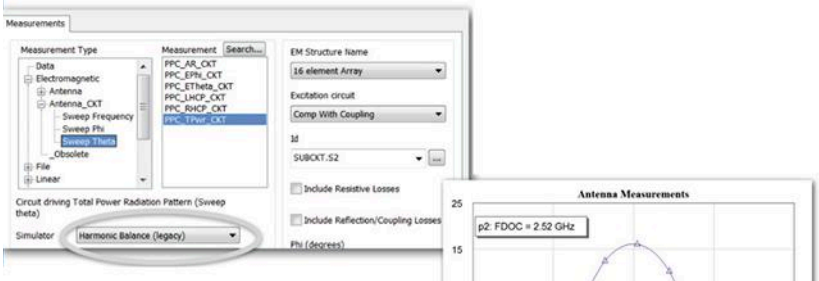


**18. Harmonic balance is used for the circuit simulation.**

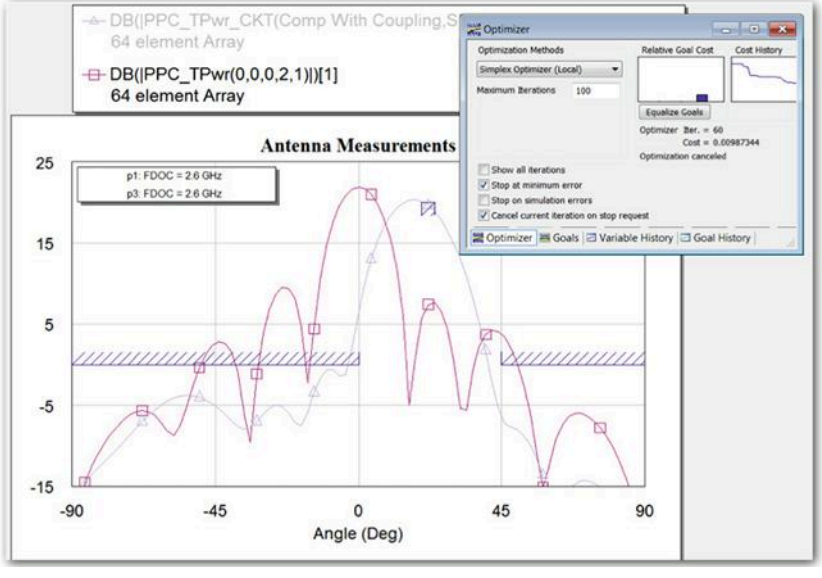


**19. The pattern is optimized by changing the phasing and attenuation.**

The pattern can then be optimized. In this case, the pattern is optimized by changing the phasing and attenuation to the array elements *(Fig. 19)*. The purple pattern in Fig. 19 indicates the broadside excitation, while the blue pattern represents optimized performance, i.e., the side lobes are below the blue bars. The PA performance can be adjusted with the optimization.

## CONCLUSION

Complex 5G and radar infrastructure requires the integration of antennas and circuitry. The challenge for EDA software is to support multiple technologies that require different circuit and EM simulators. Hierarchy at both the circuit simulation and EM level can be used to control multi-technology designs. And in-situ simulation is able to model antenna and circuit interactions. MW

NOTE: A video from EDI CON 2017 demonstrating EM/circuit co-simulation within NI AWR Design Environment is available for viewing at: https://www.youtube.com/watch?v=F_48_RXQrvM

REFERENCE:

http://www.microwavejournal.com/articles/27830-ibm-and-ericsson-announce-5g-mmwave-phase-array-antenna-module

Looking for just the right part, at just the right price...

**Connect with over 200 distributors** on the NEW SourceESB!

sourceesb

Find electronic parts fast - from the only database that verifies part authorization.

Parts | Enter part... | Enter List

**Part Lists Tool**

- Send multi-part RFQs
- Save your part lists to work on later
- Filter by authorized distributor

**www.SourceESB.com**

DYLAN STINSON | Product Manager for RF/Microwave Products
*www.tek.com*

# 5 Steps to Antenna Matching Using a Portable PC-Based VNA

**These practical tips outline an efficient way to perform impedance matching with a PC-based vector network analyzer combined with analysis software.**

Properly matching an antenna to a transceiver is one of the easiest ways to extend the signal range and battery life of a smartphone, laptop, or any other wireless device. According to the inverse square law of radio waves, only a 6-dB improvement in path loss from improved matching results in a device that transmits and receives at twice the range. A spectrum analyzer with a tracking generator can check an antenna match by looking at the voltage standing wave ratio (VSWR). But the best tool to make the impedance measurements needed to effectively design a matching network is a vector network analyzer (VNA).

Until recently, many engineers tasked with integrating an antenna into a wireless device had limited or no access to a VNA due to the historically high cost of these instruments. In fact, some have not been trained on how to use them. However, the advent of low-cost, portable VNAs coupled with intuitive PC software has made it easier and more affordable to perform antenna matching to improve the performance of wireless devices.

In this article, we'll present a straightforward process for antenna matching using a portable VNA. A similar process can be used for many other kinds

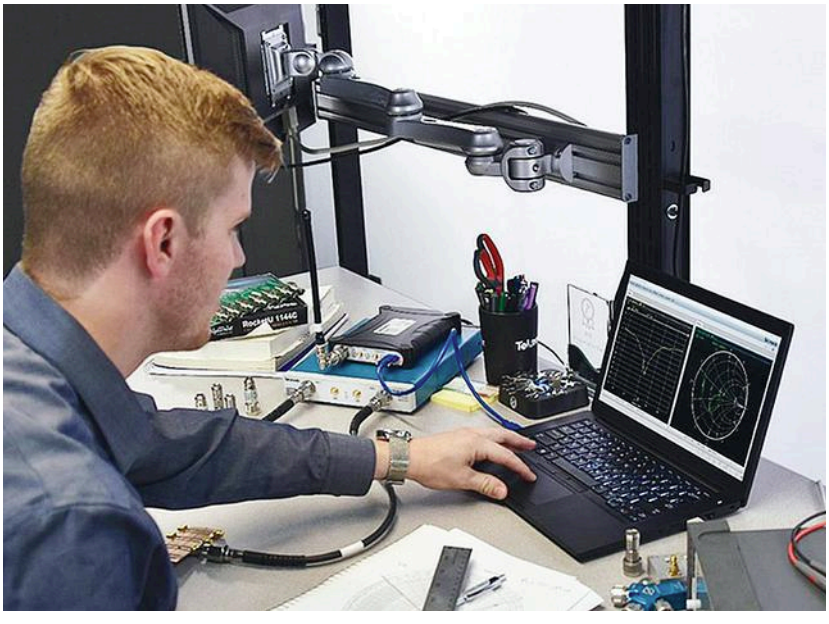

**1. With the advent of portable USB-based VNAs, it's more affordable and convenient than ever to test and create your own antenna impedance-matching network.**

of impedance matching needed to maximize power transfer between components in a system with high-frequency signals, or to check transmission-line design or characteristic impedance.

## AGENTS OF SIGNAL POWER DECLINE

Two primary factors that reduce the signal power transferred between a source and load, such as in a transceiver and antenna system, are signal reflections and power-dissipation losses. Impedance mismatches between an antenna and transceiver cause signal reflections at the feed point of the antenna, which are either absorbed back by the source or dissipated by lossy transmission lines and components.

Such reflections result in dramatically reduced signal range, dropped data packets, and wasted battery life. They can even damage the transceiver source if the reflected power is too high—an extremely dangerous situation in high-power applications.

Maximum power transfer between a source and a load occurs when their resistances are the same, or in the case of ac circuits, when their impedances are complex conjugates of one another. For example, some transceivers and antennas are specifically designed with impedances of 50 Ω (resistive) at their inputs (or outputs). In that case, they can usually be directly integrated and connected with 50-Ω transmission lines and achieve close to maximum power transfer.

In other cases, the input impedance of the antenna or load is not 50 Ω by design, or some imaginary part of the impedance (i.e., reactance) is unaccounted for that results in a mismatch. In this situation, a matching network is used to match the antenna, including its feed line, to the impedance of the source.

When it comes to antennas, a datasheet or reference design may say the impedance is 50 Ω. However, you may find that the stated value is not entirely accurate for your environment or frequency of interest. At high-enough frequencies, the input impedance of an antenna and connected feed line depends heavily on the length of the feed line.

In addition, any objects placed around an antenna, such as an enclosure or product packaging, will alter its radiation pattern and its input impedance. That's why it's important to use a VNA to measure the input impedance of the antenna (including its intended feed line) within the environment that will most closely resemble where it is intended to operate.

To combat circuit losses, the impedance-matching network in most cases consists of one or more low-loss inductors and capacitors or transmission line stubs. These components are used in a network design chosen to meet the goals of matching impedances, as well as any filtering and bandwidth (or multi-band) specifications as needed. Even an RF novice can correctly match an antenna using a VNA with a test setup similar to the one shown in *Figure 1*.

Before beginning, it's important to keep in mind that the impedance to be matched must be measured at the point where the matching network will be placed. If a transmission line, such as a feed line, sits between the antenna port and the matching-network location, it will affect the complex impedance value that must be matched with a matching network. This only starts to become significant as the length of the feed line becomes greater than about one-tenth the wavelength of the highest frequency of interest.

Likewise, a VNA measures at the plane of calibration by default, namely without de-embedding or port extensions applied. Any transmission line between the calibration plane and the matching-network location must be accounted for. A port extension can be used to extend the calibration plane to the correct location if needed. *Figure 2* illustrates these points.

**Step 1: Calibrate the VNA as close to the measurement plane as possible, ideally at the matching-network location.**

Getting the calibration plane dialed in correctly is the most crucial and difficult step in matching-network design.

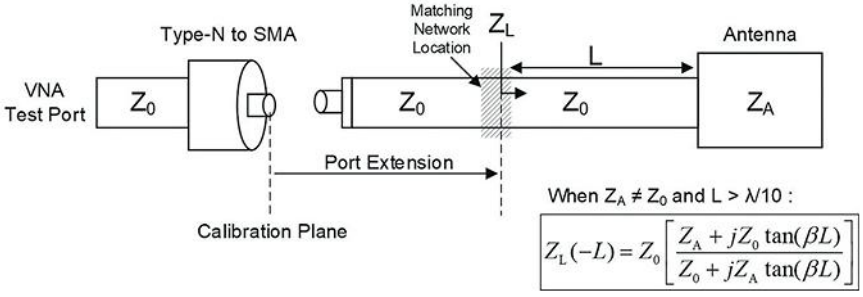


**2. The impedance measurement must be made at the point where the matching network will be placed. If additional transmission line length exists between the calibration plane and the intended matching-network location, use a port extension to extend the calibration plane to the correct location.**

A poor calibration can result in much different results. But the compact arrangement and lack of compatible access points on most circuit boards and wireless modules makes this task a challenge. Typically, you have two options:

**1. Indirect:** Calibrate with a commonly available calibration kit, such as a 3.5-mm cal kit compatible with SMA connectors, as close to the matching network as possible. You can then use a port extension to account for any adapters, transmission lines, or probes between the calibration plane and the matching network (*see Step 2 below*). One useful trick for getting the calibration plane close to the matching-network location (if you can accomplish it) is to carefully solder a U.FL connector at the matching network location of your wireless module, calibrate the VNA with a 3.5-mm cal kit, and then use an SMA-to-U.FL adapter between the calibration plane and matching network location. A port extension can then be used to remove the adapter from the measurement.

**2. Direct:** Create your own short, open, and load at the matching-network location and perform a short-open-load (SOL) calibration directly. This approach must be used very carefully, however, because it is difficult to create an ideal short, open, or load on a circuit board by soldering and de-soldering components. A big blob of solder can add a significant amount of reactance to the measured circuit. But for circuits at frequencies of 2 GHz and below, this shouldn't be much of a problem because the wavelengths are relatively large.

*Figure 3* illustrates these two approaches. The importance of a good calibration for getting an accurate impedance measurement cannot be overstated. If the calibration is off, the impedance measurement will be incorrect and the match will not behave as expected when modifying the matching network. In that case, the user will end up chasing the impedance around the 50-Ω point and waste time with multiple iterations.

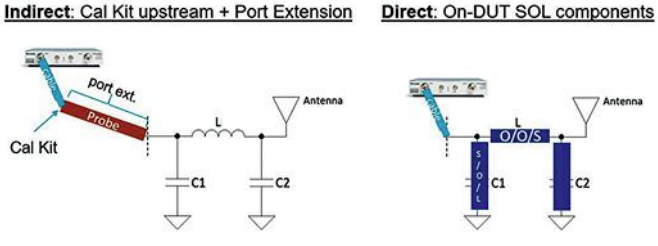


**3. Shown are indirect and direct options for calibrating and connecting the VNA.**

**Step 2: If necessary, align the calibration plane with the measurement plane by using a port extension.**

As shown in *Fig. 2*, a transmission line between the VNA calibration plane and the matching network location will impact the measured impedance. This effect can be corrected with a port extension. To understand how a port extension works and how it affects the Smith chart display, let's first review some Smith chart basics.

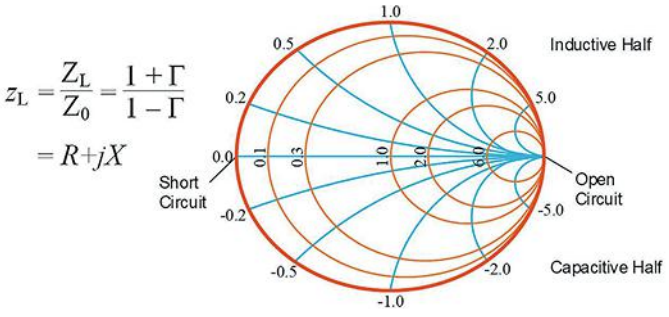


**4. The Smith chart is used to plot impedance.**

*Figure 4* shows the Smith chart, which can look intimidating to the novice, but is easy to understand when you break it down. Begin with the polar reflection coefficient chart (*Fig. 5*). Signal reflections, represented by the reflection coefficient, are related to the ratio of impedance at a mismatch.

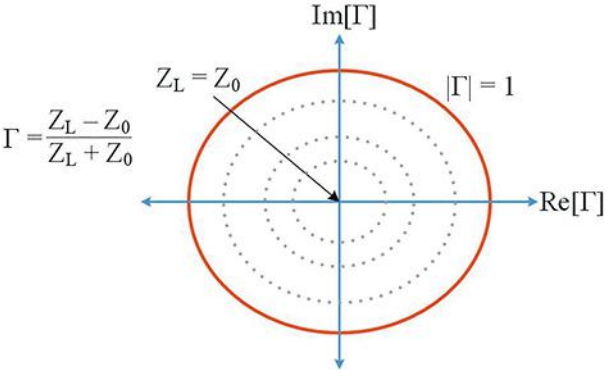


**5. Shown here is a polar reflection coefficient chart with dotted lines of constant reflection-coefficient magnitude/constant VSWR.**

Because we usually have a known reference impedance ($Z_0$) of 50 Ω, the normalized load impedance $Z_L$ (the value normalized to 50 Ω) can be mapped onto the reflection coefficient chart. Note that impedance is a complex value consisting of real and imaginary parts (i.e., Z = R + jX). When mapping $Z_L$ to the reflection coefficient chart, some useful patterns emerge: lines of constant resistance, *R* (*Fig. 6*) and lines of constant reactance, *X* (*Fig. 7*).

Finally, getting back to port extensions, changing the length of a transmission line between the measurement point and the impedance mismatch does not change the magnitude of reflection. However, it does change the measured phase. This results in a rotation on the Smith chart around the 50-Ω center point along a line of constant reflection-coefficient magnitude/constant VSWR (*Fig. 5*, *again*).

*(Continued on page 79)*

JACK BROWNE | Technical Contributor

# LDMOS Power Transistors Drive 200 W to 1300 MHz

**This article breaks down two new highly integrated Doherty PA designs that could have a major impact on 5G applications.**

Power transistors for RF/microwave applications exploit a range of different technologies, including substrate materials like the tried-and-true gallium arsenide (GaAs) to the somewhat more recent and intriguing gallium nitride (GaN). Still, silicon transistor substrates remain the longest-running foundations for high-power RF/microwave transistors in both commercial and military applications.

Among those silicon devices, lateral diffused metal-oxide-semiconductor (LDMOS) transistors have demonstrated good reliability with high performance levels. And when new silicon LDMOS power transistors arrive, they provide further options for RF/microwave power-amplifier designers faced with the challenges of trying to optimize performance parameters such as output power, gain, and efficiency over a given bandwidth.

A pair of +28-V dc silicon LDMOS power transistors from Polyfet RF Devices pack a great deal of punch for power amplifiers through about 1.3 GHz. The LA2541 and LS2541 impedance-unmatched silicon LDMOS transistors come in two slightly different push-pull packages. Each transistor is capable of as much as 200 W output power (at 1-dB compression), and versatile enough to drive continuous-wave (CW) or pulsed input waveforms with high efficiency and effective thermal management.

Depending on how they are source and load matched, the two packaged transistors (*see figure*) can be used in broadband or narrowband applications through 1300 MHz and deliver high output power with high gain and efficiency. Each device employs back-to-back gate diodes for enhanced electrostatic-discharge (ESD) protection. Their rugged metal-ceramic packages feature clearly marked and easily accessible gate, drain, and source connections to simplify installation into a circuit board.

Both packages/transistors are rated for total device power dissipation of 460 W, junction-to-case thermal resistance of 0.38°C/W, maximum dc drain current of 18 A, high maximum drain-to-gate breakdown voltage of 80 V dc, and maximum junction temperature of +200°C.

In terms of performance, the two transistors offer similar levels. For example, the LA2541 is rated for minimum common source power gain of 16 dB at 500 MHz, when measured at 28 V dc with quiescent drain current ($I_{dq}$) of 800 mA. It boasts typical drain efficiency of 60% when measured under the same operating conditions at 500 MHz. In addition, it can handle VSWR load mismatches as severe as 20.0:1 at 500 MHz, under the same operating conditions.

Supplied in its LS package with somewhat modified drain contacts, the LS2541 features the same minimum gain, typical drain efficiency, and VSWR load mismatch capabilities when measured at a test frequency of 500 MHz.

**These high-power silicon LDMOS transistors are supplied in a choice of LA (top) and LS (bottom) metal-ceramic flanged packages for ease of use and installation.**

Both power transistors are tested and characterized in three different test fixtures, at 500 MHz, 1.3 GHz, and across the frequency range of 30 to 512 MHz. The transistors share electrical characteristics and can be used almost interchangeably in power-amplifier designs, depending on packaging and layout requirements. The packaged transistors incorporate flanges based on copper/copper-molybdenum-copper/copper rather than copper-tungsten materials. This enables efficient thermal transfer from transistor die to heat sink and surrounding circuitry for effective heat flow and enhanced device reliability.

The LA2541 and LS2541 share electrical characteristics, including a gate-source voltage ($V_{gs}$) range of 2 to 5 V dc for a drain-source voltage ($V_{ds}$) at the same setting and a drain-source current ($I_{ds}$) of 200 mA. The minimum breakdown drain-source voltage ($BV_{dss}$) is 80 V dc at Ids of 5 mA and $V_{gs}$ of 0 V dc. The maximum saturated drain-source leakage current ($I_{dss}$) is 5.0 mA at $V_{ds}$ of 28 V dc and $V_{gs}$ of 0 V ds. The maximum gate leakage current ($I_{gss}$) is 1 µA for $V_{gs}$ of 10 V dc and $V_{ds}$ of 0 V dc. Both packaged power transistors exhibit a typical forward transconductance of 7.5 mhos at $V_{ds}$ of 10 V dc and $V_{gs}$ of 5 V dc.

Whichever package/transistor is specified, these are high-power RF transistors that can be impedance-matched as needed for narrowband or broadband applications. MW

**POLYFET RF DEVICES**, 1110 Avenida Acaso, Camarillo, CA 93012; (805) 484-4210, E-mail: contact@polyfet.com; *www.polyfet.com*

IMS
Connecting Minds. Exchanging Ideas.

The 2018 IEEE MTT-S
International Microwave Symposium

# Join Us in

# Enhance your IMS Experience with these

## 5G Summit, Tuesday, 12 June 2018; Room 103

The 5G Summit, at the Pennsylvania Convention Center in Philadelphia, is an IEEE event that is organized by two of IEEE's largest societies – MTT-S and ComSoc. This special collaboration, for the second year running, complements MTT-S' "hardware and systems" focus with ComSoc's "networking and services" focus. The one-day Summit features talks from experts from government, academia, and industry experts on various aspects of 5G services and applications. It's further complemented by the 5G Pavilion at the IMS2018 exhibition where table top demonstrations and "fire-side" chats are presented at the 5G theater.

### 5G Summit Speakers:

**"Bringing the World Closer Together"**

Jin Bains
Head of Connectivity, SCL, Facebook

**"AT&T Perspectives on 5G Services"**

David Lu
Vice President, AT&T

Other featured presentations from Huawei, GM, Keysight, NI, Global Foundries, MACOM as well as academia will include following topics:

- Spectrum/Regulatory
- Infrastructure/Trials, Applications
- Technologies, Circuits, Systems
- Design, Test & Measurement Challenges
- Test-bed Services for 5G

Lunchtime Panel session: "mmWave Radios in Smartphones: What they will look like in 2, 5, and 10 years"

## RF Boot Camp, Monday, 11 June 2018; Room 109B

This one-day course is ideal for newcomers to the microwave world, such as technicians, new engineers, college students, engineers changing their career path, as well as marketing and sales professionals looking to become more comfortable in customer interactions involving RF & Microwave circuit, and system concepts and terminology. The format of the RF Boot Camp is like that of a workshop or short course, with multiple presenters from industry and academia presenting on a variety of topics including:

- The RF/Microwave Signal Chain
- Network Characteristics, Analysis and Measurement
- Fundamentals of RF Simulation
- Impedance Matching & Device Modeling Basics
- Introduction to RF and Microwave Filters
- Spectral Analysis and Receiver Technology
- Signal Generation
- Modulation and Vector Signal Analysis
- Microwave Antenna Basics
- Introduction to Radar and Radar Measurements

**For complete details on IMS and Microwave Week visit www.ims2018.org**

# Philadelphia!

## not to miss events! Register Today!

### Physicians Panel Session:

**Utilization of RF/Microwaves in Medicine, Thursday, 14 June 2018; Room 204B**

Over the past three decades, collaboration between physicians and engineers has increased dramatically, to the benefit of our society. Biomedical engineering departments, the majority of which found in engineering schools and some within medical schools, offer seemingly unlimited opportunities and continue to attract a large number of students. To benefit from the merits of interdisciplinary cooperation and facilitate the transfer of technology to the market, existing large corporations, start-up medical companies, and research funding agencies now demand strong collaboration between engineers and physicians. With this in mind, IMS 2018 has made the subject of RF/microwaves in Medicine a major theme of the conference. The physicians on this panel will discuss the use of RF/microwaves in their respective fields. Topics ranging from microwave hyperthermia therapy for reoccurrences of breast cancer, advances in RF renal denervation, to back pain management using RF, will be highlighted!

**Panelists:**

1. Andrew Ng, Thomas Jefferson University Hospital, Philadelphia, PA
2. Daniel Frisch, Thomas Jefferson University Hospital, Philadelphia, PA
3. Donald Mitchell, Thomas Jefferson University Hospital, Philadelphia, PA
4. Ernest Rosato, Thomas Jefferson University Hospital, Philadelphia, PA
5. Eugene Viscusi, Thomas Jefferson University Hospital, Philadelphia, PA
6. Francis Kralick, Neurological Surgery, Shore Medical Center, Brigantine, NJ
7. Hamid RS Hosseinzadeh, School of Osteopathic Medicine, Stratford, NJ
8. Mark Hurwitz, Thomas Jefferson University Hospital, Philadelphia, PA
9. Nicholas Ruggiero, Thomas Jefferson University Hospital, Philadelphia, PA
10. William Jow, Medifocus Inc., Columbia, MD

### Exhibition Dates and Hours

| | |
|---|---|
| Tuesday, 12 June 2018 | 09:30 to 17:00 |
| Wednesday, 13 June 2018 | 09:30 to 17:00 |
| Exhibit-Only Time: | 13:30 to 15:10 |
| Industry Hosted Reception: | 17:00 to 18:00 |
| Thursday, 14 June | 09:30 to 15:00 |

### MicroApps

The Microwave Application seminars (MicroApps) offered Tuesday, 12 June through Thursday, 14 June, 2018, provide a unique forum for the exchange of ideas and practical knowledge related to the design, development, production, and test of products and services. MicroApps seminars are presented by technical experts from IMS2018 exhibitors with a focus on providing practical information, design, and test techniques that practicing engineers and technicians can apply to solve the current issues in their projects and products.

### Industry Workshops

The Industry Workshops are 2-hour industry-led presentations featuring hands-on, practical solutions often including live demonstrations and attendee participation. These Workshops are open to all registered Microwave Week attendees at a nominal charge.

**PENNSYLVANIA CONVENTION CENTER • PHILADELPHIA, PENNSYLVANIA, USA**

Exhibition Dates: 12–14 June 2018 • Symposium Dates: 10–15 June 2018

IEEE

Follow us on:

#IMS2018

MTT-S

Techonology Feature

VALENTYN SOLOMKO | Infineon Technologies
HORSON HAO | Infineon Technologies
OLIVIER PICHARD | Infineon Technologies
GILBERT LIN | Infineon Technologies
MICHAEL WILHELM | Infineon Technologies
*www.infineon.com*

# Switchable Directional Coupler IC Lends a Hand to RF Front Ends

**This directional coupler can help overcome the challenges associated with cellular and Wi-Fi coexistence in the world of cell phones.**

A directional coupler in cellular RF front ends is located between the power-amplifier/antenna-switch module and the antenna tuner. It's used as part of the power control and antenna tuning loops.

Infineon's BGC100GN6 integrated circuit (IC) contains a directional coupler, a direction switch for selecting the coupled or isolated port, and a filter for 5-GHz ISM blockers suppression (*Fig. 1*). The feedback receiver (FR) sequentially receives forward- and reverse-coupled signals by changing the position of the switch. There are several benefits to integrating the coupling, switching, and filtering functions on a single die:

- It requires only one RF feedback line from the switchable coupler IC to the FR. Since the RF feedback line must be fully isolated from the main RF path to achieve high directivity, having only one feedback line reduces the complexity and cost of the main phone board.
- The inactive coupled branch of the coupler is terminated internally via a switch by an accurate 50-Ω resistor. This allows over 20 dB of directivity to be achieved independently of the impedance of the RF feedback path.
- A filter for 5-GHz Wi-Fi signal suppression prevents the FR from mixing down the Wi-Fi blockers and distorting the cellular feedback signal. An integrated Wi-Fi filter eliminates the need (or significantly relaxes the requirements) for a discrete lowpass filter in the coupled RF feedback path.

## ADDRESSING COEXISTENCE CHALLENGES

Modern handheld devices incorporate multiple radio technologies, including cellular and Wi-Fi radios. Cellular and Wi-Fi transceivers operate simultaneously and independently from each other and may interfere at the RF level.

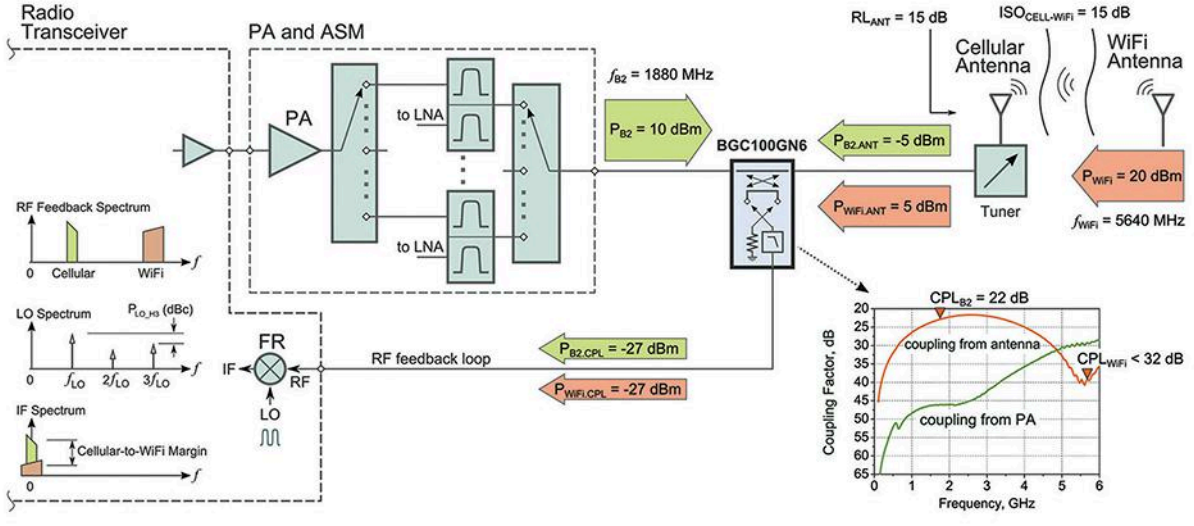


**1. A switchable directional coupler is located in the RF front end of handheld cellular devices.**

Even though the cellular and Wi-Fi antennas are physically located at opposite sides of the handheld device, finite RF isolation results in unwanted coupling of the Wi-Fi signal into the main cellular path, with further coupling into an RF feedback path via a coupler IC. As a result, an RF feedback signal applied to a FR will contain cellular and Wi-Fi spectral components (*Fig. 1, again*).

An FR is a zero-IF downconversion mixer driven by a nearly rectangular local-oscillator (LO) signal with a third harmonic that's 10 dB below the main tone. If the third harmonic happens to overlap with a Wi-Fi band, then both the Wi-Fi and cellular bands will be downconverted to the same intermediate frequency (IF).

## ANTENNA TUNING SCENARIO

Assume the cellular radio is transmitting a B2 signal at a frequency ($f_{B2}$) of 1880 MHz. Furthermore, the RF feedback loop is operating in antenna tuning mode. The switchable coupler is configured to sense an RF signal reflected from the cellular antenna. Assume the forward cellular power ($P_{B2}$) is +10 dBm and the return loss from the antenna ($RL_{ANT}$) is 15 dB. The power reflected back from the antenna is:

$$P_{B2} - RL_{ANT} = -5 \text{ dBm}$$

This power couples into the FR via a coupler with a coupling factor ($CPL_{B2}$) of 22 dB at 1880 MHz, resulting in a cellular feedback power level of:

$$P_{B2.FR} = P_{B2} - RL_{ANT} - CPL_{B2} = -27 \text{ dBm}$$

While the cellular radio operates in B2, a Wi-Fi signal at 5,640 MHz ($f_{WiFi}$) is transmitted at a power level of +20 dBm ($P_{WiFi}$). The isolation between the Wi-Fi and cellular antennas at 5,640 MHz ($ISO_{CELL\text{-}WiFi}$) is 15 dB. The power that couples into the cellular antenna is:

$$P_{WiFi} - ISO_{CELL\text{-}WiFi} = +5 \text{ dBm}$$

The signal further couples into the RF feedback loop via the coupler. If the switchable coupler has no Wi-Fi blocking filter (standard coupler), the coupling factor at 5,640 MHz ($CPL_{WiFi}$) is 22 dB, resulting in Wi-Fi power at the input of the FR equal to:

$$P_{WiFi.FR} = P_{WiFi} - ISO_{CELL\text{-}WiFi} - CPL_{WiFi} = -17 \text{ dBm}$$

Since $f_{WiFi} = 3 \times f_{B2}$, both the cellular and Wi-Fi bands are downconverted by the FR and fall into the same IF (*Fig. 1, again*). Given that the relative power of the third harmonic of the LO signal ($P_{LO_H3}$) is equal to −10 dBc, the cellular-to-Wi-Fi margin can be calculated as:

$$\Delta P_{CELL\text{-}WiFi} = P_{B2.CPL} - P_{WiFi.CPL} - P_{LO_H3} = 0 \text{ dB}$$

Such a margin is obviously not acceptable for proper antenna tuning closed-loop control. Thus, the need arises for additional lowpass filtering in the coupled path. In some cases, it's recommended to insert a discrete passive lowpass filter into the RF feedback path to suppress the unwanted Wi-Fi interference. However, this increases the phone bill of materials (BOM) and board complexity.

The BGC100GN6 coupler IC addresses the issue by using a monolithically integrated Wi-Fi filter in the coupled path. Due to the filter, the coupling factor at Wi-Fi frequencies ($CPL_{WiFi}$) is 32 dB, which is at least 10 dB better than standard coupler ICs. Hence, the cellular-to-Wi-Fi margin can be increased by 10 dB without any discrete filter in the coupled path. The table denotes two different RF feedback paths.

**POWER BUDGETS IN RF FEEDBACK PATH FOR ANTENNA TUNING SCENARIO**

| Parameter | Symbol | RF front-end with standard coupler | RF front-end with Infineon's BGC100GN6 coupler |
|---|---|---|---|
| Cellular power (dBm) | $P_{B2}$ | 10 | 10 |
| Wi-Fi power (dBm) | $P_{WiFi}$ | 20 | 20 |
| Wi-Fi-to-cellular antenna isolation (dB) | $ISO_{CELL\text{-}WiFi}$ | 15 | 15 |
| Cellular antenna return loss (dB) | $RL_{ANT}$ | 15 | 15 |
| Coupling factor of coupler at cellular band (dB) | $CPL_{B2}$ | 22 | 22 |
| Coupling factor of coupler at Wi-Fi band (dB) | $CPL_{WiFi}$ | 22 | 32 |
| LO third harmonic (dBc) | $PL_{O_H3}$ | −10 | −10 |
| Cellular-to-WiFi margin (dB) | $\Delta P_{CELL\text{-}WiFi}$ | 0 | +10 |
| $\Delta P_{CELL\text{-}WiFi} = (P_{B2} - RL_{ANT} - CPL_{B2}) - (P_{WiFi} - ISO_{CELL\text{-}WiFi} - CPL_{WiFi} + P_{LO_H3})$ | | | |

## IMPROVING CELLULAR-TO-WI-FI MARGIN

For most front ends, the power margin achieved with the BGC100GN6 coupler IC is sufficient. The margin improves automatically with an increase in cellular power or

reflection from antenna. Among the degrees of freedom for further improvement of cellular-to-Wi-Fi margins at the application level are:

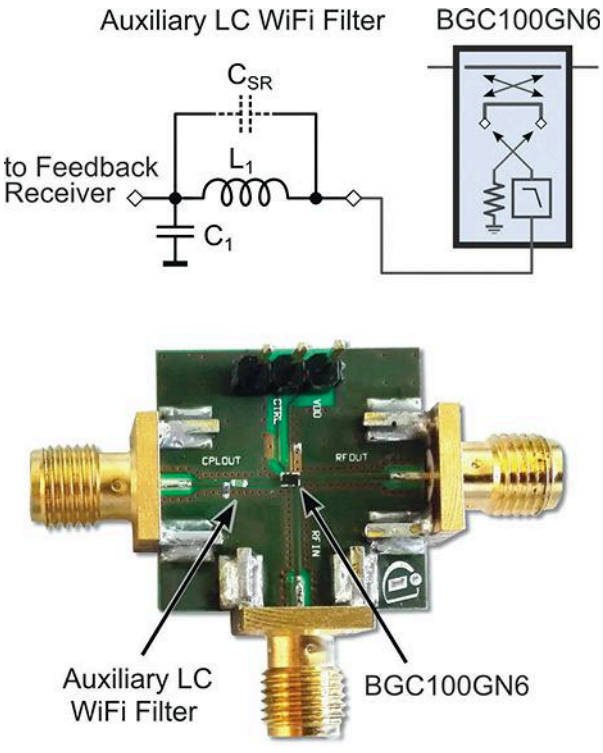


**2. This evaluation board contains the BGC100GN6 coupler with an auxiliary LC Wi-Fi filter.**

- Increasing isolation between the Wi-Fi and cellular antennas ($ISO_{CELL\text{-}WiFi}$), achieved by physical separation and proper orientation of antennas.

- Addition of a discrete lowpass filter into the coupled RF feedback path for further suppression of Wi-Fi blockers.

The former may be required for high-end RF front ends to achieve the best sensitivity of power control and antenna tuning loops. Since the BGC100GN6 already offers 30 dB of isolation within frequencies from 4.9 to 5.9 GHz, there's no need for a high-order ceramic filter. A simple LC lowpass filter, implemented with two low-cost surface-mount-device (SMD) components, would provide a total isolation of 50 dB or higher.

The filter could consist of a series inductor followed by a shunt capacitor. Self-resonance of the inductor caused by an inter-winding parasitic capacitance ($C_{SR}$) improves isolation at Wi-Fi frequencies and should be set between 6 and 7 GHz.

An evaluation board with the BGC100GN6 and a discrete Wi-Fi filter are depicted in *Figure 2*. The filter, which is located 4 mm away from the coupler IC to avoid any parasitic EMI coupling from the main path into the filter output, consists of a low-cost Murata LQG15HS4N3S02 inductor and a 1-pF capacitor. The inductor reaches self-resonance at 6.7 GHz.

*Figure 3* shows the frequency response of the circuit. *Fig. 3a* illustrates the intrinsic BGC100GN6 response with 30 dB of isolation at Wi-Fi frequencies. Utilizing an auxiliary Wi-Fi filter results in more than 48 dB of isolation from 4.9 to 5.9 GHz (*Fig. 3b*). This is at least 18 dB higher when compared with just the BGC-100GN6 IC. In essence, the cellular-to-Wi-Fi margin improves by 18 dB, reaching 28 dB for the worst-case antenna tuning scenario.

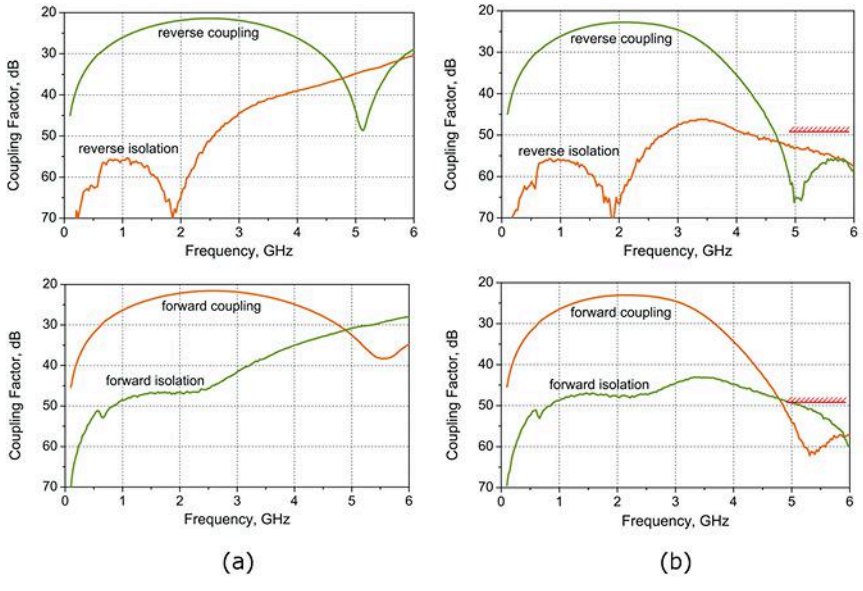


**3. Shown is the measured response of the BGC100GN6 coupler IC without (a) and with (b) a discrete LC lowpass filter in the coupled path.**

## CONCLUSION

Infineon's BGC100GN6 switchable wideband directional coupler IC with integrated direction switch and Wi-Fi lowpass filter is designed and optimized for RF front ends in cellular handheld devices. With an auxiliary discrete lowpass filter, the BGC100GN6 coupler IC provides a signal-to-distortion ratio suitable for the most demanding high-end systems. mw

*(Continued from page 72)*

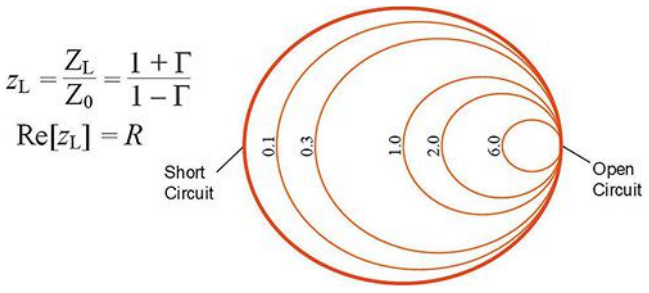


**6. Shown is the Smith chart with lines of constant resistance (*R*).**

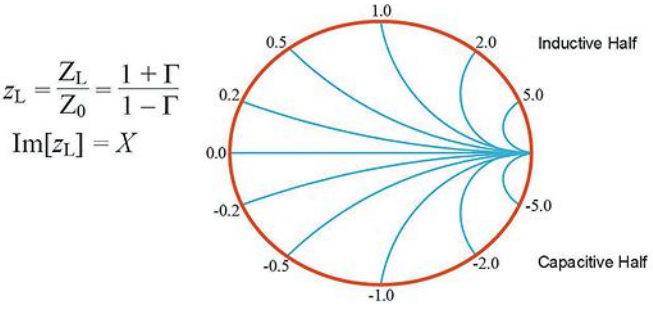


**7. In this case, the Smith chart depicts lines of constant reactance (*X*).**

An increase in transmission-line length will result in a clockwise rotation along the Smith chart. If this phase difference is not accounted for, the impedance value measured by the VNA will be different than the value at the matching-network location and the wrong matching-network values will be chosen to match the antenna. The phase correction can be made using a VNA by applying a port extension.

*Figure 8* illustrates the rotation of a trace on a Smith chart using a port extension with vector analysis software and a portable, PC-based VNA. The value referred to as delay length in the port-extension dialogue box is the physical length between the calibration plane and the desired measurement plane.

An easy way to correctly set the port extension is to place an open or short circuit at the desired measurement plane (the matching-network location) and incrementally adjust the delay length or delay time until the $S_{11}$ trace moves to the corresponding position on the right (open) or left (short) side of the Smith chart (*Fig. 8b*). Adding a positive value results in a counterclockwise rotation; a negative value results in a clockwise rotation.

In most cases, removing the device under test (DUT), i.e., matching network, will conveniently leave a suitable open at the desired reference plane. However, an open is susceptible to fringing capacitance and other parasitics at higher frequencies that make it less than ideal. Therefore, it may be best to use a short if your center frequency is above 1 or 2 GHz.

Now you're ready to measure the unmatched impedance at the matching network location.

**Step 3: Measure the unmatched impedance at the frequency of interest.**

Using a VNA, measure $S_{11}$ and view the trace on a Smith chart display. To get a clearer, more relevant trace, configure the VNA to sweep only over the frequency span covering the band(s) of interest (*Fig. 9*). Depending on your approach in the following Step 4, save the trace to a *.s1p* file or record the R + jX impedance value at the frequency of interest.

Setting a marker at the midband point(s) will help you identify how the trace needs to move on the Smith chart to get to the 50-Ω match point. If you only need the single impedance value in the middle of a band, you could also simply configure a zero-span trace at the midband frequency to easily distinguish the impedance at that frequency point.

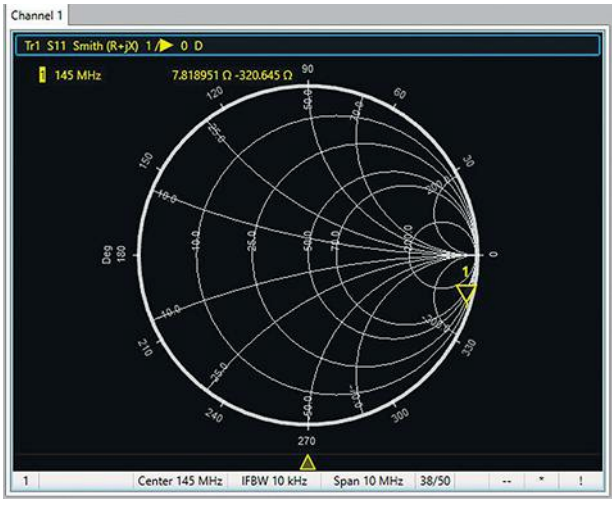


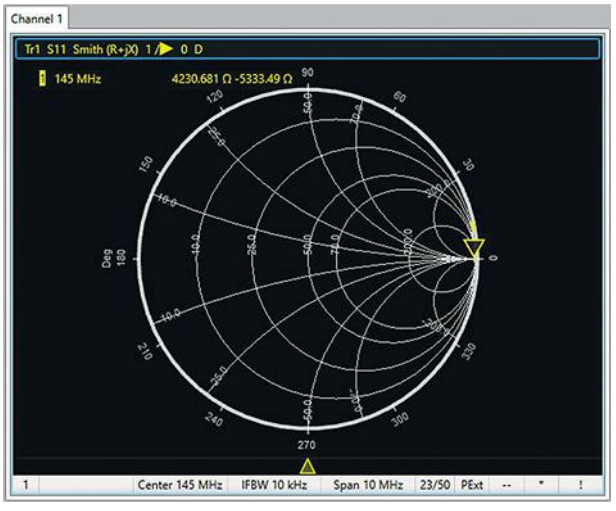


**8. This figure shows a Smith Chart display with no port extension applied (a) and then with a 4.9-cm port extension (b).**

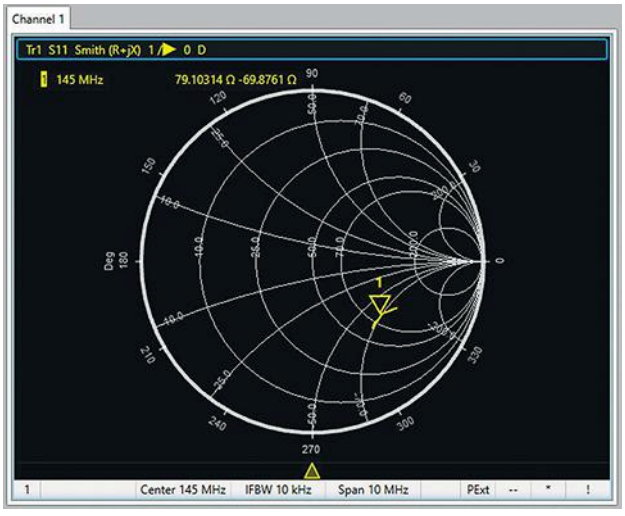


**9. Shown is an example of an unmatched antenna impedance measurement ($Z_L$ = 79.1 - j69.87 Ω). One can either save the full *.s1p* file or record the center frequency impedance value to calculate the matching network.**

**Step 4: Determine the matching-network component values and integrate the components.**

These days, few people calculate the matching-network component values by hand (although this author applauds those who still do). There are a variety of matching-network circuit simulators available, ranging from free downloadable tools to professional tools that provide powerful features to optimize a matching network based on multiple performance needs and design constraints. A PC-based VNA saves you time by making it easy to save S-parameter files from the VNA (containing the impedance measurement information) and import them into the circuit simulator.

The Smith chart is rarely used these days to calculate matching component values. Nonetheless, it is a very useful tool for visualizing how the choice of components will move the impedance from the unmatched value along the chart lines to the 50-Ω center point.

**Step 5: Confirm the matched impedance and adjust if needed.**

Once the matching network is integrated, re-measure the impedance as in Steps 2 and 3. If you followed the proper calibration and test methods, with a little luck, the trace will be centered and the antenna will now be matched to 50 Ω. If the impedance did not shift on the Smith chart consistent with what was predicted based on the matching circuit design, the most likely culprit is that the measured impedance was incorrect due to an inaccurate calibration, or improperly applied port extension (*Fig. 10*).

In such cases, try re-performing the calibration or establishing the calibration with a different approach. Using a calibration kit may be a preferred option instead of trying to create an SOL on the printed-circuit board (PCB). You may also have difficulty establishing a clean calibration because of the sensitivities of impedance measurement to board and test-setup parasitics. In that case, you can try to iterate the matching-network component values through trial and error until the antenna match is acceptably close to 50 Ω.

By following these five steps and using a portable VNA coupled with analysis software, anyone can improve their wireless device's performance without breaking the bank. MW

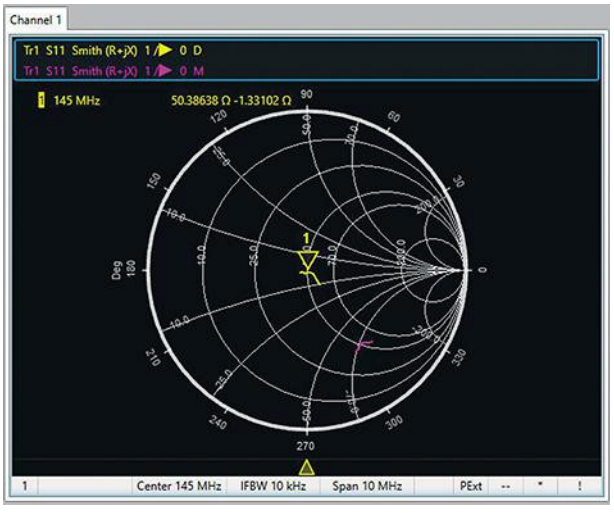


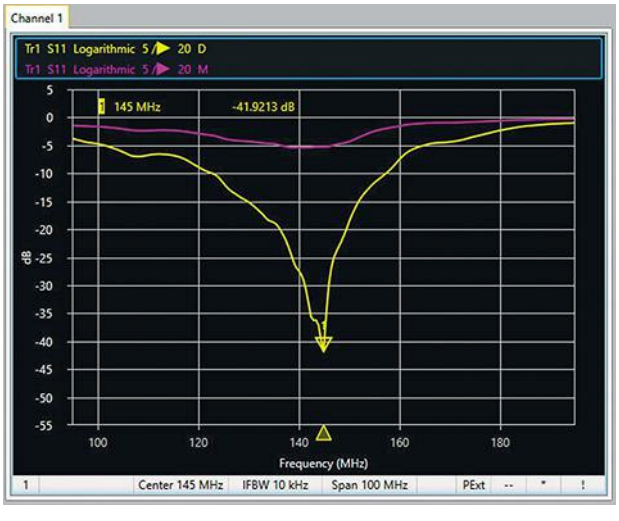


**10. In this example, the unmatched antenna (purple) is only achieving 4 to 5 dB return loss, resulting in as much as 30% to 40% of reflected power. The fully matched antenna (yellow) is achieving greater than 40 dB return loss, indicating a reflected power of less than 1%.**

CHRIS DeMARTINO | Technical Editor

# How Port Tuning Makes Filter Design More Efficient

**In this article, the design of a miniature hairpin resonator filter is presented to demonstrate how port tuning can accelerate the design of planar filters.**

It goes without saying that filters are crucial for achieving acceptable RF/microwave system performance. For engineers who are tasked with designing filters, software tools are available to streamline the design process. This article dives into one such example by presenting a design process of a miniature hairpin resonator filter, which can be designed in a short amount of time thanks to the capabilities of current software tools.

One company that specializes in filter design software is Nuhertz Technologies (*www.nuhertz.com*). The company's FilterSolutions software can be used to design lumped-element, distributed, active, and digital filters. In addition, FilterSolutions can be used together with various third-party electromagnetic (EM) simulators, as filter designs in FilterSolutions can be exported to third-party EM simulators for simulation and analysis.

In the example presented in this article, the Nuhertz FilterSolutions software will be used to design a microstrip miniature hairpin resonator filter.[1] This filter design will then be exported to the AXIEM 3D planar EM simulator within the NI AWR Design Environment (*www.awrcorp.com*) where it is optimized to obtain the desired performance. Nuhertz's port tuning feature enables the overall design process to be completed in a short amount of time.[2]

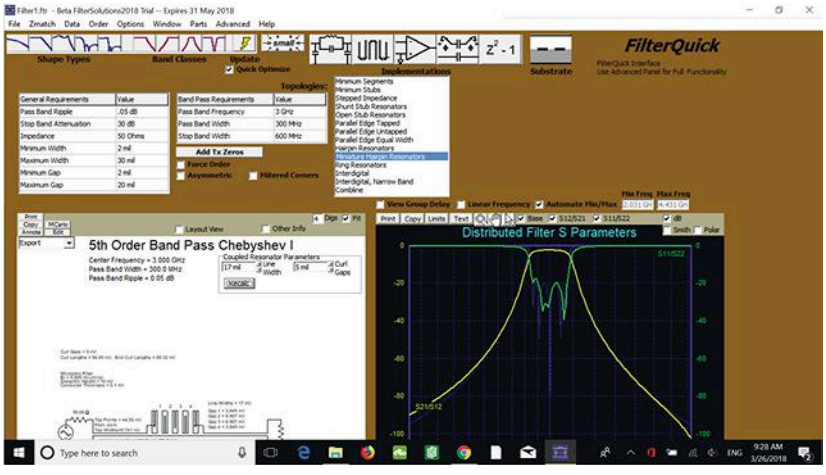


**1. Shown here is the FilterQuick user interface. The parameters for the filter have been entered.**

As an overview, the design process involves first creating the filter in the FilterSolutions program. Next, the design is exported to AXIEM with the port tuning feature enabled (this feature will be explained in more detail later).

After being exported to AXIEM, the filter is then optimized with the port tuning feature enabled. Since the tuning process is iterative, the filter is then imported back into FilterSolutions and then re-exported to AXIEM with the port tuning feature still enabled. This process is repeated until desirable simulation results are achieved, which is usually accomplished in one to three cycles. Tuning ports rely on small perturbation adjustments for accuracy. Hence, the first pass tends to rough out the optimization, while the second pass tends to fine-tune it.

Once the desired performance is attained, the filter is imported back into FilterSolutions and then re-exported to AXIEM again, but without the port tuning feature enabled. By disabling the port tuning feature, the final EM model can be generated in AXIEM for simulation and fabrication.

## STARTING THE DESIGN PROCESS

The FilterSolutions software lets users choose either quick or advanced user design panels. The quick panel, known

as *FilterQuick*, is intended to provide a more simplified approach to designing filters and helps new users learn the tool. More advanced users are sure to take advantage of the comprehensive advanced design panel. Both panels support the port tuning feature.

For this example, *FilterQuick* is used. *Figure 1* shows the parameters for this filter. Among them are a center frequency of 3 GHz and a stopband attenuation of 30 dB. Furthermore, the substrate for this filter is 10-mil-thick alumina. *Figure 1* also shows the frequency response.

## EM ANALYSIS WITH THE PORT TUNING FEATURE

EM analysis is the next step in the design process. As stated earlier, filter designs in FilterSolutions can be exported to various third-party EM simulators. Exporting a filter is accomplished via the *Export* dropdown menu (*Fig. 1*). Clicking this dropdown menu reveals several options that users can choose from. For this example, *AWR Setup* is selected.

Selecting *AWR Setup* displays a subsequent user interface (*Fig. 2*). *Extract to Axiem* was then selected from the *EM Extraction* dropdown menu that can be seen in *Figure 2*. The *Port Tune Format* checkbox located directly underneath the *EM Extraction* dropdown menu was then checked. Additional options include setting the number of EM points to simulate, setting the cell size in AXIEM, and much more.

Next, clicking *Overwrite to Axiem* exports the filter design to the AXIEM EM simulator. The filter is then generated in AXIEM in just a matter of seconds. *Figure 3* shows the generated AXIEM EM layout.

As can be seen in *Fig. 3*, internal ports are automatically incorporated into the AXIEM EM structure by enabling the port tuning feature during the filter exporting process. These internal ports provide connection points for tuning elements (components) located in strategic locations. The associated schematic in the AWR design environment contains the EM

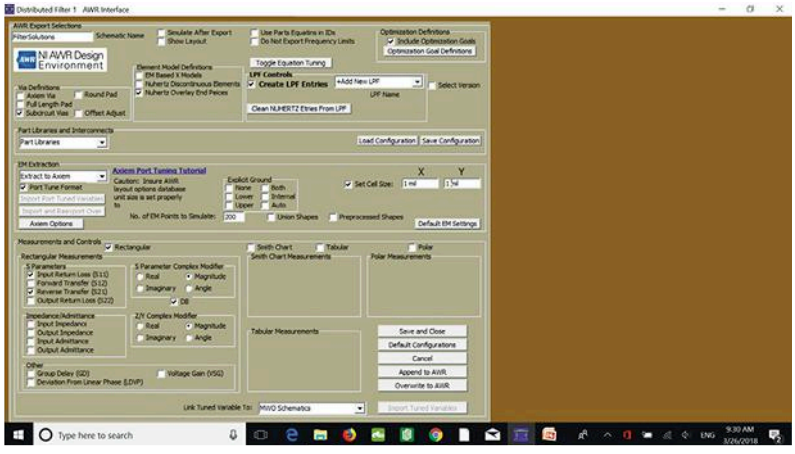

**2. This is the user interface that is displayed after choosing *AWR Setup*.**

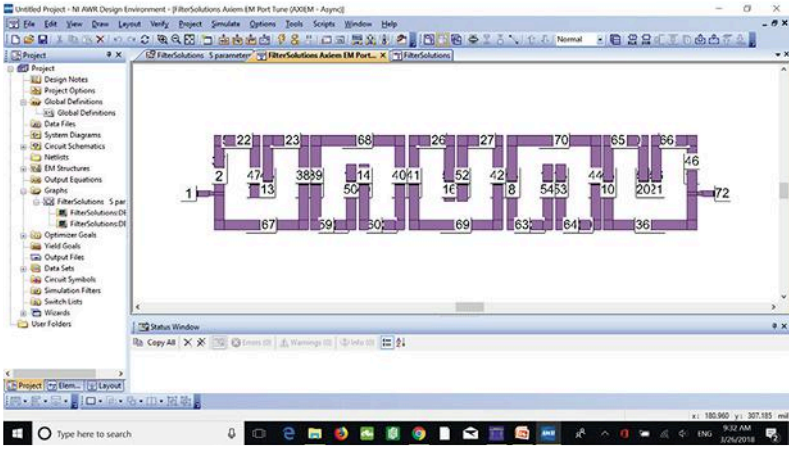

**3. Shown is the EM layout that is generated in AXIEM after exporting. In addition to the input and output ports, a large number of tuning ports are present here.**

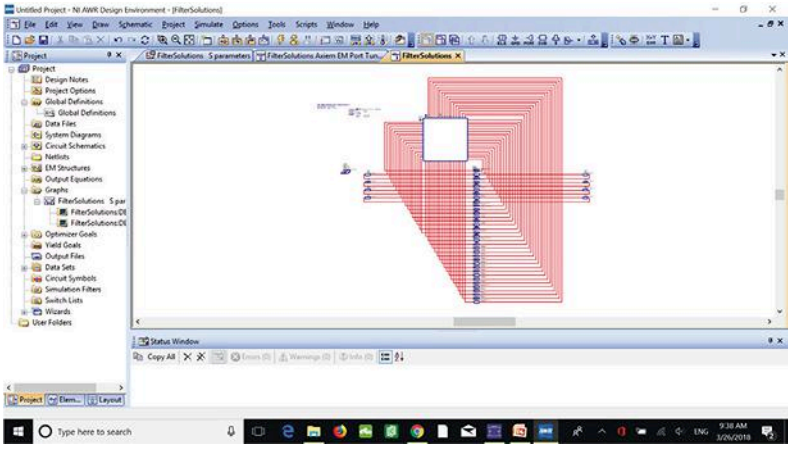

**4. The schematic contains the EM structure (large square) along with many tuning elements.**

# X-Series
# REFLECTIONLESS FILTERS

## DC to 30 GHz!

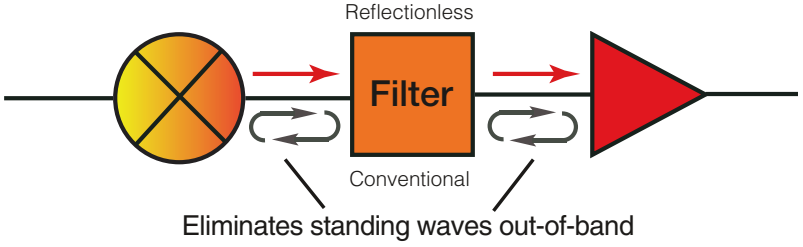


Eliminates standing waves out-of-band

## Now over 50 Models to Improve Your System Performance!

Now Mini-Circuits' revolutionary X-series reflectionless filters give you even more options to improve your system performance. Choose from over 50 unique models with passbands from DC to 30 GHz. Unlike conventional filters, reflectionless filters are matched to 50Ω in the passband, stopband and transition, eliminating intermods, ripples and other problems caused by reflections in the signal chain. They're perfect for pairing with non-linear devices such as mixers and multipliers, significantly reducing unwanted signals generated and increasing system dynamic range.[2] Jump on the bandwagon, and place your order today for delivery as soon as tomorrow. Need a custom design? Call us and talk to our engineers about a reflectionless filter to improve performance in your system!

*from* $6.95 *ea. (qty. 1000)*[1]

- High pass, low pass, and band pass models
- Patented design eliminates in-band spurs
- Absorbs stopband signal power rather than reflecting it
- Good impedance match in passband, stopband and transition
- Intrinsically Cascadable[3]
- Passbands from DC to 30 GHz[4]

[1] Small quantity samples available, $9.95 ea. (qty. 20)
[2] See application note AN-75-007 on our website
[3] See application note AN-75-008 on our website
[4] Defined to 3 dB cutoff point

Protected by U.S. Patent No. 8,392,495 and Chinese Patent No. ZL201080014266.I. Patent applications 14/724976 (U.S.) and PCT/USIS/33118 (PCT) pending.

Mini-Circuits®

www.minicircuits.com P.O. Box 350166, Brooklyn, NY 11235-0003 (718) 934-4500 sales@minicircuits.com 550 Rev D

structure itself along with tuning elements that are connected to the tuning ports (*Fig. 4*). These tuning elements can be optimized to obtain the desired frequency response using parameters that are derived from tuning variables contained in the schematic.

*Figure 5* shows the results of the initial AXIEM simulation prior to optimizing the filter. The results of the EM simulation demonstrate that the filter should be optimized, since it appears that the response at the low end of the frequency range needs to be improved.

## OPTIMIZING THE FILTER

Optimizing the filter first requires specifying the optimization goals. FilterSolutions automatically produces its own default set of optimization goals. Of course, designers can also modify these goals to meet their own requirements. *Figure 6* shows the optimization goals used here, one of which is an $S_{11}$ of less than −18 dB from 2,854 to 3,154 MHz.

The average amount of time needed to optimize the filter in this case was approximately 52 sec. (note that this average was calculated after performing the optimization 10 consecutive times for verification purposes). *Figure 7* shows the simulation results after optimization, revealing an improved frequency response.

## IMPORTING AND RE-EXPORTING

The tuning process is iterative, meaning a few cycles are generally needed to obtain the desired performance. Hence, the next step is to return to the FilterSolutions software and select *Import and Reexport Over* from the user interface (*Fig. 2*). The filter is again generated in AXIEM with internal ports. However, while the EM layout of this newly generated filter essentially looks the same, it now has certain resonator dimensions that have been re-computed.

The associated schematic contains this new EM structure along with the tuning elements connected to the tuning ports. The same process of optimizing the filter is then repeated. *Figure 8* shows the simulation results after optimization.

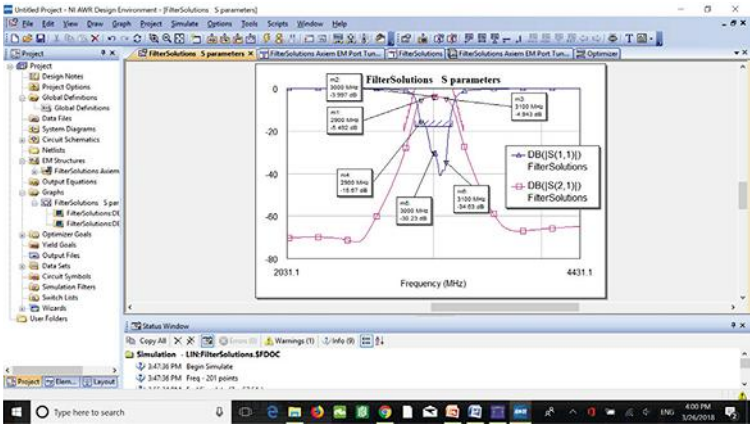


**5. Shown are the initial AXIEM simulation results.**

| Measurement | Enabled | Cost | Weight | L | X Start | X Stop | Y Start | Y Stop | Type |
|---|---|---|---|---|---|---|---|---|---|
| FilterSolutions:DB(\|S(2,1)\|) | ☑ | 0 | 0.5 | 2 | 3154 MHz | 3247 MHz | -0.05 | -20.05 | Meas < Goal |
| FilterSolutions:DB(\|S(2,1)\|) | ☑ | 0 | 0.5 | 2 | 2772 MHz | 2854 MHz | -20.05 | -0.05 | Meas < Goal |
| FilterSolutions:DB(\|S(1,1)\|) | ☑ | 12.74 | 1 | 2 | 2854 MHz | 3154 MHz | -18 | -18 | Meas < Goal |

**6. The optimization goals are shown here.**

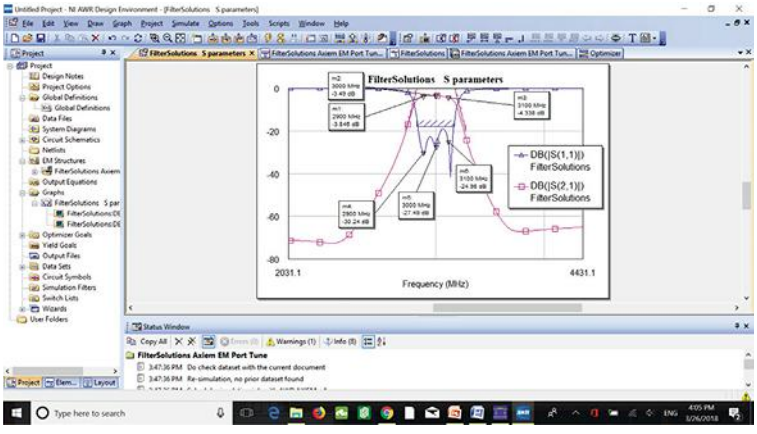


**7. Shown are the simulation results after optimization, illustrating an improved filter response.**

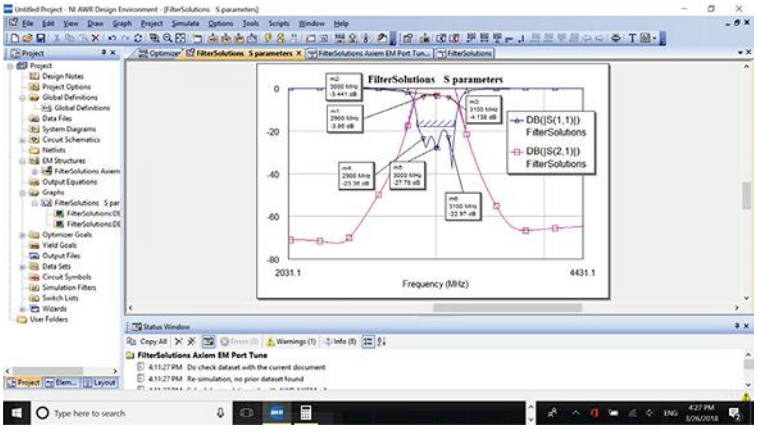


**8. After selecting *Import and Reexport Over* in FilterSolutions, the filter was again optimized in AXIEM. Shown here are the simulation results.**

As stated, the tuning process is iterative, as it may require a few cycles. Hence, the same process of returning to FilterSolutions and selecting *Import and Reexport Over* was performed again. However, the simulation results obtained after optimizing the filter once again remained almost the same as the results obtained after the previous optimization. Hence, this step may not have been necessary for this design.

## IMPORTING AND RE-EXPORTING WITHOUT PORT TUNING

Now that a desirable filter response has been achieved, the last step in the design process is to perform a final design verification using the EM simulator without the tuning elements. The internal ports are removed by disabling the port tuning feature in the FilterSolutions program by unchecking the *Port Tune Format* checkbox. Next, *Import and Reexport Over* is selected to export the filter into AXIEM again to confirm that the design goals have been met.

*Figure 9* shows the generated AXIEM EM layout. As can be seen, the internal ports are no longer present due to disabling the port tuning feature. *Figure 10* shows the associated schematic, which contains an EM extraction block. *Figure 11* shows the simulation results of this filter, demonstrating good performance.

To summarize, the port tuning feature is a fast and effective way of designing distributed filters. The design of a microstrip miniature hairpin resonator filter was presented in this article to validate this process. Those who are interested can take advantage of the software tools featured in this article to design their own filters. mw

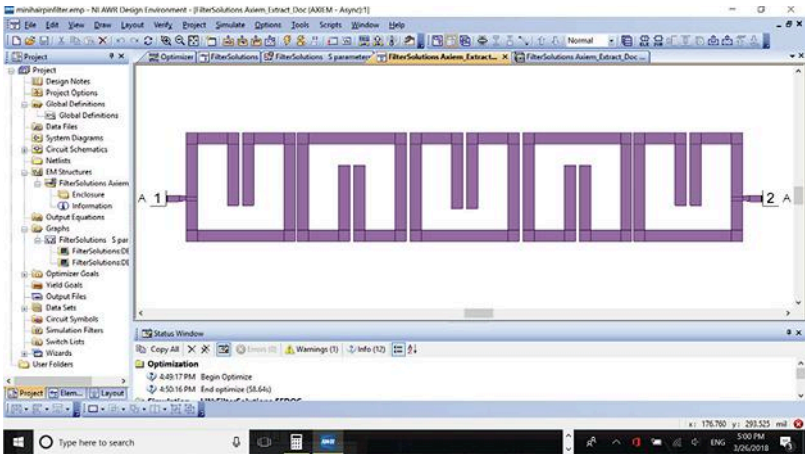

**9. The filter is now generated in AXIEM without any tuning ports.**

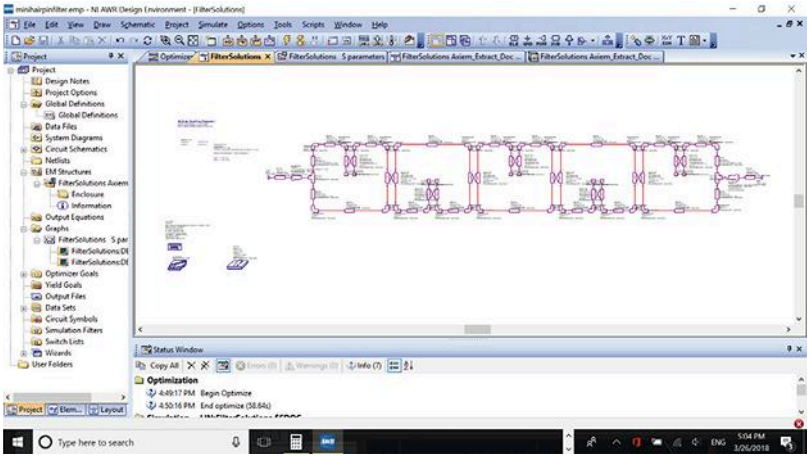

**10. Shown is the schematic in the AWR design environment that includes an EM extraction block.**

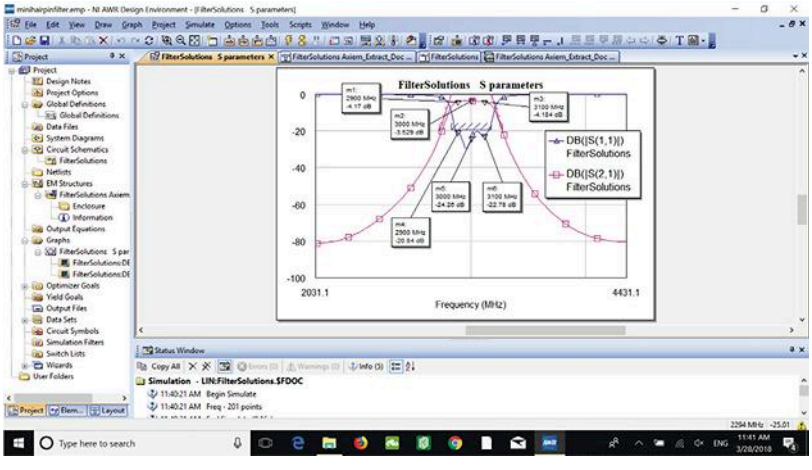


**11. This figure illustrates the final simulation results of the filter.**


REFERENCES

1. Shivhare, Jagdish. "A Compact Fourth-Order Multi-fold Hairpin Line Microstrip Bandpass Filter at 1650 Mhz for Rf Wireless Communications," *International Journal of Research in Engineering and Technology*, May 2014, pp. 683-686.
2. Rautio, James C. "Perfectly Calibrated Internal Ports in EM Analysis of Planar Circuits," 2008 *IEEE MTT-S International Microwave Symposium Digest*, June 15-20, 2008, pp. 1,373-1,376.

### USB/Ethernet Programmable Attenuator Covers 0.1 to 30.0 GHz

**MODEL RCDAT-30G-30** is a programmable attenuator with extremely wide bandwidth of 0.1 to 30.0 GHz. It provides precisely controlled attenuation values from 0 to 30 dB in 0.5-dB steps and can be operated by means of computer control using its integral USB or Ethernet ports. As many as 25 attenuators can be controlled with a single connection by "daisy-chaining" the attenuators. The RoHS-compliant attenuator has full software support, including for Windows and Linux 32- and 64-b environments. Attenuation accuracy is typically ±0.6 dB or better at all frequencies for attenuation values to 10 dB and typically ±2.65 dB or better for attenuation values to 30 dB across the full frequency range. Typical VSWR is 1.40:1 across the full frequency range. The programmable attenuator operates on 5 V dc via USB or serial control.

**MINI-CIRCUITS,** P. O. Box 350166, Brooklyn, NY 11235-003; (718) 934-4500, *www.mini-circuits.com*

### Broadband SMT Mixer Translates 1 to 6000 MHz

**THE SMD-6000** is a broadband, surface-mount-technology (SMT), double-balanced mixer suitable for a wide range of applications. It features an RF/LO frequency range of 1 to 6000 MHz and an intermediate-frequency (IF) range of dc to 700 MHz. It exhibits typical conversion loss of 8.5 dB, working with nominal LO power of +10 dBm. The output 1-dB compression point is typically +3 dBm, with an input third-order intercept point (IP3) of typically +15 dBm. The LO-to-RF isolation is at least 15 dB and typically 25 dB; the LO-to-IF isolation is at least 12 dB and typically 18 dB; and the RF-to-IF isolation is at least 12 dB and typically 15 dB. The RoHS-compliant 50-Ω mixer is available in a compact SMT housing measuring just 0.500 × 0.375 × 0.165 in. Operating temperature range is –40 to +75°C.

**SYNERGY MICROWAVE CORP.,** 201 McLean Blvd., Paterson, NJ 07504; (973) 881-8800, E-mail: sales@synergymwave.com, *www.synergymwave.com*

### Circuit Materials Support Multiple-Layer Designs

**RO4835T LAMINATES ARE** designed for inner-layer use in multilayer circuit-board designs. The spread-glass-reinforced, ceramic-filled thermoset materials exhibit a dielectric constant (Dk) of 3.3 and are available in thicknesses of 2.5, 3.0, and 4.0 mil as a complement to RO4835 circuit laminates. The materials are compatible with standard FR-4 epoxy-glass circuit fabrication processes. As an additional complement, RO4450T bonding materials are low-loss, glass-reinforced, ceramic-filled bonding materials with a Dk of 3.2 to 3.3 designed to work with RO4835T circuit materials, typically in multilayer circuit assemblies.

**ROGERS CORP.,** Advanced Connectivity Solutions, 100 S. Roosevelt Ave., Chandler, AZ 85226; (480) 961-1382, *www.rogerscorp.com*

### VCO Shaves Phase Noise at 2176 MHz

**THE DCSR2176-6** is a voltage-controlled oscillator (VCO) with fundamental-frequency output of 2176 MHz and tuning sensitivity of 2.75 to 3.50 MHz/V for a tuning voltage range of 0.5 to 5.0 V dc. It achieves low phase noise of –115 dBc/Hz offset 10 kHz from 2176 MHz, and provides enough tuning bandwidth margin to cover effects from long-term aging, thermal drift, pulling, and pushing. The 50-Ω oscillator delivers +2 dBm minimum output power while drawing only 30 mA typical current from a 6-V dc supply. The typical pulling is 4 MHz at a 1.75:1 VSWR. Harmonic rejection is typically –27 dBc. The RoHS-compliant VCO comes in a surface-mount package measuring just 0.500 × 0.500 × 0.180 in.

**SYNERGY MICROWAVE CORP.,** 201 McLean Blvd., Paterson, NJ 07504; (973) 881-8800, E-mail: sales@synergymwave.com, *www.synergymwave.com*

### Surface-Mount Mixers Convert Signals to 26 GHz

**MODELS MMIQ-0520LSM** and MMIQ-0626LSM are surface-mount versions of low-barrier-diode in-phase/quadrature (I/Q) frequency mixers. The two mixers offer wide RF/LO bandwidths of 5 to 20 GHz and 6 to 26 GHz, respectively, and are designed to operate effectively with a low drive level of +3 dBm. They are available in 4- × 4-mm QFN surface-mount packages or in evaluation modules with connectors.

**MARKI MICROWAVE INC.,** 215 Vineyard Ct., Morgan Hill, CA 95037; (408) 778-4200, *www.markimicrowave.com*

## Coaxial LNA Has Level Gain to 18 GHz

**MODEL PE2-30-1R018R0-4R5-22-12-SFF-1** is a coaxial low-noise amplifier (LNA) with 30-dB typical gain from 1 to 18 GHz. It maintains gain flatness within ±1.5 dB across that frequency range with maximum noise figure of 4.5 dB and at least +22 dBm output 1-dB compression point. The rugged amplifier draws 500 mA typical current from a voltage supply of +12 to +15 V dc and is supplied with removable SMA female connectors.

**PMI,** 7311-F Grove Road, Frederick, MD 21710; (301) 662-5019, FAX: (3010) 662-1731, *www.pmi-rf.com*

## Attenuators Pad Signals to 6 GHz

**A LINE OF** quick-connect attenuators consists of 31 models for a total frequency range of dc to 6 GHz. With attenuation values from 0 to 20 dB and VSWRs as low as 1.15:1, the attenuators are available with QMA, QN, or 4.3-10 connectors for easy mating in radio heads, base stations, and antennas. The attenuators can handle power levels as high as 15 W.

**FAIRVIEW MICROWAVE INC.,** 301 Leora Ln., Ste. 100, Lewisville, TX 75056; (800) 715-4396, (972) 649-6678, *www.fairviewmicrowave.com*

## Coupler Commands 690 to 6000 MHz

**MODEL IPP-7148** is a 90-deg. surface-mount coupler for applications from 690 to 6000 MHz. It combines two signals and handles as much as 130 W CW combined power. It comes in a tiny package measuring just 0.50 × 1.00 × 0.167 in. Insertion loss across the full band is less than 0.80 dB. Amplitude balance is well controlled, while VSWR is better than 1.35:1. The coupler provides better than 16.5 dB isolation between ports.

**INNOVATIVE POWER PRODUCTS,** 1170 Lincoln Ave, No. 8, Holbrook, NY 11741; (631) 563-0088, *www.innovativepp.com*

## Dish Antenna Makes Strong Point-to-Point Connections

**MODEL KPPA-29-5GHZDPFHA** is a dish antenna well-suited for point-to-point radios operating from 4900 to 5900 MHz. The feed-horn reflector dish antenna boasts more than 27-dBi gain and more than 30-dB front-to-back isolation for a 6.5-deg. 3-dB beam width. The antenna exhibits less than 1.50:1 VSWR with better than 14-dB return loss. The 28-in.-diameter antenna comes equipped with two Type N female connectors and a J-arm pole mount to handle high winds and also adjustments for vertical/horizontal and ±45-deg. slant polarization schemes. It features better than 32-dB front-to-back ratio. And better than 24-dB cross polarization rejection. The 50-Ω antenna handles as much as 25 W input power per port.

**KP PERFORMANCE ANTENNAS,** 15497 117 Ave., Edmonton, Alberta TM53X4, Canada; (855) 276-5772, (780) 702-7577; E-mail: info@kpperformance.ca, *www.kpperformance.ca*

## Waveguide Switches Span E- and W-Band Ranges

**A LINE OF GAAS PIN-DIODE** waveguide switches covers millimeter-wave frequency bands of E-band (60 to 90 GHz) and W-band (75 to 110 GHz) for communications, radar, and test applications. The single-pole, single-throw (SPST) and single-pole, double-throw (SPDT) switches feature typical insertion loss of 4 dB with 25-dB isolation between ports, and fast switching speeds of better than 300 ns. The E- and W-band components are equipped with TTL driver circuitry and fully integrated WR10 and WR12 waveguide ports, respectively. All of the switch models require a dual voltage bias of +5 and –5 V dc and are designed for operating temperatures of –55 to +85°C.

**FAIRVIEW MICROWAVE INC.,** 301 Leora Ln., Ste. 100, Lewisville, TX 75056; (800) 715-4396, (972) 649-6678, *www.fairviewmicrowave.com*

| ADVERTISER | PAGE |
|---|---|
| **A** | |
| ARRA INC. | C3 |
| *www.arra.com* | |
| ANALOG DEVICES | 11 |
| *www.analog.com/LTC5596* | |
| ASELSAN ELEKTRONIK | 56 |
| *www.aselsan.com.tr* | |
| AVTECH ELECTROSYSTEMS LTD. | 6 |
| *www.avtechpulse.com* | |
| **C** | |
| CIAO WIRELESS INC | 17 |
| *www.ciaowireless.com* | |
| COILCRAFT | C4 |
| *www.coilcraft.com* | |
| COMMUNICATION CONCEPTS INC | 68 |
| *www.communication-concepts.com* | |
| CUSTOM MMIC | 2 |
| *www.custommmic.com/calculators* | |
| **D** | |
| DBM CORP | 7 |
| *www.dbmcorp.com* | |
| **E** | |
| E360 MICROWAVE.COM | 4 |
| *www.e360microwave.com* | |
| ECLIPSE MICROWAVE | 66 |
| *www.eclipsemdi.com* | |
| **F** | |
| FAIRVIEW | 22,23 |
| *www.fairviewmicrowave.com* | |
| **H** | |
| HEROTEK INC | 13 |
| *www.herotek.com* | |
| **I** | |
| IMS | 74-75 |
| *www.ims2018.org* | |
| INDIUM CORPORATION | 49 |
| *www.indium.com/MICRV* | |
| **J** | |
| JFW INDUSTRIES INC | 37 |
| *www.jfwindustries.com* | |

| ADVERTISER | PAGE |
|---|---|
| **M** | |
| M/A COM TECHNOLOGY SOLUTIONS, INC | 8-9 |
| *www.macom.com/home* | |
| MICRO LAMBDA WIRELESS,INC | 29 |
| *www.microlambdawireless.com* | |
| MINI-CIRCUITS/SCI COMPONENTS | 12,14-15,21,25,30-31,43, 61,65,83 |
| *www.minicircuits.com* | |
| **N** | |
| NI AWR CORPORATION | C2 |
| *www.awrcorp.com/5g* | |
| NI MICROWAVE COMPONENTS | 36 |
| *www.ni-microwavecomponents.com/quicksyn* | |
| **P** | |
| PASTERNACK ENTERPRISES | 26 |
| *www.pasternack.com* | |
| PICO TECHNOLOGY | 55 |
| *www.picotech.com/A72* | |
| PLANAR MONOLITHICS INDUSTRIES | 1 |
| *www.pmi-rf.com* | |
| POLYFET RF DEVICES | 67 |
| *www.polyfet.com* | |
| PULSAR MICROWAVE CORP | 20 |
| *www.pulsarmicrowave.com* | |
| **R** | |
| ROHDE&SCHWARZ GMBH&CO KG | 48 |
| *www.rohde-schwarz.com/5G* | |
| **S** | |
| SAGE MILLIMETER INC | 40-41 |
| *www.sagemillimeter.com* | |
| SKYWORKS SOLUTIONS INC | 33 |
| *www.skyworksinc.com/Sky5* | |
| SYNERGY MICROWAVE | 3,51 |
| *www.synergywave.com* | |
| **W** | |
| WAVELINE INC | 16 |
| *www.wavelineinc.com* | |


*This index is provided as an additional service by the publisher, who assumes no responsibility for errors or omissions.*

Subscription Assistance and Information:
(ISSN 0745-2993)
Microwaves & RF is published monthly. Microwaves & RF is sent free to individuals actively engaged in high-frequency electronics engineering. In addition, paid subscriptions are available. Subscription rates for U.S. are $95 for 1 year ($120 in Canada, $150 for International). Published by Informa Media Inc., 9800 Metcalf Ave., Overland Park, KS 66212-2216. Periodicals Postage Paid at Kansas City, MO and additional mailing offices. POSTMASTER: Send change of address to Microwaves & RF PO Box 2100, Skokie, IL 60076-7800. For paid subscription information, please contact Microwaves & RF at PO Box 2100, Skokie IL 60076-7800. Canada Post Publications Mail agreement No. 40612608. Canada return address: IMEX Global Solutions PO Box 25542, London ON N6C 6B2.

Back issues of MicroWaves and Microwaves & RF are available on microfilm and can be purchased from National Archive Publishing Company (NAPC). For more information, call NAPC at 734-302-6500 or 800-420-NAPC (6272) x 6578. Copying: Permission is granted to users registered with the Copyright Clearance Center, Inc. (CCC) to photocopy any article, with the exception of those for which separate copyright ownership is indicated on the first page of the article, provided that a base fee of $1.25 per copy of the article plus 60 cents per page is paid directly to the CCC, 222 Rosewood Dr., Danvers, MA 01923. (Code 0745–2993/02 $1.25 +.60) Copying done for other than personal or internal reference use without the expressed permission of Informa Media Inc., is prohibited. Requests for special permission or bulk orders should be addressed in writing to the publisher.
Copyright 2018 • Informa Media Inc. • All rights reserved. Printed in the U.S.

# The sweetest & largest assortment of Miniatures in the world...

## from ARRA, of course!

*For your "sweet tooth"...*

## Miniature Variable Attenuators

*Bands from* DC–18GHz

Some models feature:

- ♥ Extremely flat attenuation vs. frequency response
- ♥ Constant phase with △ attenuation.

The ultimate in reliability, and wear-free performance ...achieved with ARRA's non-contacting method of attenuating.

Most units incorporate ARRA's proprietary attenuating elements which give excellent stability over a wide temperature range.

*Customerized* to *your* requirements.

**Call us, write or Fax your specs to 631-434-1116**

*...the last word in variable attenuators*

# ARRA INC.

**Visit our website at www.arra.com**

**15 Harold Court, Bay Shore, N.Y. 11706 • 631-231-8400**

# Introducing our new Common Mode Choke Finder

## There's nothing common about it!

### Search and compare hundreds of common mode choke options in four easy steps.

**Step 1:** Search parts by Impedance, Attenuation or Inductance at your operating frequency.

**Step 2:** View results in a sortable table with complete performance specifications and select parts for further analysis.

**Step 3:** Make direct comparisons of up to six components on single impedance and attenuation graphs.

**Step 4:** Request free samples of the most interesting parts for evaluation and testing.

## It's that Simple!

Try it at **coilcraft.com/CMCfinder.**

coilcraftdirect.com
No min order. Next day delivery.

Coilcraft®

WWW.COILCRAFT.COM